Improving Discharge Prediction for Poorly Gauged Hydropower Potential Sites – A Case Study of Mabula Kapi Site

By

Reynolds Mukuka

A thesis

submitted in fulfilment of the requirements for the

Master of Engineering Degree in Water Resources Engineering,

THE UNIVERSITY OF ZAMBIA

LUSAKA

2022

Copyright Declaration

I declare that this thesis is my own original work and, to the best of my knowledge and belief, it does not: Breach copyright or other intellectual property rights of a third party.

Declaration

This thesis represents the Author's own work. It has not previously been submitted for a degree, diploma or other qualification at this or any other University;

Signature: …… Date: …….

Certificate of Approval

This thesis of Reynolds Mukuka has been approved as fulfilling the requirements for the award of Master of Engineering Degree in Water Resources Engineering by the University of Zambia;

Board of Examiners:

Chairperson

Name…… Signature ……

Date……

Examiner 1

Name: ……... Signature ……

Date……

Examiner 2

Name…… Signature ……

Date……

Abstract

Kafue Gorge Regional Training Centre (KGRTC) intends to carry out full feasibility studies for the development of Mabula Kapi hydropower site located on Kaombe River in Serenje District. KGRTC installed a hydrological gauging station at the site in September 2019. However, the small hydropower potential site is considered to be poorly gauged since it lacks adequate streamflow and/or rainfall data required for hydropower planning and design. Mabula Kapi was initially investigated to prefeasibility study level, using hydrological data from an adjacent catchment on Lusiwasi River, which was considered to be hydrologically similar. The catchment area-ratio method which was applied is a simple approximation because catchment characteristics between donor and target catchments rarely match perfectly. For Mabula Kapi site, the presence of a natural lake on the Lusiwasi donor catchment raised uncertainties about similarities in the drainage network and therefore the accuracy of transposing hydrological data. Additionally, anticipated future climate changes raised uncertainties about the sustainability of the proposed hydropower plant.

In this study, several discharge prediction methods were reviewed and rainfall-runoff computer modelling was selected as the most suitable method for predicting discharge for Mabula Kapi Catchment. The method was applied to accurately predict discharge time series by creating a conceptual representation of relevant hydrological processes for Mabula Kapi Catchment in a computer-based open-source model known as PITMAN. The PITMAN model was largely selected due to limitations in local input data availability and project budget. Satellite rainfall point data known as the Climate Hazards Group InfraRed Precipitation with Station data (CHIRPS) was adopted as one of the modeling inputs because of its good correlation with ground measured data. A 30-year discharge time series was simulated for Mabula Kapi site using the PITMAN model. The model was calibrated by matching simulated discharge and observed discharge time series from the newly installed gauging station at Mabula Kapi site. The derived time series were used to estimate the installed capacity (8.2 MW), annual energy yield (38 GWh) and design flood ($120 m^3/s$). Runoff simulations done in the model using future rainfall and temperature projections indicated that the average annual energy for the power plant is likely to reduce by 11% from 2040 to 2059. It is recommended that the estimated energy reduction be taken into account when conducting financial analysis for the project and that further climate tests be done using other credible climatic projections which may be available.

Key words: CHIRPS, Hydropower, Modelling, Rainfall, Streamflow

Acknowledgements

I wish to express my sincere gratitude to the Management of Kafue Gorge Regional Training Center for allowing me to conduct my research at Mabula Kapi hydropower potential site. I am grateful for the support rendered to me during the studies, especially the financial support extended to me during site visits. I definitely want to thank my supervisors Dr. Edwin Nyirenda and Dr. Joel Kabika for the guidance given to me throughout my study. I am grateful that Dr. Nyirenda took personal interest in my research work and even took time from his busy schedule to visit Mabula Kapi site.

I am very grateful to my wife Bithiah and to my son Ray for the support rendered to me during my research. I am very thankful to my God Jehovah for the gift of life I have enjoyed during this period and for according me the opportunity to appreciate his marvelous scientific wisdom.

Table of Contents

List of Tables

List of Figures

List of Abbreviations

AARD	Average Annual Runoff Depth
ADCP	Acoustic Doppler Current Profiler
AE	Actual Evaporation
CC	Coefficient of Correlation
CHIRPS	Climate Hazards Group Infrared Precipitation
CKP	Climate Knowledge Portal
DEM	Digital Elevation Models
EV	Extreme value
FAO	Food Agriculture Organization
FDC	Flow Duration Curve
GCM	General Circulation Models
GIS	Geographic Information System
GRG	Generalized Reduced Gradient
GWh	Gigawatt-hour
HPP	Hydropower Plant
IPCC	International Panel on Climate Change
KGRTC	Kafue Gorge Regional Training Centre
kWh	Kilowatt-hour
LPS	Linear Programming Solver
MAE	Mean Absolute Error
MAR	Mean Annual Rainfall
MW	Megawatt
OPPPI	Office for Promoting Private Power Investment
PDF	Probability Density Function
PE	Potential Evaporation
PMF	Probable Maximum Flood
RCM	Regional Climate Models
RCP	Representative Concentration Pathways
RET	Renewable Energy Technology
SAAR	Standard Average Annual Rainfall
SADC	Southern Africa Development Community
SHP	Small Hydropower Plant
SRTM	Shuttle Radar Topography Mission
SSP	Shared Social-Economic Pathways
TAMSAT	Tropical Applications of Meteorology using Satellite
WARMA	Water Resources Management Authority
ZMD	Zambia Meteorological Department

1 Chapter One: Introduction

1.1 Background

1.1.1 Overview

According to estimates from previous energy studies, Zambia has a hydropower generation potential of more than 6,000 MW (Tokyo Electric Power Company, 2008). Most of the hydropower potential sites are in rural areas and their capacities range from small to large. Development of small hydropower plants which are widely considered to be renewable energy technology will help to foster sustainable development as well as increase access to electricity in the country. In 2015, only 31% of households had access to electricity in Zambia. The electrification rates for rural and urban households were estimated to be 4.4% and 67.3% respectively (Republic of Zambia, 2015)

Most rivers in Zambia hosting small hydropower potential sites do not have gauging stations and therefore adequate hydrological time series required for hydropower planning. This presents a real challenge for developers wishing to establish technical viability of hydropower projects. Developers are therefore expected to apply suitable methods for predicting discharge at a particular site of interest.

ZESCO Limited, a national vertically integrated power utility, has played a key role in the development of small hydropower plants in Zambia. In 2015, ZESCO begun to undertake in-house project preparation activities for development of small hydropower plants (HPP). Several small hydropower plants were identified, and preliminary studies were conducted ranging from reconnaissance to prefeasibility studies. Mabula Kapi (formerly known as Kaombe) hydropower potential site located in Serenje District, Central |Province of Zambia was identified from this program. ZESCO conducted prefeasibility studies for Mabula Kapi potential site in 2018 and it was conceptualised as a 7.4MW run-of-river power plant (ZESCO, 2018).

1.1.2 Mabula Kapi site attributes

Mabula Kapi site is located on Kaombe River, in the Central Province of Zambia on latitude 13º 19' 28.02" and Longitude 30º 47' 14.02" in WGS84 coordinate system. The location of the site is illustrated in Appendix 5. The project site can be accessed from Serenje district by road on a total distance of 121 Km, out of which 83Km is on a bituminous paved road , 25Km is on a gravel road and the last 13 Km is on an earth road. The site is in Chieftainess Serenje Chiefdom (ZESCO, 2018).

Prefeasibility studies established that construction of the proposed Mabula Kapi HPP would be technically feasible with a minimum power installed capacity of 7.4MW and an average annual energy of 34 GWh. In terms of power evacuation, it was proposed that the power generated from the proposed Kaombe HPP be evacuated through a 22Km double circuit line from the proposed Kaombe HPP to connect into the existing 66kV Pensulo-Lusiwasi line 2.

1.1.3 Proposed Feasibility Study

In 2019, Kafue Gorge Regional Training Centre (KGRTC) requested ZESCO for assistance in identifying a suitable hydropower site for feasibility study and possible development. Following successful negotiations, ZESCO handed over the site and the prefeasibility study report to the Training Institution. KGRTC eventually applied for feasibility study rights for Mapula Kapi site through the office for promoting private power investment (OPPPI) of the Ministry of Energy and they were granted feasibility study rights. KGRTC has managed to implement one of the recommendations from the prefeasibility study to install a stream flow gauging station on Kaombe river, upstream of the proposed intake for the hydropower station. The station was installed in September 2019 in collaboration with the Water Resources Management Authority (WARMA).

KGRTC intends to carry out feasibility studies for development of Mabula Kapi hydropower site in collaboration with ZESCO. A larger part of the engineering feasibility studies will be undertaken by KGRTC and ZESCO staff. Only a few identified specialized works such as drone topographical surveys and geotechnical

investigations will be outsourced. The Author has offered to undertake hydrological analysis for development of Mabula Kapi hydropower plant.

1.2 Problem Statement

1.2.1 Hydrological uncertainties

Kaombe river on which Mabula Kapi hydropower potential site is located did not have a gauging station for many years. During prefeasibility studies conducted by ZESCO, streamflow data from a nearby gauging station located on Lusiwasi River was transposed onto the Mabula Kapi site for preliminary design. This was done using the catchment area ratio method. However, the method is a simple approximation, which works best when the gauging station is close to the respective intake (Nruthya & Srinivas, 2015). This method does not consider the influences of vegetation, soil type, and geology on the flow in the investigated area. Use of this method may leave hydrological uncertainties which present a risk to hydropower development (Fitchner, 2015).

This research study is an opportunity to verify and firmly establish discharge time series required for the design of Mabula Kapi HPP with a view to minimize hydrological uncertainties.

1.2.2 Climate risks for hydropower plants

Another challenge encountered in recent years is the susceptibility of hydropower facilities to climate risks (IHA, 2019). Zambia has continued to experience climate change and climate variability.

Although there are several uncertainties regarding the forecast climatic changes, it is becoming standard practice to evaluate the effects of climate change on water resources infrastructure. Failure to consider climate risks may lead to deficiencies in technical and financial performance, safety aspects, and environmental functions

(IHA, 2019). It is therefore prudent that a climate resilient design be evaluated for the proposed Mabula Kapi HPP.

1.3 Objectives

1.3.1 Overall objective

To predict discharge time series for the proposed Mabula Kapi hydropower plant and to estimate its power output and energy yield.

1.3.2 Specific objectives

The specific objectives of this research project are as follows:

a) To identify, compare and select suitable techniques and methods for predicting discharge time series at Mabula Kapi HPP site
b) To predict discharge time series required for estimating the power potential and energy yield for Mabula Kapi HPP site
c) To determine the power potential and energy output for a possible climate resilient power plant at Mabula Kapi with minimal shortcomings in safety, technical and financial performance.

1.4 Research questions

This research answers the following questions:

a) What are the available methods for reliably predicting discharge time series for Mapula Kapi HPP site?
b) Based on available data, which is the most suitable method for predicting discharge time series for Mabula Kapi HPP site and how can it be applied?
c) Based on available data, which is the most suitable open-source rainfall-runoff model to be used for simulation of discharge time series for Mabula Kapi HPP site?
d) Based on the predicted discharge time series, what would be the design flood and design discharge for proposed Mabula Kapi HPP?
e) What is the anticipated impact of climate change on Mabula Kapi HPP site?

f) What would be the energy yield for a climate resilient plant at Mabula Kapi site?

1.5 Significance of the Study

The study will contribute to the development of renewable energy in Zambia. Small hydropower plants like Mabula Kapi are widely considered to be renewable due to their anticipated minimal impacts on the environment. However, the lack of reliable hydrologic data on several hydropower potential sites poses a challenge. The study will provide a more complete and reliable hydrologic analysis to predict discharge time series required for design of Mabula Kapi HPP. It will also help to assure technical and financial viability of the power plant through consideration of future climate impacts.

2 Chapter Two: Literature Review

2.1 Mabula Kapi site attributes

Mabula Kapi site is located on Kaombe River, in the Central Province of Zambia on latitude 13º 19' 28.02" and Longitude 30º 47' 14.02" in WGS84 coordinate system. The location of the site is illustrated in Appendix 5. The project site can be accessed from Serenje district by road on a total distance of 121 Km, out of which 83Km is on a bituminous paved road, 25Km is on a gravel road and the last 13Km is on an earth road. The site is in Chieftainess Serenje Chiefdom (ZESCO, 2018).

Prefeasibility studies established that construction of the proposed Mabula Kapi HPP would be technically feasible with a minimum power installed capacity of 7.4MW and an average annual energy of 34 GWh. In terms of power evacuation, it was proposed that the power generated from the proposed Kaombe HPP be evacuated through a 22Km double circuit line from the proposed Kaombe HPP to connect into the existing 66kV Pensulo-Lusiwasi line 2.

2.2 Previous hydrological studies at Mabula Kapi site

During the prefeasibility studies conducted by ZESCO Limited in 2018, hydrological data for preliminary conceptualisation of the Mabula Kapi HPP was transposed from a nearby catchment gauging station located on Lusiwasi River. The gauging station catchment is located in Serenje District on station 5-670, at Masase approximately 40 km downstream from Lake Lusiwasi storage reservoir managed by ZESCO Limited (ZESCO, 2018). Discharge time series from November 1965 to September 2015 were used during the study.

In transposing the hydrological data, annual rainfall was considered to be the same for the two catchments because of their geographical proximity and as deduced from rainfall isohyetal maps. The catchment area for Lusiwasi River at Masase was noted to be 1040km^2 while the catchment area for Mabula Kapi site was calculated as 543 km^2 (ZESCO, 2018). Other parameters assumed to be similar included topography, land use and geology. However, similarities were not established in detail and there

was concern over the differences in the drainage network of the two catchments. It was noted that the catchment area for the Masase gauging station had a natural lake in the headwaters of Lusiwasi River. This could potentially affect the flow regime of the river (ZESCO, 2018).

The limitations of the catchment area ratio method were documented during prefeasibility studies and recommendations were made for application of other methods to improve the reliability of the plant at feasibility study stage.

2.3 Hydropower technology

2.3.1 Water dependency

Electricity from water is usually referred to as hydropower. A continuous inflow of water and a difference of height between the water level of the upstream intake of the power plant and its downstream outlet are required to generate electricity (IIT, 2008). Hydropower is dependent on the hydrologic cycle. The key components of the hydrologic cycle include precipitation, evaporation, evapotranspiration, infiltration, overland flow, streamflow, and ground water flow (Bedient, et al., 2013). As a low carbon technology, hydropower is estimated to produce almost two-thirds of the world's renewable electricity generation and will make a significant contribution to achieving the targets of the Paris Climate Agreement and the Sustainable Development Goals (IHA, 2019).

2.3.2 Calculation Hydropower potential

a. Formula and parameters

The gross head, H_0, at a hydroelectric plant is the difference in water level between the reservoir behind the dam and the water level in the tail race. For run of river plants, this head is determined from the water level in the head tank or forebay. Because of the variable inflow and operating conditions of the plant these levels vary. The effective or net head, H, is the head available for energy production after the

deduction of losses in the conveying system of the plant. The water falling from a high-level source drives turbines, which in turn drive generators that produce the electricity. The hydraulic power is given by

$$P = \frac{\eta p g Q H}{1000} \ (KW) \qquad \text{Equation 2-1}$$

where η is the turbine efficiency, p the density of water, g is the acceleration due to gravity and Q is the flow rate (in m^3/s) under a head of H (m). The hydraulic efficiency of the plant is the ratio of net head to gross head, and the overall efficiency is equal to the product of the hydraulic efficiency and the efficiency of turbine and generator. The installed capacity of a hydro power plant is the maximum power which can be developed by the generators at normal head with full flow. The unit of electrical power is the kilowatt, and that of the electrical energy, defined as the power delivered per unit time, is the kilowatt-hour (kWh) (Novak, et al., 2007).

b. Energy modelling using software

Hydropower simulation models can be used to compute power and energy outputs. Open-source models are available on the market. RETScreen is one such hydropower energy modelling software freely available for users. RETScreen is a clean energy awareness, decision-support and capacity building tool. The core of the tool consists of a standardised and integrated clean energy project analysis software that can be used to evaluate the energy production, life-cycle costs and greenhouse gas emission reductions for various types of energy efficient and renewable energy technologies (RETs), including hydropower, solar, wind and bioenergy technologies.

Each RETScreen technology model is developed within an individual Microsoft Excel spreadsheet called a “Workbook" file. The Workbook file in-turn comprises a series of worksheets. These worksheets have a common look and follow a standard approach for all RETScreen models. In addition to the software, the tool includes cost databases which can be used for cost estimates (RETScreen International , 2004).

2.3.3 Design flood estimation

Energy production is not the only concern for hydropower plant developers. Stream flow in the form of floods is also a potential threat to all structures built in rivers. Thus, hydrological investigation must address not just water availability for production, but also frequency and severity of floods so as to design flood protection and control into the hydropower scheme (ESHA, 2004).

For medium and low hazard dams such as weirs, the requirements often specify that the spillway capacity shall exceed the peak flow of a flood with a specific return period, typically between 100 and 1000 years.

The requirements for estimating design floods are usually specified in national legislation or industry guidelines, and distinguish between high, medium and low hazard structures. Typical design flood requirements are given in Table 2-1.

Table 2-1: Typical design flood requirements

[Source: *(ESHA, 2004)]*

Structure	**Design Flood**
High Hazard	Maximum Inflow Design Flood: PMF, Probable Maximum Flood or similar. Alternatively, 10.000-year flood Normal Operation Design Flood: 1000-year flood.
Medium Hazard	100- to 1000-year flood
Low Hazard	Typically, 100-year flood although in some countries no formal requirements exist.

There are basically two methods of estimating a design flood (ESHA, 2004):

- Statistical analysis of stream flow records
- Hydrological modelling of the catchment area

The statistical analysis is used for less important structures that would not cause severe consequences downstream, to life and society, whereas hydrological modelling is required for more important and potentially dangerous large dams in case of failure. The object of the hydrological modelling is to estimate a Probable Maximum Flood (PMF), or similar, to be used for dam and spillway design. Frequency analysis is basically a statistical method to calculate the probability of an event based on a series of historical events (ESHA, 2004).

The estimation of the return period of flows is based on records of annual maximum flows. The annual maximum flows or peak flows are derived from records of mean daily discharge (Wilson, 2011). For the evaluation, a probability distribution that fits to the phenomenon should be chosen.

Use of probability distributions in flood estimation

A probability distribution describes the behavior of random variables. Every possible outcome of an experiment is given a numerical value according to a discrete probability mass function (PMF) or a continuous probability density function (PDF). Many continuous PDFs are used in hydrology and flood estimation, but the most common are the normal, lognormal, gamma (Pearson type 3), log-gamma (log Pearson type 3) and the extreme value (EV) family of distributions (Bedient, et al., 2013). Such distributions can be evaluated using a frequency factor K, which may be a function of other distribution parameters such as skewness.

The most common means used in hydrology to indicate the probability of an event is to allocate a return period, or recurrence interval, to the event. An annual maximum event has a return period of T years if its magnitude is equaled or exceeded once, on the average, every T years. The reciprocal of T is the exceedance probability of the event—that is, the probability that the event is equaled or exceeded in any one year.

For a given return period, the magnitude of a flood x can be found using the following equation (Bedient, et al., 2013):

$$x = \bar{x} + z.S_x \qquad \textit{Equation 2-2}$$

Where

x = Magnitude of a flood

$\bar{x}$ = Mean value of annual flood record

z = Frequency factor K for a given distribution and return period

S_x = Standard deviation of the annual flood record

For the normal, lognormal, gamma (Pearson type 3), log-gamma (log Pearson type 3) the frequency factor K, may be calculated using statistic tables found in virtually every statistics text.

Generally, log Pearson 3 is widely recommended for flood estimation as it allows for non-symmetrical probability distributions around the mean value, which is often the case in hydrology, however the lognormal and the Weibull (gumbel) distributions are also widely used.

Typically, In the graphical method, the annual maximum floods are arranged in order of size and then plotted on probability paper applicable for the desired distribution. The ordinate represents the flood value and the abscissa represents the probability. The data are expected to fit, as close as possible, to a straight line. In this case the graph can be used for interpolation, extrapolation or comparison purposes. In cases of extrapolation, the effects of errors may be magnified and caution needs to be exercised.

2.3.4 Climate resilient design of hydropower scheme

a. Climate risk assessment

Hydropower plants have traditionally been designed using historical data (IHA, 2019). Since a single instantaneous measurement is not useful for designing the plant, discharge time series with a minimum period of 15 years would typically be used to

in the design (Fitchner, 2015). However, in designing a hydropower scheme the engineer needs to identify and apply modern best practices which will consider climate risk. For example, the International Hydropower Agency (IHA, 2019) has published a climate resilient guide to assist engineers to address climate risk. The guide also seeks to evolve from the default use of historical data, the assumption that hydrological variability will remain the same over the lifetime of a project and the limited knowledge of how best to access, use and interpret climate change modelling and observed climate data. The conventional approach neglects to consider the short- and long-term impacts that climate change may have on investments due to the high uncertainty inherent to actual climate change predictions (IHA, 2019).

The World Bank Group also provides data on its online climate knowledge portal (World Bank, 2022). Engineers can use data provided on the website to analyze long-term historical data on temperature and precipitation. They can also access climate data projections for temperature and precipitation which can be used to carry out sensitivity analysis for planned hydropower projects. Such modern guidelines need to be applied to the design of small hydropower plants to ensure sustainability and viability.

The need to qualitatively assess whether climate change may have a significant influence on the project cannot be overemphasized. The assessment can be done by focusing on project performance metrics that may not be achieved or risk thresholds that could potentially be exceeded. Table 2.3 shows the questions which need to be answered to assess whether a climate risk assessment is necessary (IHA, 2019).

Table 2-2: Questions to assess the need for a climate risk assessment

[*Source: (IHA, 2019)]*

Could a change of the hydrological regime significantly affect the hydropower project's economic viability?	Yes/No
Could a change in the hydrological regime affect service continuity/access to electricity in the region it serves?	Yes/No
Could any of the performance metrics for the project be unachievable by potential climate change effects?	Yes/No
ecosystems?	Yes/No

Table 2-2 Continued

Would a breach of the project's main dam or other associated infrastructure have significant adverse consequences on downstream populations, strategic infrastructure or protected ecosystems?	Yes/No

If the answer to at least one question is yes, it is necessary to undertake a climate risk assessment. This involves applying climate change projections in risk assessment.

b. Climate change projections

Historical data, whether local ground observations or global gridded datasets, describes local historical behavior of rainfall, temperature and other relevant hydro-climatic variables, and also indicates trajectories to inform expectations for the future. On the other hand, climate change projections from experiments performed with General Circulation Models (GCMs) and Regional Climate Models (RCMs) provide insight into behavioral changes that the climate might undergo in a future of ocean atmospheric processes affected by warmer ambient temperatures. Future emission scenarios can be derived from GCMs. The International Panel on Climate Change (IPCC) of the United Nations provides a range of greenhouse emission scenarios. In the fifth and sixth IPCC assessment reports these scenarios are knows as Representative Concentration Pathways (RCPs) and Shared Socioeconomic Pathways (SSPs) respectively. These pathways are identified by their approximate total radiative forcing at 2100 relative to 1750 (New Zealand Government, 2018):

a) 2.6 W m-2 for RCP or SSP 2.6
b) 4.5 W m-2 for RCP or SSP 4.5
c) 6.0 W m-2 for RCP or SSP 6.0
d) 8.5 W m-2 for RCP or SSP 8.5

These RCPs or SSPs include (New Zealand Government, 2018):

a) One mitigation pathway (RCP/SSP 2.6, which requires removal of some of the carbon dioxide presently in the atmosphere)

b) Two mitigation pathways (RCP/SSP 4.5 and RCP/SSP 6.0)
c) One pathway with very high greenhouse concentrations (RCP/SSP 8.5)

The processes undertaken in making climate projections include (IHA, 2019):

a) Establishing a consistent baseline against which to measure potential changes to future system performance, with the understanding from the historical observations and climate change projections. In most cases, the baseline would be the hydro-meteorological conditions of the most current 30-year period.
b) Reviewing the latest Intergovernmental Panel on Climate Change (IPCC) ensemble of climate projections. For regionally-specific climate change projections, a number of sources are available, including the World Bank Climate Change Knowledge Portal (CKP).
c) Reviewing climate change projections of relevant variables, such as the annual averages, seasonal variability, or changes in monthly maximum and minimum values of precipitation and temperature. As a minimum, two different Representative Concentration Pathways (RCPs) or Shared Social Economic Pathways (SSPs) need to be considered. For example RCP or SSP 2.6 (optimistic) and RCP or SSP 8.5 (pessimistic)). A minimum of two future 30-year time periods (most relevant to the project and asset lifetime) is also recommended for assessment of climatic projections.

2.4 Hydrologic elements supporting hydropower

2.4.1 Hydrologic cycle

Hydropower is dependent on the natural hydrologic cycle. The elementary components of the cycle include precipitation, evapotranspiration, infiltration, overland flow, streamflow, and ground water flow. For any hydrologic system, a water budget can be established to account for various pathways and storage components (Bedient, et al., 2013). The hydrologic continuity equation for any system can be written as

$$I - Q = \frac{dS}{dt} \qquad \textit{Equation 2-3}$$

Where

$I =$ inflow in volume/time

$Q =$ outflow in vol/time

$\frac{dS}{dt}$ = change in storage in vol/time

It can be understood from the above equation that the difference between accumulated inflow and outflow at any time represents detention storage volume that is eventually released from storage (Bedient, et al., 2013). This concept can be applied to small or large catchment areas. An overall water budget for a given catchment can be written as a conceptual mathematical model in units of depth (mm) as follows

$$P - R - G - E - T = \Delta S$$

Where

$P =$ precipitation

$R =$ surface runoff

$G =$ ground water flow

$E =$ evaporation

$T =$ transpiration

$\Delta S =$ change in storage

It should be noted that infiltration I is a loss to the surface system and a gain to the ground water. It thus cancels out from the overall budget (Bedient, et al., 2013).

2.4.2 Rainfall-runoff processes

Hydropower technology is depended on streamflow, a product of rainfall-runoff processes. In the rainfall-runoff processes, input rainfall is distributed into various components of evaporation, infiltration, detention or depression storage, overland flow, and eventually streamflow (Bedient, et al., 2013). The hydrologic response to rainfall is governed by catchment or watershed characteristics.

A hydrologic catchment or watershed can be defined as a continuous area that drains to an outlet, such that precipitation that falls within the area runs off through that single outlet. The boundary of the catchment area is defined by ridges below which the waters within the catchment flow through a network of streams and rivers and basins to the single outlet. Catchments are often characterised by one main channel and by tributaries that drain into a main channel at one or more confluence points (Bedient, et al., 2013). Factors that influence the hydrologic response of a catchment include:

a) Rainfall intensity and pattern
b) Areal distribution of rainfall over the catchment
c) Duration of the storm event
d) Size of catchment
e) Shape of catchment
f) Slope of the land and main channel
g) Soil type
h) Storage detention in the catchment
i) Land use
j) Land cover
k) Drainage network

The land surface condition can affect hydrologic processes such as runoff and evapotranspiration. A geographical information systems (GIS) map of the land use and associated cover is an important descriptor of the hydrology, whether it is vegetative, such as pasture or forest, or the surface is modified with asphalt or concrete pavement. Land use and land cover GIS data are compiled for many applications and may be useful for hydrologic modeling (Bedient, et al., 2013).

During a rainfall event, hydrologic processes such as infiltration, depression storage, and detention storage must first be satisfied before surface runoff begins. As the depth of surface detention increases, overland flow may occur in some portions of the basin. Water eventually moves into small channels, and finally to the main stream of the catchment. Some of the water may infiltrate the soil and move laterally through the upper soil zones until it enters a stream or channel. This portion of runoff is called interflow or subsurface stormflow. Some precipitation may percolate to the water

table usually several meters below the ground surface, and contribute to a stream or river as base flow if the water table intersects the stream channel (Bedient, et al., 2013).

2.4.3 Catchment area delineation

Advances in GIS have paved way for computer-based catchment area delineation. GIS is a computerised system used to capture, retrieve, analyse and display spatial data. Data is captured by many ways including remote sensing using satellite and airborne platforms (Johnson, 2009).

Digital Elevation Models (DEM) are a type of data set generally produced by photogrammetry techniques but also through interpolation of elevation data (Bedient, et al., 2013).A DEM is basically a raster data set of elevation. One of the freely available DEM is the Shuttle Radar Topography Mission (SRTM) DEM which is accessible at 90m and 30m resolution. The resolution of a DEM is the area of land represented by a single grid cell. A DEM can be used for delineation of hydrologic catchments. Common GIS software use the following steps for delineation of catchments (Johnson, 2009)

a) DEM reconditioning - imposes linear features onto the elevation data
b) Fill sinks - ensure that water has drainage to an outlet
c) Flow direction - upstream to downstream
d) Flow accumulation - accumulated number of cells upstream from a given cell
e) Stream definition - stream path begins at a set area upstream
f) Stream segmentation - segments between junction nodes
g) Catchment grid delineation - assigns grid cells to a catchment
h) Catchment polygon processing - defines the catchment boundary

There is several GIS software that can be used to delineate catchments. These include ArcMap, Global Mapper, Mike Hydro and Quantum GIS (QGIS).

2.5 Streamflow

The accuracy of stream prediction for ungauged sites is greatly enhanced if on-site (observed) data is available. If appropriate stream flow time series cannot be found, discharge should preferably be measured directly for at least a year (ESHA, 2004). A new gauging station may need to be installed on an ungauged river to derive reasonable time series.

2.5.1 Stream flow gauging stations

Streamflow gauging stations are facilities used by hydrologists to determine the rate of flow or discharge in streams or rivers. Discharge at a gauging station is determined through measurement of the river cross-sectional area and the mean velocity of the water through it (ESHA, 2004). A relationship between measured discharge and the water level at the gauging station must be established. The relationship is established by taking several discharge measurements covering the whole range of anticipated water levels or gauge heights at the gauging station. The relationship between discharge and water level or stage is known as a rating curve.

2.5.2 Rating curves

Rating curves are relations used to model discharge as a function of one or more variables (Rainville, et al., 2016). Discharge ratings for gauging stations are usually determined empirically by means of discharge measurements made in the field (World Meteorological Organization , 2010) . Based on such measurements, a rating curve is developed by balancing it through a scatter- plot of the measurements (Tilrem, 1997). In computing the stage discharge relation, mainly two types of equations are used, namely the power equation and the square equation. The power equation is widely used for fitting stage discharge data while the square equation is more suitable for extrapolation purposes (Boiten, 2003). The power equation can be written as follows:

$$Q = a(h_w - h_0)^b \qquad \textit{Equation 2-4}$$

Where

$Q = discharge\ \left(\frac{m3}{s}\right)$

$h_w = measured\ water\ level\ (m)$

$h_0 = water\ level\ for\ Q = 0$

$a, b = station\ parameters$

Logarithmic transformation of the power equation gives

$log\ Q = \log a + b \log(h_w - h_0)$

Substituting $Y = \log Q,\ \ a_0 = \log a\ \ and\ X = \log(h_w - h_0)$ gives

$Y = a_0 + b\ X$ *Equation 2-5*

Then parameters a_0 , $a\ and\ b$ can be calculated using the following relationship:

$\sum Y = \ a_0\ .N + b\ .\sum X$ *Equation 2-6*

$\sum XY = \ a_0\ .\sum X + b\ .\sum X^2$ *Equation 2-7*

Equations (2-7) and (2-8) are collectively referred to as the least squares method, where N is the number of data. Substitution of the values found for $\boldsymbol{h_o}$, **a** and **b** in the power equation (2-5) yields the mathematical model of the rating curve (Boiten, 2003).

Excel solver, an add-in available in excel can also be used to solve complex mathematical relationships. It has the capability to optimize linear as well as nonlinear equations by changing specified parameters. Excel solver consists of a linear programming solver (LPS), a generalized reduced gradient (GRG) solver, and an evolutionary solver which optimises nonlinear equations. Since rating equations are basically of nonlinear form, GRG nonlinear solver and evolutionary solver may be

used to obtain the optimum values of rating curve parameters (Alam & Mohammad, 2018).

Sufficient information is required to justify the level of complexity assumed in any rating structure. Generally, the size of the measurement sample should be twice as large as the number of parameters that have to be calibrated in any rating. More specifically:

a) For each rating segment, the parameters $\boldsymbol{a}$, $\boldsymbol{b}$ and $\boldsymbol{h_o}$ from the power equation should be calibrated using at least 6 measurements (Rainville, et al., 2016).

b) Any *transition* between segments corresponds to a single parameter which should be defined using at least 2 measurements (Rainville, et al., 2016).

The number of measurements used to establish a rating curve is not the only important factor during its calibration. The sample distribution and other site observations are as important as the number of measurements available. Measurements should be evenly spread over the entire range of the rating, ensuring that each segment and transition is defined by sufficient and significant information (Rainville, et al., 2016).

The procedure for establishing the discharge rating curve can generally be summarized as follows (Tilrem, 1997):

a) Plot all discharge measurements on ordinary arithmetic scale, with the gauge height on vertical scale and the discharge on horizontal scale

b) A curve is fitted to the data points by visual estimation. If the curve is fit manually, a method known as series of differences is used to smooth/fit the curve until the rating curve is of a fairly regular shape.

c) The water level for stage of zero flow, h_0 is determined using a suitable method. Various methods can be used to determine h_0. Available methods include graphical, arithmetic, and various parameter optimization techniques.

   One arithmetic method requires that a curve be plotted between Q and h and three values of discharge Q_1, Q_2 and Q_3 be selected from the curve so that $Q_2^2 = Q_1Q_3$. If the corresponding values of the stages are h_1, h_2 and h_3, then it can be verified that:

$$h_0 = \frac{h_1 .h_3 - h^2}{h_1 + h_3 - 2h_2}$$ *Equation 2-8*

Apart from graphical and arithmetical methods, various optimization techniques can be used to obtain the best value of h_0. The value of h_0 can be determined by trial-and-error method (Subramanya, 2008).

d) After determination of h_0, values of Q against $h_w - h_0$ are plotted on a log-log graph and they will lie approximately in a straight line between shifts in control (Boiten, 2003).

e) When the curve has been found acceptable, the mathematical equation for each straight-line segment is calculated. The mathematical equation is referred to as a rating equation.

f) Finally, each straight-line segment is tested for biasness and goodness of fit. One common statistical method for testing biasness is the student paired t-test.

The student's paired t-test of the differences between the measured discharge and the discharge estimated by the rating curve is used to check whether a rating curve on an average basis, gives significant overestimates or under estimates as compared with the discharge measurements on which the curve is based (Tilrem, 1997). A few statistical parameters need to be computed to apply the student's paired test. A percentage deviation of each discharge measurement from the estimated discharge by the rating curve, is first computed, after which is calculated the standard deviation and the standard error of the percentages (Tilrem, 1997).

Thus, the percentage deviation is

$$P = \left(\frac{Q_m - Q_r}{Q_r}\right) * 100\%$$ *Equation 2-9*

the percentage standard deviation then is

$$S_D = \left(\frac{\sum (P - \bar{P})^2}{n-1}\right)^{1/2}$$ *Equation 2-10*

and the percentage standard error is

$$S_E = \frac{S_D}{n^{1/2}}$$ *Equation 2-11*

where

Q_m = measured discharge (m^3/s),

Q_m = discharge estimated by the rating curve (m^3/s),

P = percentage deviation,

$\bar{P}$ = mean percentage deviation,

S_D= standard deviation of the percentage deviation p

S_E= standard error of the percentage deviation p

n = number of discharge measurements

A test statistic t, to be used for the student's t-test is then computed from the following relationship:

$$t = \frac{\bar{P}}{S_E}$$ *Equation 2-12*

The calculated values of t are then compared against t values from tables of t-distribution, to determine biasness in terms of levels of significance. Tables of the t-distribution giving values of t for different levels of significance are virtually available in every statistics text book. On the other hand, the quality of fit of the rating curve can be assessed by the coefficient of determination, the so-called r-squared value (DeCoursey, 2013). This can be calculated using the equation:

$$r^2 = 1 - \frac{SSE}{SST}$$ *Equation 2-13*

where SSE is obtained by evaluating each of the error terms and then computing a numerical value for the sum of squares of the errors using the formula

$$SSE = \sum_{i=1}^{n}[y_i - f(x_i)]^2$$ *Equation 2-14*

and SST represents the sum of the squares of the deviations about the mean

$$SST = \sum_{i=1}^{n}[y_i - y]^2 \qquad \textit{Equation 2-15}$$

where

y = log Q (m^3/s)

x= log ($h_w - h_o$) in metres.

The r-squared value varies between 0 and 1. Note that r^2 will equal 1 when SSE equals zero. Hence, an r^2 value close to 1 (which means that the sum of the square errors is small) generally indicates a good fit.

2.6 Prediction of Discharge for poorly gauged sites

Lack of sufficient hydrological data at many hydropower potential sites presents a real challenge in establishing viability of hydropower plants. To establish if a scheme will be viable, it is necessary to begin by evaluating the water resource existing at the potential hydropower site. The energy potential of the scheme is proportional to the product of the discharge and the head. Except for very low heads, the gross head can usually be considered as constant, but the flow varies over the year. To select the most appropriate hydraulic equipment and compute the sites energy and power, a flow-duration curve is typically used (ESHA, 2004). A single measurement of instantaneous flow in a stream cannot be used to establish viability of a hydropower plant. Various methods and techniques can be applied to predict streamflow at poorly gauged sites. These vary from simple methods that can only be used for preliminary estimates of power potential to complex methods that may be used to establish technical and financial viability.

2.6.1 Statistical and Empirical Methods

a. Mean annual flow method

One of the simple methods used at early stages for evaluation of flow and power potential at ungauged sites is the determination of the mean annual flow (Q) using the average annual runoff depth (AARD) and the site's catchment area (Jha & Smakhtin, 2008). The difference between standard average annual rainfall (SAAR) and actual evaporation (AE) is assumed to be equal to the AARD (ESHA, 2004), while actual evaporation (AE) is estimated from potential evaporation (PE). The mean annual flow (Q) estimated using the AARD and the catchment area can be used to estimate the power potential. Although the mean annual flow gives an idea of a river's power potential, a firmer knowledge of the river's flow regime, as obtained from a flow duration curve, is needed (ESHA, 2004).

b. Catchment area ratio method

The area ratio method is one of the simplest methods used to predict streamflow at poorly gauged sites (Nruthya & Srinivas, 2015). It involves the use of hydrological data from a gauging station with sufficient discharge time series which is located on the same river or a nearby river (Fitchner, 2015) . The data is transposed to the ungauged site by using the ratio between catchment areas. In some cases, the ratio between the average annual rainfall may also be used if the sites receive different amounts of rainfall. However, this method does not consider a number of factors (Yilmaz & Onoz, 2020). These include site geology, soil type, land use and vegetation which have a significant influence on the unique flow characteristics (Fitchner, 2015). It may be difficult to establish similarities of these aspects between the gauged catchment and the ungauged catchment.

c. Simultaneous Flow Measurement

A temporary gauging point (so-called control profile) is established at a point of interest (intake location or its vicinity) along the river, usually upstream of an existing gauging station. The two points are measured simultaneously considering that the same weather conditions prevail at the two sites. Measurements of the control profile (temporary station) with those of the gauging station can then be correlated. In other cases, a new gauging station at a point of interest (intake location or its vicinity) along a river may be compared with an existing gauging station in a nearby catchment with similar hydrological and meteorological conditions (INSHP, 2019). The two points can be measured simultaneously considering that the same weather conditions prevail at the two sites. Measurements of the new gauging station can then be correlated with those of the existing gauging station. Next, historical hydrological data with sufficient time series are transposed from the existing gauging station to the proposed intake. To cover all flow conditions, measurements must be undertaken during dry and wet periods. The more simultaneous measurements there are, the better the accuracy of the correlation (Fitchner, 2015).

Correlation is a measure of the strength of association between two random variables, say x and y. Correlation coefficients are one class of measures that can be used to determine this association between the variables (Helsel & Hirsch, 2002). It is assumed for this analysis that x and y are related linearly, so the usual correlation coefficient gives a measure of the linear association between x and y. This is calculated as (DeCoursey, 2013)

$$r = \frac{\sum_{i=1}^{n}(x_i-\bar{x})(y_i-\bar{y})}{\sqrt{\sum_{i=1}^{n}(x_i-\bar{x})^2(y_i-\bar{y})^2}} \qquad \textit{Equation 2-16}$$

Here r reflects the extent of the linear relationship between the two variables y and x. For a perfect correlation, r is equal to 1.0. However, a value of r between 0.6 and 1.0 is generally considered a good correlation (Subramanya, 2008).

d. Relationship between specific runoff and attitude

Another approach used to empirically predict discharge for ungauged sites is to derive a relationship between specific runoff [l/s/km2] and average catchment area altitude. Data from several gauging stations and control profiles in the area are used to generate a regional function or curve. This method is based on the idea that, the higher the catchment area, the more expected runoff per km². After average flow (MQ) is determined, the value is compared to the MQ at the next gauging station and the correlation is determined, then historical hydrological data can be transposed to the intake. The accuracy of hydrological data obtained by this method depends on the accuracy of data used to prepare the regional function and the method used to the average height of the catchment area (Fitchner, 2015).

2.6.2 Rainfall-runoff models

Advances in computer methods have made the use of simulation models possible in hydrology and hydropower planning. Many hydrologic models are available which can be used for catchment rainfall-runoff simulation (Bedient, et al., 2013). Computer modelling offers a solution to investigate hydrological processes and make predictions on what the flow might be in a river given a certain amount of rainfall. There are different types of models, with differing amounts of complexity (Davie, 2008). Although there are many ways to classify models, not all models fit into a one category because they are developed for a variety of purposes (Singh, 1995).

Hydrologic models may be classified as empirical, conceptual, and physical (Sitterson, et al., 2017). Each type calculates runoff differently. Researchers use different ways to classify and divide models based on spatial resolution, input/output type, model simplicity, etc. The models can further be classified based on the spatial interpretation of the model's catchment area separating them into lumped, semi-distributed, and distributed models (Sitterson, et al., 2017).

In a lumped model, parameters do not vary spatially with the basin and response is only evaluated at the outlet, without explicitly accounting for the response of individual subbasins. In a semi-distributed model parameters are partially allowed to

vary in space by dividing the basin into several smaller subbasins. The advantage is that the structure is more physically based than lumped models. In a distributed model, parameters are fully allowed to vary in space at a resolution chosen by the user. The model attempt to incorporate data including spatial distribution of parameter variation together with computational algorithms (Eldho, 2015). Semi-distributed models are therefore less demanding on input data than distributed models.

Based on characteristics that need to be studied, the objectives to be met and the funds available, the Engineer should make a choice of the available simulation models. The selection of the model will also depend on the study objectives, catchment characteristics, availability of data and the project budget. Some models require inputs data such as rainfall, infiltration, evaporation, evapotranspiration, physiography, land use, reservoir data, terrain data and streamflow. A model will need to be calibrated to get good results. Model calibration and verification is extremely important in fitting the model parameters and producing accurate results. Model calibration involves selecting a measured set of input data. The controlling parameters are adjusted until a "best fit" is obtained between observed and simulated data (Bedient, et al., 2013).

The relationship between simulated and observed data is measured by a number of statistical goodness-of-fit criteria. There are many types of objective functions available but the choice of which to employ is related to the model application. The coefficient of determination, r^2 and the coefficient of efficiency, also referred to as the Nash-Sutcliffe are able to provide a satisfactory assessment of the correspondence between observed and simulated time series. (Mwelwa, 2004). The Nash-Sutcliffe formula can be written as:

$$CE = 1 - \frac{\sum_1^n (y_i - y_{i,simulated})^2}{\sum_1^n (y_i - \bar{y})^2} \qquad \text{Equation 2-17}$$

Where,

CE = Coefficient of efficiency

y_i = Observed values of the variable of interest

$y_{i,simulated}$ = Simulated values

$\bar{y}$ = Mean value of observed values

The coefficient of efficiency is sensitive to systematic errors such as the general over or under prediction between observed and simulated flow, where the r^2 is not (Mwelwa, 2004).

a. Rainfall

Rainfall is the most important input to any hydrological or water resources study (Pitman & Bailey, 2021). However, rainfall data from meteorological station observations are inadequate over many parts of the world, especially in developing countries due to sparse or non-existent observation networks, or limited reporting of gauge observations. As a result, satellite derived rainfall estimates have been used as an alternative or as a supplement to station observations (RMetS, 2018).

Many satellite-derived rainfall products with long time series suffer from coarse spatial and temporal resolutions and inhomogeneities caused by variations in satellite inputs. There are however some satellite rainfall products with reasonably consistent time series, but they are often limited to specific geographic areas. For example, the Climate Hazards Group Infrared Precipitation (CHIRP) and CHIRP combined with station observations (CHIRPS) are recently produced satellite-derived rainfall products with relatively high spatial and temporal resolutions and quasi-global coverage (RMetS, 2018).

Different validation statistics can be used to evaluate the different satellite derived products. These include bias, mean error (ME), mean absolute error (MAE) and correlation coefficient (CC) which can be used for evaluating monthly timescales. The formulae for these statistical measures are indicated in Table 2-4.

Table 2-3: Validation Statistics and formulae

[*Source: (RMetS, 2018)*]

Statistics	**Formula**	**Range**	**Unit**	**Best value**
Correlation Coefficient	$r = \frac{\sum_{i=1}^{n}(G_i - \bar{G})(S_i - \bar{S})}{\sqrt{\sum_{i=1}^{n}(G_i - \bar{G})^2 (S_i - \bar{S})^2}}$	-1 to 1	None	-1 or 1
Mean Error	$ME = \frac{1}{N}\sum_{i=1}^{n}(S_i - G_i)$	-∞ to ∞	mm	0
Mean Absolute Error	$MAE = \frac{1}{N}\sum_{i=1}^{n}\lvert(S_i - G_i)\rvert$	0 to ∞	mm	0
Bias	$Bias = \frac{\sum S}{\sum G}$	0 to ∞	None	1

Where,

G =gauge rainfall measurements

$\bar{G}$ =average of the gauge measurements

S =satellite rainfall estimate

$\bar{S}$ = average of the satellite rainfall estimates

N =number of data pairs

The correlation coefficient r indicated in Table 6-3 is the most used measure of correlation and sometimes it is called the linear correlation coefficient because *r* measures the linear association between two random variables y and x (Helsel & Hirsch, 2002). The square of the correlation coefficient, r^2 is called the coefficient of determination (DeCoursey, 2013). The coefficient of determination is interpreted as the proportion of observed y variation that can be explained by the simple linear regression model (attributed to an approximate linear relationship between two variables y and x). The higher the value of r^2, the more successful is the simple linear regression model in explaining the y variation. When regression analysis is done by a statistical computer package such as excel, r^2 (the percentage of variation explained by the model) is a prominent part of the output. If r^2 is small, an analyst will usually

want to search for an alternative model (either a nonlinear model or a multiple regression model that involves more than a single independent variable) that can more effectively explain y variation (Devore, 2012).

b. Evaporation & evapotranspiration

Several hydrologic computer models use evaporation or evapotranspiration inputs in rainfall-runoff modelling. These are important components in the water balance. Evaporation data may be obtained from meteorological stations as pan evaporation. Evapotranspiration may be estimated from pan evaporation as reference crop evapotranspiration. When pan evaporation is used to estimate the reference crop evapotranspiration, a comparison can be made between the evaporation from the water surface in the pan and the evapotranspiration of the standard grass (Food and Agriculture Organization of the United Nations, 2021).

The Food Agriculture Organization (FAO) has provided an equation known as the FAO Penman -Monteith equation for determining the evapotranspiration from a hypothetical grass reference surface . The equation was derived from the original Penman-Monteith equation and the equations of the aerodynamic and canopy resistance. The FAO Penman-Monteith equation is written as follows (Food and Agriculture Organization of the United Nations, 2021):

$$ET_0 = \frac{0.408\Delta(R_n - G) + \gamma \frac{900}{T + 273} U_2(e_s - e_a)}{\Delta + \gamma(1 + 0.34U_2)}$$

Where

ET_0= Reference crop evapotranspiration [mm/day]

R_n= Net radiation at the crop surface [MJ m^2/day]

G= Soil heat flux density [MJ m^2/day]

T= Air temperature at 2m height [^{o} C]

U_2= Wind speed at 2m height [m/s]

e_s = Saturation vapour pressure [kPa]

e_a= Actual vapour pressure [kPa]

$e_s - e_a$= Saturation vapour pressure deficit [kPa]

Calculations of the reference crop evapotranspiration are usually computerised. A number of software packages use the Penman-Monteith equation to determine the reference crop evapotranspiration. CROPWAT software is an open-source software that is recommended for calculating reference crop evapotranspiration (Food and Agriculture Organization of the United Nations, 2021).

Evapotranspiration can also be determined from pan evaporation. Pan evaporation is measured from standard pans at meteorological stations. The pans are usually made of stainless steel with specific dimensions. The pan is normally installed in a grassy location, away from bushes, trees and other obstacles which may obstruct the natural flow of air around the pan. The result of evaporation and precipitation is usually measured daily within a still well, by means of a high-quality evaporation micrometer. The pans make possible the measurement of the integrated effect of radiation, wind, temperature and humidity on the evaporation from an open water source. Standard pans are used to measure evaporation and in the absence of rain, the amount of water evaporated during a period (mm/day) corresponds with the depth in that period (Food and Agriculture Organization of the United Nations, 2021).

An evaporation pan provides a measurement of the combined effect of temperature, humidity, wind speed and sunshine on the reference crop evapotranspiration ETo. The pan evaporation is related to the reference evapotranspiration by an empirically derived pan coefficient (Eijkelkamp, 2009):

$$ET_O = K_{pan}\ E_{pan}$$

Where,

ET_O= Reference crop evapotranspiration

K_{pan}= Pan coefficient

E_{pan}= Pan evaporation

When using the evaporation pan to estimate ET_O, a comparison is made between the evaporation from the water surface in the pan and the evapotranspiration of the

standard grass. Since the water in the pan and the grass do not react in exactly the same way to the climate, the pan coefficient, K_{pan} is used to relate one to the other. The pan coefficient depends on the type of pan used, the environment, the humidity and the wind speed. Evaporation pans may be provided in different classes. For example, a class A standard pan is 54mm in height and 1026mm in diameter. The K_{pan} for such a pan varies from 0.35 and 0.85, with the average value being 0.70. If the pan factor is not known the average value can be used (Eijkelkamp, 2009).

3 Chapter Three: Methodology

3.1 Selection of suitable prediction methods

Broadly speaking, both statistical and hydrologic modelling can be used for prediction of discharge at Mabula Kapi Site. However, the selection of the specific methods to use depends on several factors. For Mabula Kapi site, the rainfall-runoff modelling method has been selected as the best method for prediction of discharge.

The other methods discussed in section 2.6 have not been selected for accurate prediction of discharge due to the following reasons:

a) The Mean Annual Flow method – While this method gives an idea of a river's power potential, it does not provide a firmer knowledge of the river's flow regime as obtained from a flow duration curve.
b) Catchment Area Ratio method – This method does not consider several factors including site geology, soil type, land use and vegetation which have a significant influence on the unique flow characteristics.
c) Relationship between Specific runoff and Altitude method – This method requires use of data from several gauging stations and profiles in the area to generate a regional function. The scarcity of data in the Mabula Kapi region presents a challenge for application of this method.
d) Simultaneous flow measurement method – In this method, a new gauging station at a point of interest (intake location or its vicinity) along a river may be compared with an existing gauging station in a nearby catchment with similar hydrological and meteorological conditions. Manangwa gauging station (for Mabula Kapi catchment) can be correlated with measurements taken from an existing gauging station in a nearby catchment. Masase gauging station located on Lusiwasi River is located about 30 km away Manangwa gauging station. This station which is managed by ZESCO limited has a discharge time series of over 50 year. The proximity of the two gauging stations and their catchments is shown in Figure 3.2.

   The simultaneous flow measurement method in this case was not selected due to a major difference in the drainage network between the two catchment

areas. The Lusiwasi catchment has a lake in its head waters as shown in Figure 3-1.

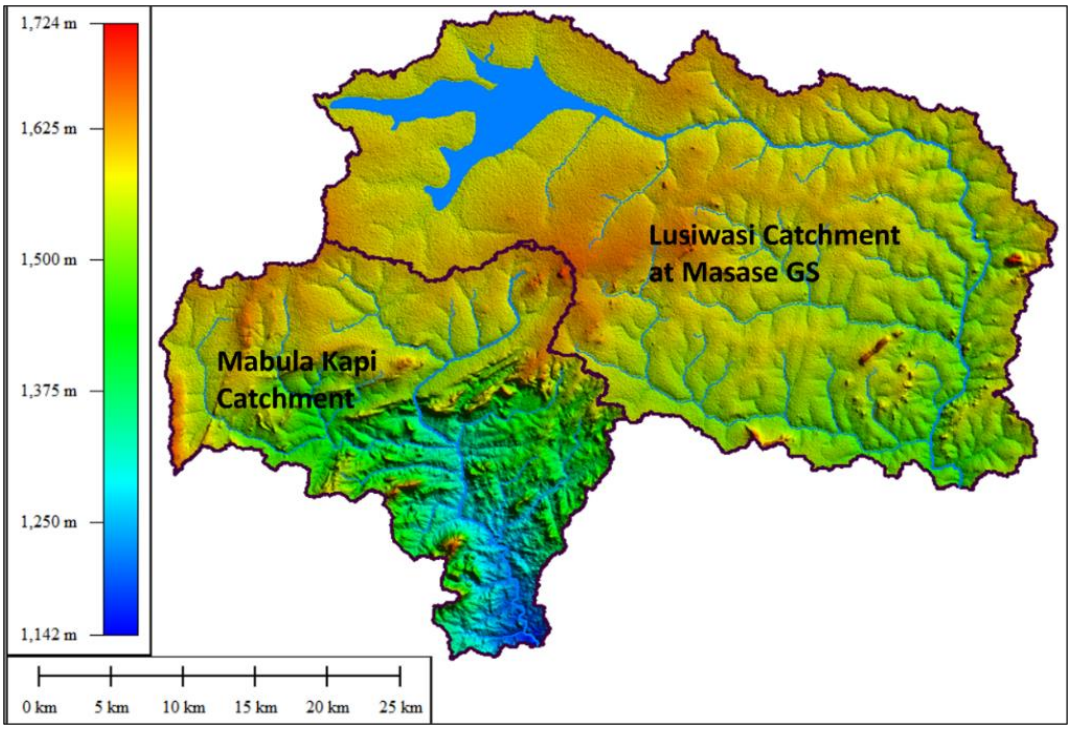

[Source: (ZESCO, 2018)]

Figure 3-1: Proximity of Mabula Kapi and Lusiwasi Catchments

3.1.1 Rainfall – runoff model (PITMAN model)

a. Model definition and structure

Following careful and extensive review of available open-source hydrologic modelling software, the Author selected a model known as the WRSM/PITMAN model for rainfall-runoff modelling of the Mabula Kapi catchment. The model can create a conceptual representation of relevant processes and storages in a hydrologic catchment such as interception, soil moisture capacity, groundwater flow, wetlands, lakes, and attenuation in channel systems. There are currently three versions of the of the model as follows

a) WRSM/Pitman version 2.7 which is a monthly time step version

b) WRSM2000/Pitman version 2.6 which is a daily time step version with limited distribution. It also has the monthly time step but users are recommended to use it only for daily time step analyses and
c) WRSM2000/Pitman version 2.11 which is the latest monthly time step version with enhanced features

WRSM stands for Water Resources and Simulation Model. The WRSM/Pitman model is a conceptual semi distributed model, consisting of storages such as interception, soil moisture and groundwater, linked by functions designed to represent the main hydrological processes at the subbasin scale such as infiltration, excess flow, saturation excess flow, direct overland flow, and ground water flow (Hughes, et al., 2006). The model was initially developed in 1969 and has been subject to several enhancements over the years. There have been various changes to its name over the years. Currently the model is known either as the WRSM2000 model or the Pitman model (Pitman, et al., 2015). WRSM2000 model has been applied to many different hydro climatic regions in Africa (Raphael , et al., 2014).This study will refer to it as PITMAN model.

The Author attended a two-day training course for the PITMAN model in October 2021. Based on knowledge acquired, he proposed to employ version 2.11 of the PITMAN model which is a monthly time step, for general hydrological modelling and simulation of discharge time series. However, for the purpose of flood frequency analysis, the version 2.6 which is a daily time step was adopted. It is important to note that version 2.6 employs the same time series of monthly catchment rainfall as used by the monthly model. The daily time step model was designed to generate daily flows using as input daily and monthly rainfall and average monthly potential evaporation. The structure is similar to that of the monthly time step. (Pitman, et al., 2015).

The PITMAN model is of a modular construction (running under Windows), with five different types of modules linked by means of routes:

a) The Runoff module
b) The Reservoir module
c) The Irrigation module
d) The Channel module

e) The Mining module

The runoff module is said to be the of heart the PITMAN model. This module uses various input data including climate data to simulate runoff. The reservoir module is applied if the river network has a reservoir such as a large dam or a small network of farm dams. The irrigation module is used if the river network contains irrigation systems that demand or abstract water from the river network. The channel module is used to link abstractions, return flows as well as other modules. It can also be used to include wetlands identified in the river system. The Mining module is used to include mines, if they are part of the river network (Pitman, et al., 2015).

The PITMAN model has been selected for the following reasons:

a) It is an open-source application
b) It can be used to extend natural flow records as far as rainfall records allow
c) It can be used to calibrate flow records taking land-use changes over time into account
d) It can be used to simulate flows for present or future conditions
e) It can be used estimate flows in ungauged catchments by transferring parameters
f) Input data required for the model is readily available
g) Model developers are available to provide virtual training workshops
h) It is user friendly
i) It has been used throughout South Africa, Southern Africa Development Community (SADC) countries and even in certain overseas countries

Each of the 5 modules in the PITMAN model contains one (or offers a choice between more than one) hydrological models that simulate a particular hydrological aspect. The modules are linked to one another by means of routes. A connection of different modules, together with the routes, form a network. By choosing and linking several modules carefully, virtually any real-world hydrological system can be represented. The first step in simulating any hydrological system is to set up the network of modules and routes to represent this system. The PITMAN model allows for large networks to be created and offers interactive creation and editing of all modules, routes and networks. The program supports the user by means of extensive error checking (Pitman, et al., 2015).

The PITMAN model simulates flows in a catchment and allows for a comparison of simulated flows against observed flows. The user can analyse statistics and graphs of various water resource parameters and manipulate calibration parameters to achieve a good 'fit' between observed and simulated flows.

b. Runoff module

The runoff module is the most critical module of the PITMAN model. The main inputs and drivers of streamflow in the runoff module are:

a) Catchment area
b) Rainfall
c) Pan evaporation
d) Calibration parameters

Land use and water use in the catchment is defined by afforestation, alien vegetation and paved areas. The model requires substantial manipulation of the rainfall data prior to use.

PITMAN model applies several calibration parameters which govern the amount, rate and timing of the runoff generated. It initiates the first simulation with default parameters which the user can change to match or calibrate the simulated and observed flows as closely as possible. The calibration parameters are listed in the Table 3-1.

Table 3-1: Calibration parameter description

[*Source: (Pitman, et al., 2015)*]

Parameter	**Description**	**Unit (If applicable)**
POW	Power in the soil moisture / subsurface flow equation	-
SL	Power in the soil moisture recharge equation	-
ST	Soil moisture capacity	Mm

Table 3-1 Continued

Parameter	Description	Unit (If applicable)
FT	Sub-surface flow at full soil moisture capacity	-
GW	Maximum groundwater flow	mm/month
HGGW	Maximum soil moisture recharge	-
ZMIN	Minimum catchment absorption rate	mm/month
ZMAX	Maximum catchment absorption rate	mm/month
PI	Interception storage	mm
TL	Lag of flow (excluding groundwater)	-
GL	Lag of groundwater flow	-
R	Coefficient in the evaporation / soil moisture equation	-

c. Detailed description of calibration parameters

A detailed description of the calibration parameters and their influence on runoff generation as explained in the PITMAN model theory manual (Pitman & Bailey, 2012) is given below:

a) Power in the soil moisture / subsurface flow equation (POW)

Determines rate at which subsurface flow (interflow plus groundwater) reduces as soil moisture is depleted. The higher the value means that the subsurface flow will drop more rapidly during periods between rainfall events

b) Power in the soil moisture recharge equation (SL)

Soil moisture level below which all subsurface flow ceases. Below this level the only soil moisture depletion is via evapotranspiration. When this parameter is increased, baseflow will cease more often as SL approaches ST. SL is a parameter which should remain as 0 unless sub-surface flow ceases before soil moisture depleted.

c) Soil moisture capacity (ST)

Soil moisture capacity is the moisture holding capacity of soil. High values of this parameter would result in less surface runoff but increase the potential for more subsurface flow.

d) Sub-surface flow at full soil moisture capacity (FT)

As FT is increased, a greater sub-surface flow will occur, at the expense of evaporation and surface flow, particularly in dry periods. Arid areas will have a value of 0 where baseflow is absent. If a good fit is obtained with a value of near/over 100, this is an unrealistic value and other parameters should be adjusted rather than increasing FT to such a high value.

e) Maximum groundwater flow (GW)

GW (and GL) are only included if we do not achieve sufficiently sustained baseflows throughout the dry season. A value of 0 is not excluding groundwater flow, it is merely lumping it with the other subsurface flow because the time lags (TL and GL) are not sufficiently different to warrant modelling groundwater separately.

f) Minimum catchment absorption rate (ZMIN)

Minimum rainfall intensity required to initiate surface runoff; below this intensity all rainfall is absorbed by the soil. A higher ZMIN value represents less frequent (and less volume) of surface runoff events as it will require a higher intensity to initiate runoff.

g) Maximum catchment absorption rate (ZMAX)

In conjunction with ZMIN, ZMAX determines the average infiltration to soil moisture. A higher ZMAX value will cause a reduction in the volume of surface runoff because the soil is able to absorb more water.

h) Interception storage (PI)

Interception storage is the amount of water which is intercepted by vegetative cover before it reaches the ground and can either run off or infiltrate into the soil. A higher value therefore represents a reduction in the quantity of rainfall available for infiltration.

i) Lag of flow - excluding groundwater (TL)

Lag of surface runoff and subsurface flow from the upper zone (interacts with GW); an increase in this parameter produces a greater delay in the catchment's response to rainfall. This parameter is adjusted primarily based upon the seasonality graph, which easily and visibly shows a in the lag of the streamflow. This parameter will not significantly affect the amount of runoff and is used primarily to adjust the seasonality of flow (where one see's the misalignment of peaks). The user will change this value iteratively until the seasonality of simulated and observed matches.

j) Lag of groundwater flow (GL)

This refers to lag of sub-surface flow in the lower zone. An increase in lag will cause the baseflow in a river to decline more slowly, yielding higher dry season flows.

k) Coefficient in the evaporation / soil moisture equation (R)

R controls the rate at which evaporation reduces as soil moisture is depleted

d. Calculation Procedure

The PITMAN theory manual (Pitman & Bailey, 2012) outlines the steps used in the monthly PITMAN model for calculating runoff each month as follows:

a) Compute runoff from impervious area;

b) Determine interception loss;

c) Synthesize mass curve of rainfall for the month and calculate rainfall for each time step;

a) Subtract interception loss from rainfall;

b) Compute surface runoff;

c) Perform mass balance of soil moisture to determine soil moisture at end of time interval.

d) If soil moisture capacity is exceeded calculate the excess water (SPILL) and apportion it to baseflow (to be lagged by GW) and remaining flow (lag of TL) as per step 9;

e) The quantity SPILL × GW/FT is added to baseflow and the remainder is added to the component to be lagged by TL.

f) Compute the runoff components originating from soil moisture;

g) Accumulate runoff components for the month;

h) After all months have been processed perform the routing (lagging) procedure and combine runoff components to obtain total monthly runoffs and

i) Convert monthly runoffs from depths (mm) to volumes (million cubic metres).

The daily time step PITMAN model (version 2.6) was designed to generate daily flows using daily and monthly rainfall and average monthly potential evaporation as input. The structure is similar to that of the monthly time step with similar calibration parameters. Assumed soil moisture conditions is determined from initial catchment discharge, precipitation is stored as interception and as soil moisture and this is subject to evaporation and transpiration. The quantity of precipitation that is not absorbed by the soil is the source of surface runoff. A portion of the precipitation held as soil moisture percolates into groundwater before entering the river system. The various components are suitably lagged and the total runoff at the catchment outlet is computed on a mass balance basis (Pitman & Bailey, 2012).

The model has been designed to balance the catchment's water budget and to determine the runoff using different time steps. For days during which there is no rain, a one-day time step is used. When a rain-day is encountered, the duration of the fall is computed and the total rainfall is distributed as hourly amounts in order that the water budget may be computed at one-hour time intervals. After cessation of the storm a single time step of n hours is employed, where n = 24 – duration of the rainfall. It is thus evident that the onset of rain is assumed to coincide with the beginning of the day (Pitman & Bailey, 2012).

In terms of interception, vegetation and soil surfaces may be initially dry before a storm and a small amount of moisture is needed to wet these surfaces before runoff and infiltration can occur. This function is represented by assuming an interception storage which must be filled before precipitation is available for infiltration and runoff. Moisture from interception storage is removed at the potential evapotranspiration rate until all moisture is exhausted. Surface runoff it is taken to be

derived from two sources namely: Runoff from impervious areas and Runoff resulting from rainfall that has not infiltrated into the soil (Pitman & Bailey, 2012).

Regarding infiltration, the quantity of water entering storage as soil moisture is simply the residual precipitation after interception and surface runoff have been subtracted. As for evaporation, the algorithms used are identical to those used in the monthly model. Regarding groundwater discharge, numerous trials revealed that the adoption of a single recession constant would not be satisfactory. The model therefore uses a variable recession constant, related to the groundwater storage state, which gives more accurate results (Pitman & Bailey, 2012).

In terms of time delay and attenuation of runoff, the response of the whole catchment is characterised by the processes taking place at a representative location, the components of model runoff may have to be lagged to indicate the runoff at the catchment outlet. Furthermore, surface runoff is subject to attenuation as it moves across the land surface and then through the channel system (Pitman & Bailey, 2012).

In terms of calibration, model developers have provided suggestions on the relationship/conversion between the monthly and daily calibration parameters as shown in Table 3-2 (Pitman & Bailey, 2012).

There are two distinct modes for analysing daily flows as follows in the model:

a) Daily naturalised flow - The user is only interested in the naturalised flows. Naturalised flows are stream flows that could be expected if human-made dams and reservoirs cannot reduce flows during a flood. They are determined by removing the effects of regulation from the historical flow record.
b) Daily streamflow that would occur in a system with various land uses where the user may want to compare simulated streamflow against daily observed streamflow (Pitman & Bailey, 2012).

Table 3-2: Conversion from monthly to daily calibration parameters

[Source: (Pitman, et al., 2015)]

Calibration Parameter	**Monthly**	**Daily**	**Suggested Rule**
POW	2	2	No difference
SL	0	0	Usually, 0

Table 3-2 Continued

Calibration Parameter	Monthly	Daily	Suggested Rule
ST	160	160	No difference
FT	20	0.3	FT (Daly) = 0.024 (= 0.48)
AI	variable	0	
Zmin	999	0	None (range 0-3)
Zmax	999	15	None (range 6 -15)
PI	1.5	1.5	
TL	0.25	5	TL (daily) = 1 + 0.00025 x Area (km2) x TL (monthly model – months) / 0.25
Lag	Not used	0	
GL		10	GL (daily model -days) = 25 x GL (monthly model -months) If Pitman method used otherwise default value
R	0.5	0.5	No difference

3.2 Input Data Processing

3.2.1 Catchment area data

The catchment area at Manangwa gauging station was delineated using global mapper software. It was delineated using a 12.5m resolution digital elevation model downloaded from Alaska Satellite Facility website (NASA, 2021). The catchment area was delineated and calculated as 511km^2 as shown in Figure 3-2.

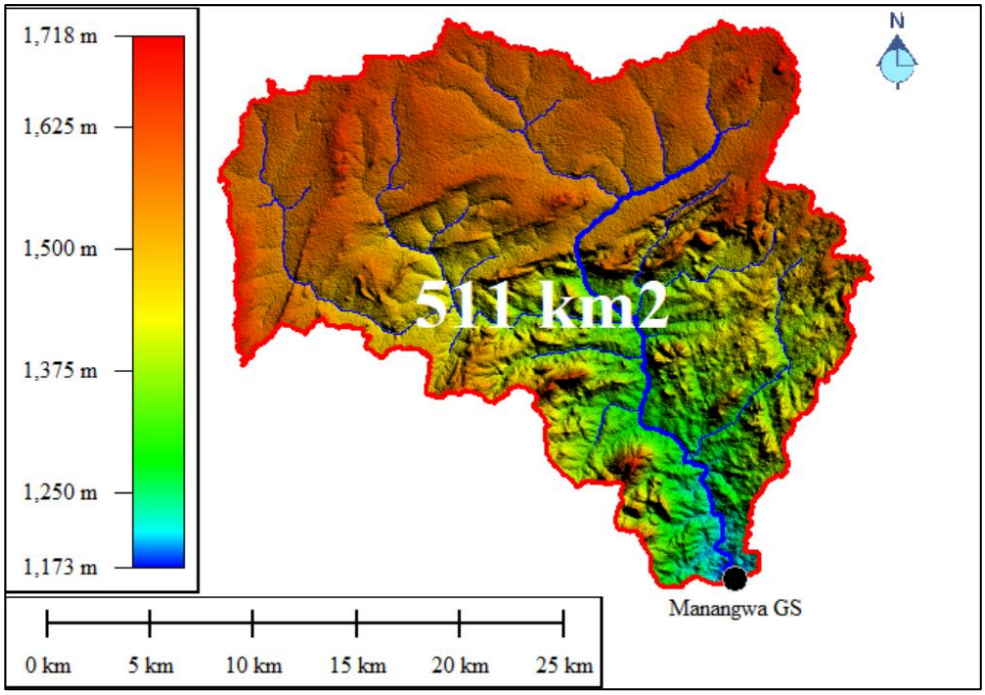

(Source: Author's delineation using Global Mapper software)

Figure 3-2: Delineated catchment for Mabula Kapi

3.2.2 Discharge

Improving the prediction of discharge for Mabula Kapi is heavily dependent on acquisition of on-site streamflow data. The on-site stream flow data collected must be entered and updated regularly to produce a discharge time series for discharge prediction.

a. On-site measurements

KGRTC had employed a gauge reader to take daily water level (stage) readings at Manangwa gauging station following its installation in September 2019. However, discharge measurements only commenced about a year later. KGRTC and the Water Resources Management Authority (WARMA) collaborated to carry out quarterly discharge measurement at the gauging station. The measurements were done using the Acoustic Doppler Current Profiler (ADCP) equipment from WARMA. A record of the discharge measurements undertaken at Manangwa station is indicated in Table 3-3.

Table 3-3: Discharge measurement record at Manangwa

(*Source: KGRTC*)

Quarterly Reading No.	Date	Water level (m)	Discharge (m3/s)
1	28-01-2021	1.400	9.152
2	01-05-2021	1.3	7.433
3	22-07-2021	1.04	3.303
4	01-10-2021	0.87	1.21
5	08-12-2021	0.68	0.58
6	01-02-2022	1.26	5.594
7	17-02-2022	2.51	81
8	15-03-2022	1.54	10.173
9	29-03-2022	1.400	9.153

b. Plotting points and curve fitting

All discharge record measurements were plotted on ordinary arithmetical scale with gauge height on vertical scale and discharge on horizontal scale. A curve was fitted to the plotted data using excel trendline options. The power trendline provided the most suitable fit to the data. The curve obtained from the power trendline is shown in Figure 3-4.

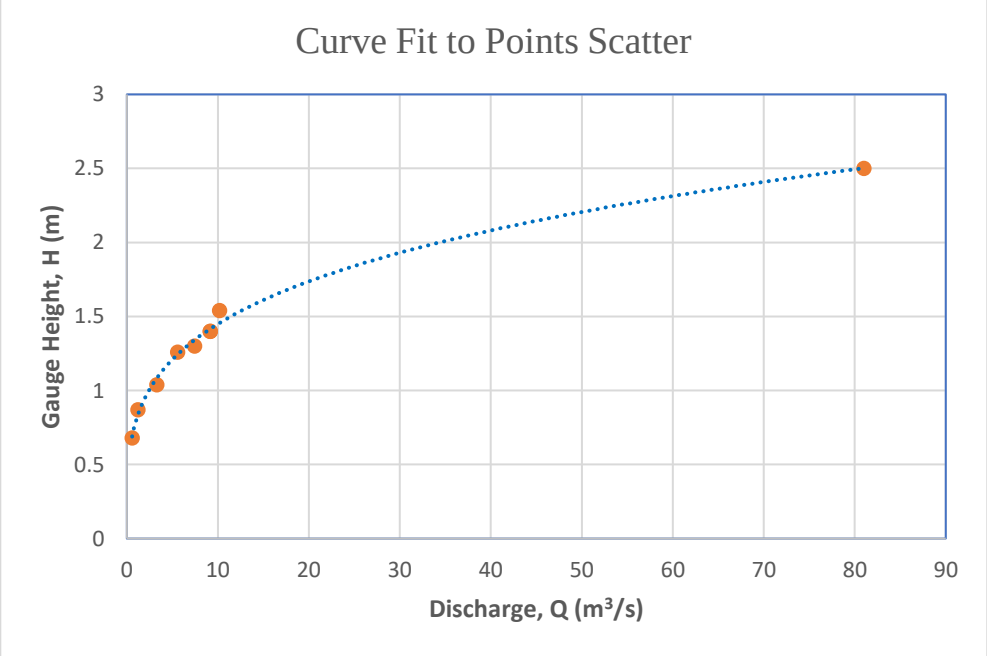

(Source: Author's computation using MS excel)

Figure 3-3: Curve fit to measured points

Three values of discharge Q_1, Q_2 and Q_3 were selected from the curve in Figure 3-4 as **5.0**, **17.320** and **60** respectively, such that $Q_2{}^2 = Q_1Q_3$. The corresponding values of h_1,h_2 and h_3 were found to be **1.209**, **1.672** and **2.313** respectively. These values were applied to equation (2-9) and h_0 was computed as zero (0).

A plot of discharge Q against $h_w - h_0$ was done on a log-log graph in excel as shown in Figure 3-5 below. The points were observed to be roughly lying in a straight line. The curve was deemed to represent one portion or segment, requiring only one mathematical equation.

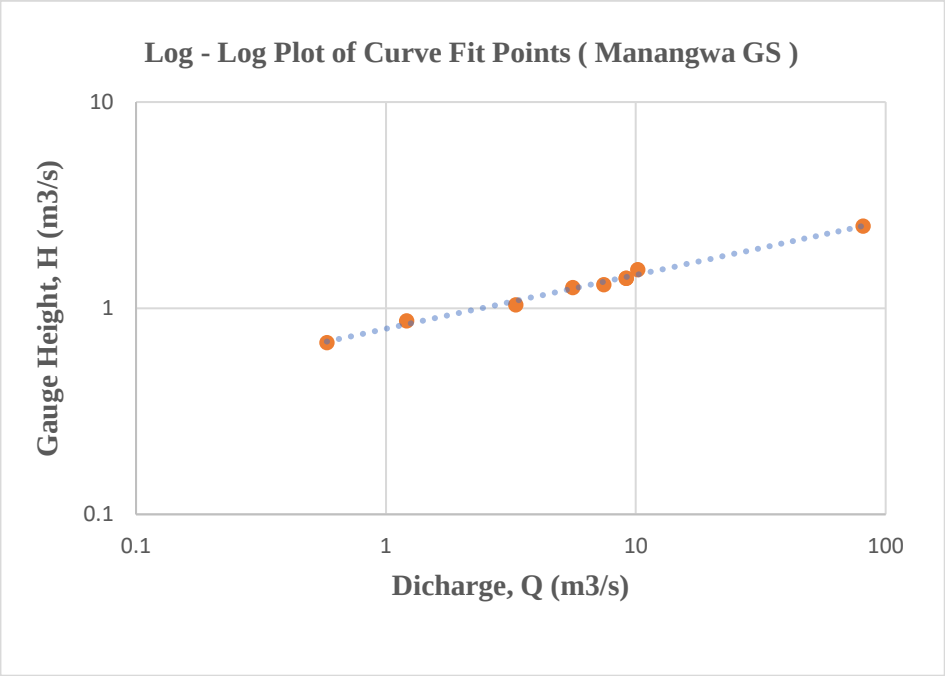

(Source: Author's computation using MS excel)

Figure 3-4: Log-log plot graph

c. Determination of rating equation

A mathematical equation was derived using the least squares method from equation (2-7) and (2-8):

Table 3-4: Calculation of the Rating Curve Using the least squares method

(Source: Author's computation using MS excel)

Stage (H)	Discharge (Q)	hw-h0	X = Log (h_w-h_0)	Y = Log Q	XY	X^2	Y^2
0.68	0.58	0.68	-0.17	-0.24	0.04	0.03	0.06
0.87	1.21	0.87	-0.06	0.08	-0.01	0.00	0.01
1.04	3.30	1.04	0.02	0.52	0.01	0.00	0.27
1.26	5.59	1.26	0.10	0.75	0.08	0.01	0.56
1.3	7.43	1.30	0.11	0.87	0.10	0.01	0.76
1.4	9.152	1.40	0.15	0.96	0.14	0.02	0.92
1.4	9.153	1.40	0.15	0.96	0.14	0.02	0.92
1.54	10.17	1.54	0.19	1.01	0.19	0.04	1.01
2.5	81.00	2.50	0.40	1.91	0.76	0.16	3.64
		Sum	0.88	6.82	1.45	0.29	8.16

Using the method of least squares, the following relationship was established, based on calculated values from Table 3-4.

$$\mathbf{6.82 = 9a_0 + 0.88b} \quad \textit{and} \quad \mathbf{1.45 = 0.88\,a_0 + 0.29\,b}$$

The coefficients$\boldsymbol{a_0}$, **a** and **b** were calculated as **0.386**, **2.433** and **3.800** respectively. The resulting rating curve equation is:

$$\boldsymbol{Q = 2.433(h_w)^{3.8}} \qquad \textit{Equation 3-1}$$

d. Testing the discharge rating curve

The discharge rating curve was tested for biasness using the student's t-test statistical methods. Table 3-5 shows the discharge measurements and computations of statistical parameters.

Table 3-5: Discharge measurements and computation of statistical parameters

(Source: Author's computation using MS excel)

Measured		Rating	Percentage deviation				$(P-\bar{P})^2$
			P		P-$\bar{P}$		
H	Q_m	Q_r	Plus	Minus	Plus	Minus	
0.68	0.58	0.562	1.02		0.62		0.74
0.87	1.21	1.433		-15.58		-15.97	255.04
1.04	3.303	2.824	16.96		16.56		257.67
1.26	5.594	5.855		-4.46		-4.86	23.62
1.3	7.433	6.594	12.73		12.33		152.03
1.4	9.152	8.738	4.73		4.34		18.84
1.4	9.153	8.738	4.75		4.35		18.92
1.54	10.173	12.552		-18.95		-19.35	374.42
2.5	81	79.125	2.37		1.97		3.88
		Sum	42.55	-38.99	40.18	-40.18	1105.17

The percentage deviation was computed using the formula $P = \left(\frac{Q_{m-Q_r}}{Q_r}\right)$ 100

Mean percentage deviation of P, $\bar{P} = \frac{P_1+P_2+P_3+\cdots\ldots\ldots+P_n}{n} = \frac{42.55-38.99}{9}$ = 0.396%

Standard percentage deviation of P, $S_D = \left(\frac{\sum(P-\bar{P})^2}{n-1}\right)^{1/2} = \frac{1105.17}{8}$ = 11.75%

Standard percentage error of P, $S_E = \frac{S_D}{n^{1/2}} = \frac{11.75}{9^{1/2}}$ = 3.92%

Test statistic, $t = \frac{\bar{P}}{S_E} = \frac{0.396}{3.92}$ = 0.101

The test statistic t has been calculated and is equal to 0.101. On the other hand, the value of t from the t-distribution table at the 5% significance level and for a sample size of 9 is found to be equal to 2.306 (two-tailed test, (n-1) = 8 degrees of freedom).

The conclusion is that since the calculated value of t is less than 2.306, the rating curve is free of bias as judged by this method.

The rating curve is also judged to be a good fit as the r^2 value was computed to be 0.9924 using Microsoft excel application.

e. Application of rating curve

The rating curve developed for Manangwa gauging station was used to compute corresponding discharges for daily stage readings recorded at Manangwa gauge station from October 2019 to September 2021, covering two hydrological years. The resulting hydrograph is shown in Figure 3-6 below.

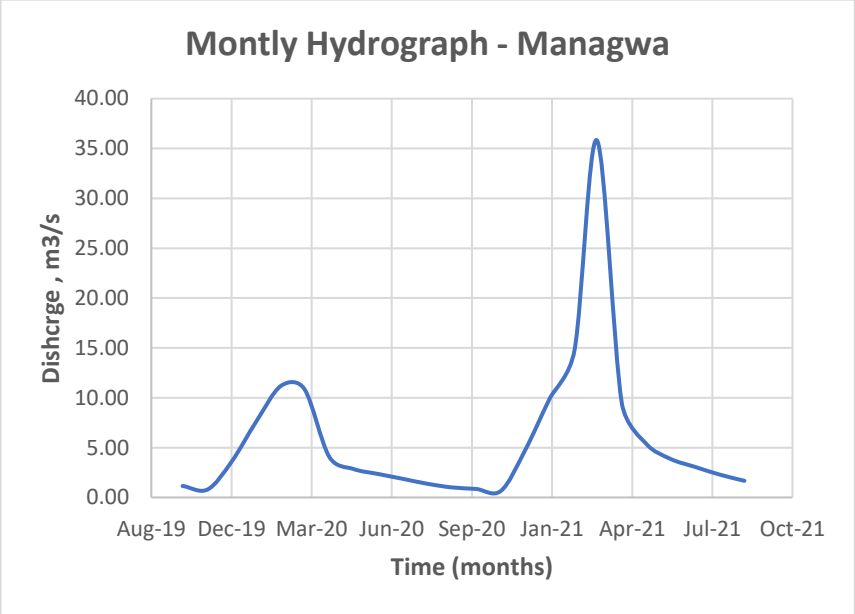

(Source: Author's computation using MS excel)

Figure 3-5: Hydrograph – Manangwa gauging station

3.2.3 Rainfall and Evaporation Data

a. On-site data

Rainfall and evaporation data are required as input in hydrological modelling of Mabula Kapi catchment. For calibration of the rainfall-runoff model, the rainfall time

series to be used in modelling should correspond to the measured discharge time series at Mangawa streamflow gauging station. The updated streamflow record runs from September 6 , 2019 to April 30, 2022. Unfortunately, there is no rainfall station within Mabula Kapi catchment to provide on-site rain fall input data for modelling. The nearest weather stations operated by the Zambia Meteorological Department (ZMD) are in Kabwe, Serenje, Mkushi and Mpika Districts.

Data from these nearby stations can be used to calculate the areal precipitation over the Mabula Kapi catchment. However, the data collected contain gaps and do not have time series for the period spanning from September 6, 2019 to April 30, 2022 which is required for calibration of the model. Table 3-6 shows the rainfall time series collected for four rainfall stations.

Table 3-6: Rainfall time series for local stations

(Source: Author's computation using MS excel)

Station Location	Data period	% Missing data (gaps)
Serenje	1981 - 2017	12 %
Mkushi	1993 - 2015	2.9 %
Mpika	1981 - 2012	0%
Kabwe	1981 - 2015	38%

b. Use of satellite data

A decline in the number of rainfall stations has motivated scientific studies to understand the extent to which satellite data can fill the gap left by the availability of rainfall stations. In recent years, studies have been conducted to compare satellite data with measured data from rainfall stations. A 2021 study in South Africa compared rainfall data sourced by the Climate Hazards Group InfraRed Precipitation with Station data (CHIRPS) satellite database with data from several rainfall stations. The analyses yielded good results overall, except in the winter rainfall region, where CHIRPS performed poorly. The study concluded that CHIRPS would have a role to play in future water resources studies (Pitman & Bailey, 2021).

CHIRPS data has been considered and analysed for possible use on the Mabula Kapi catchment. CHIRPS is downloadable from a google climate engine website (Desert

Research Institute, 2021). Rainfall data was downloaded as point data for Serenje, Mkushi, Kabwe Mpika using coordinates for the local meteorological stations from the google climate engine facility. Average point rainfall over Mabula Kapi catchment was also downloaded to ascertain its suitability for modelling. Both data sets span from span from January 1, 1981 to September 30, 2021.

To determine the suitability of CHIRPS data, a comparison has been made between the four rainfall stations near Mabula Kapi site and CHIRPS point data downloaded at these station locations. A comparison of daily time-steps showed a very poor correlation. Nevertheless, a monthly time-step comparison yielded a good association. Figures 3-7, 3-8,3-9 and 3-10 below are presentations of scatter plots showing the association between the two sets of data for Serenje, Kabwe, Mkushi and Mpika respectively.

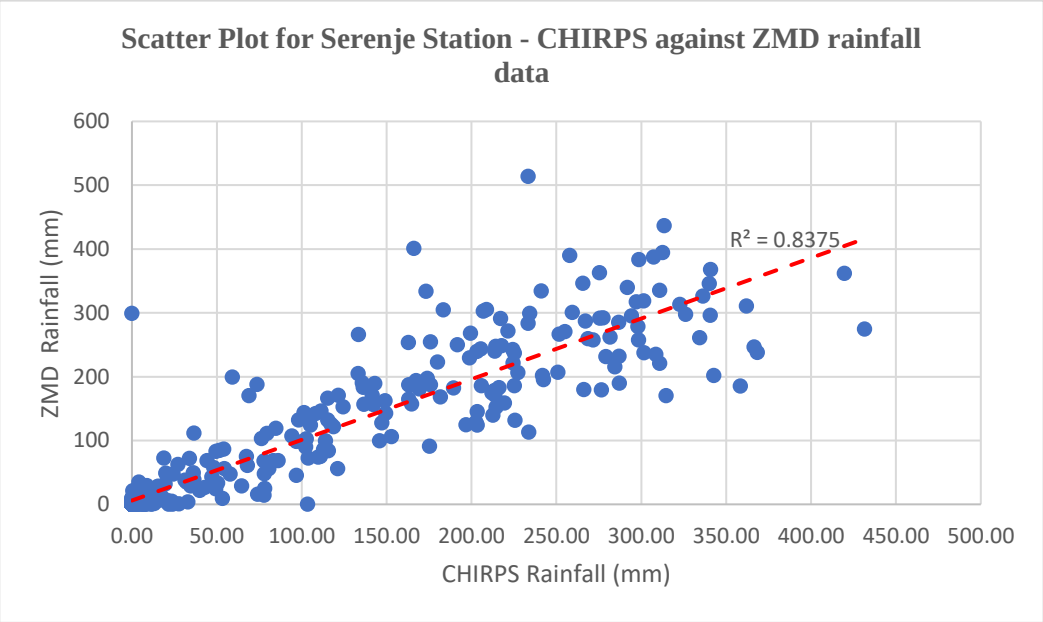

(Source: Author's computation using MS excel)

Figure 3-6: Scatter plot for Serenje rainfall against CHIRPS data (1981 -2017)

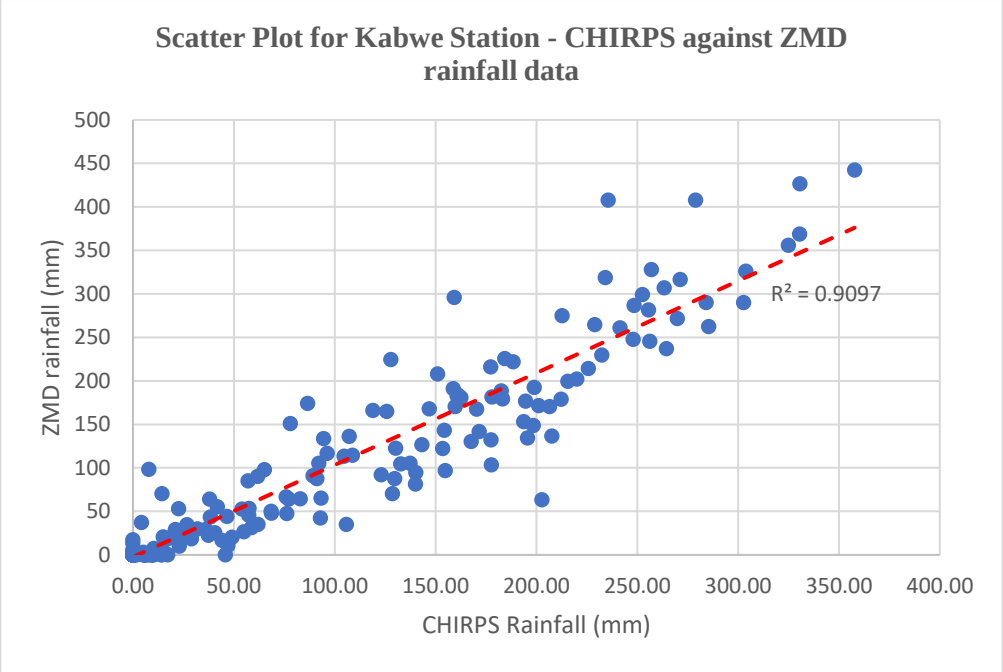

(Source: Author's computation using MS excel)

Figure 3-7: Scatter plot for Kabwe rainfall against CHIRPS data (1981 -2015)

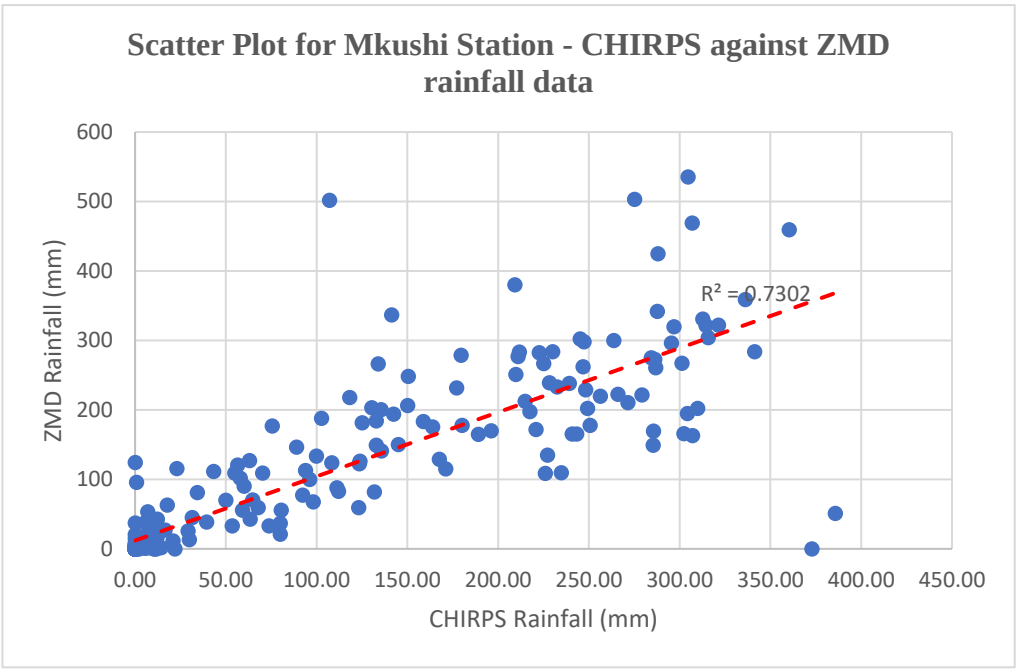

(Source: Author's computation using MS excel)

Figure 3-8: Scatter plot for Mkushi rainfall against CHIRPS data (1993 -2015)

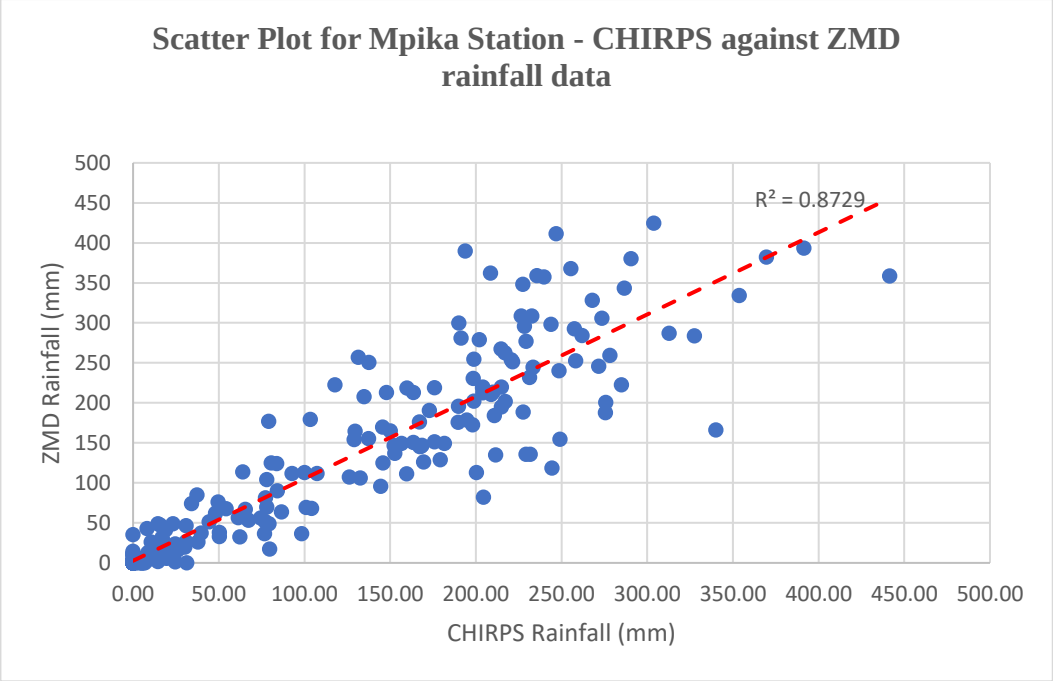

(Source: Author's computation using MS excel)

Figure 3-9: Scatter plot for Mpika rainfall against CHIRPS data (1981 -2012)

Statistical validating parameters used to compare the gauge data and CHIRPS data indicate a close relationship. Correlation coefficients for all sites indicate a very close association. The bias, the mean error and the mean absolute error are very low for all the sites as shown in Table 3-7.

Table 3-7: Validation statistics results between local stations and CHIRPS rainfall data

(Source: Author's computation using MS excel)

Station Name	Correlation Coefficient	Mean Error	Bias	Mean Absolute Error
Serenje	0.91	-2.13	0.96	28.23
Kabwe	0.95	-0.45	1.11	17.91
Mkushi	0.85	-5.66	0.93	30.31
Mpika	0.93	-2.67	0.96	21.76

The close association between the point rainfall data at Serenje, Mkushi, Kabwe and Mpika justify the use of CHIRPS data as an input to rainfall-runoff modelling on

Mabula Kapi site. The monthly time-step CHIRPS rainfall data is therefore recommended to be used in the PITMAN model for prediction of discharge.

3.2.4 Catchment Characteristics

a. Topographical characteristics

The topographical assessment for Kaombe area is based on a report obtained from the Geological Survey of Zambia for Kanona area. Kanona area is made up two zones namely the plateau and escarpment.

The northern part of the Kanona area is a plateau lying at 1500m to 1600m asl. It extends along the Luangwa-Luapula watershed. A widely spaced drainage system is characterized by the development of dambos. In the almost perennially waterlogged grassy areas of the dambos, underground seepage supplies sluggish runnels in the center of the dambos to give a small but constant supply of water throughout the year.

Kaombe site is mostly located in the escarpment zone which lies in between the plateau and the lukusashi rift ranging from 600m to 1500m asl. The boundary between the plateau and the escarpment is gradational in the west but sharply defined in the east. An early erosional stage is represented by a belt of country extending east- west across the Centre of the Kanona area immediately south of the plateau. This early erosion produced an undulating to hilly topography with the streams flowing in shallow valleys. Two later erosional stages may be defined in the south and south-east associated with deeply incised topography. Over most of the area there is a well-defined break of slope between the surface of these stages and that of the older erosional stage to the north. Waterfalls on the Kaombe River occur at the upper nick point. The smaller water courses are perennial and flow through steep gullies. The escarpment streams follow highly irregular courses and appear to be mainly joint controlled (ZESCO, 2018).

b. Geological characteristics

The geological assessment for Mabula Kapi site was based on a report obtained from the Geological Survey of Zambia for Kanona area. The area comprises some 2,970km^2, bounded by latitudes 13^o 00^o and 13^o 30' south, and longitudes 30^o 30' east (ZESCO, 2018).

Regarding soils, much of the area has a cover of pallid, light-textured, sandy soil. The lower part of the soil profile includes a lateritic horizon composed of nodular limonite and quartz gravel which may be up to 1m thick. The escarpment soils are generally thin and variable in composition with much rock rubble and quartz gravel on the hillsides. The central parts of the Kanona area where Mabula Kapi site is located are underlain by Muva rocks of Mesoproterozoic age and quarzites of possible Katangan age. The project site is underlain with Granite gneiss; coarse grained and porphyroblastic with microcline porphyroblasts; common xenoliths of banded and biotite rich gneiss. Other parts of the project site are underlain by leucocratic quartz with little or no biotite. The hillsides are generally covered with quartz scree, and whereas granite gneisses are exposed, quartzites are rarely seen in the outcrop (ZESCO, 2018).

c. Land use and cover characteristics

Agricultural production is the prime occupation with minor fishing activities in the catchment especially in the plateau areas. Agriculture can be said to be the major land use. Only a few farmers own livestock (cattle and goats). Some farmers keep local chickens at subsistence level. Farming is largely subsistence. Settlements are linearly aggregated in plateau area along access roads. The areas away from the road is sparsely populated (ZESCO, 2018). In terms of land cover, the catchment is predominantly covered by trees and scrub as shown in Figure 3-10 below.

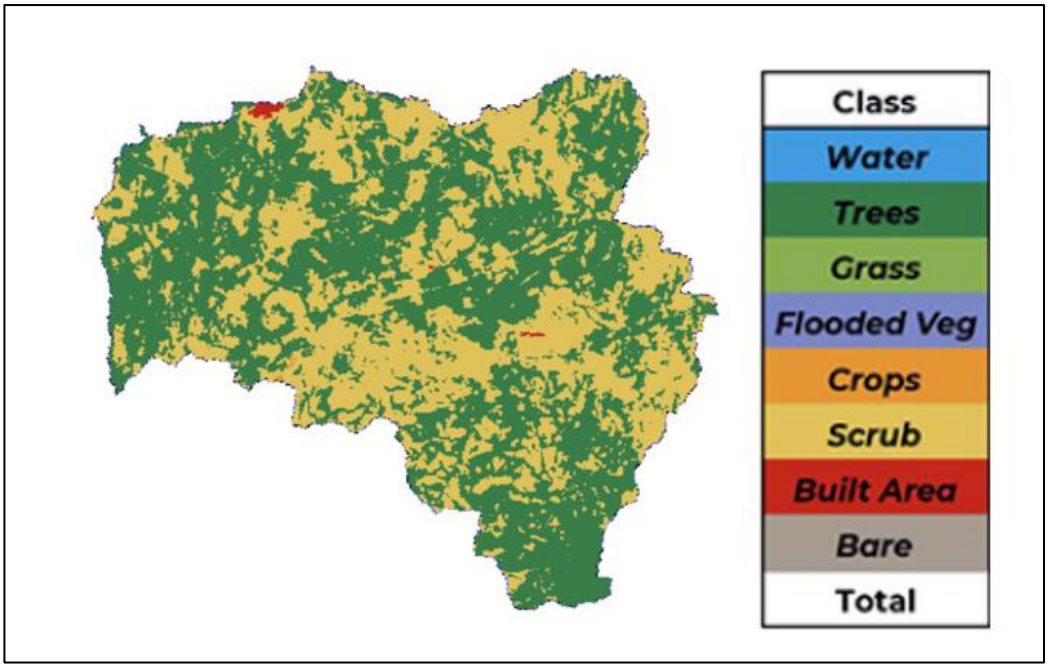

(Source: ESRI 2020 Land cover map)

Figure 3-10: Land cover map for Mabula Kapi catchment

d. Rainfall

The average annual rainfall over Mabula Kapi catchment is between 1000 to 1100mm. This is based on data provided the Meteorological Department of Zambia for a period 30-year period from 1931 to 1960 (ZESCO, 2018).

3.2.5 Climatic Projections

Ideally, a climate assessment or test should be done by considering the performance for the baseline condition as well as for locally-credible GCM or RCM-based climate projections. CHIRPS rainfall data set used in rainfall-runoff modelling of Mabula Kapi site do not have climatic projections. Thus, the Author opted to use other available climate projection time series to try to understand the proportionate impact of climate change on Mabula Kapi site.

Climate projection data from Climate Knowledge Portal (CKP) of the World Bank has been recommended as credible by a number of experts. The Author adopted the

datasets from the CKP for use on Mabula Kapi site. The data from the CKP is modelled from the global climate model compilations of the Coupled Model Inter-comparison Projects (CMIPs), overseen by the World Climate Research Program. Data downloaded by the Author is CMIP6 derived from the Sixth phase of the CMIPs. The CMIPs form the data foundation of the IPCC Assessment Reports. CMIP6 supports the IPCC's Sixth Assessment Report. The data is presented at a 1.0º x 1.0º (100km x 100km) resolution (World Bank, 2022).

The downloaded datasets are for watershed number 417 as classified on the CKP. It mainly covers the central parts of Zambia including Mabula Kapi catchment. Watershed 417 is shown in Figure 3-11 below. It must be noted that in terms of accuracy, this data set is significantly different from the CHIRPS data set used in rainfall-runoff modeling and calibration. Thus, the simulated time series from rainfall-runoff modelling using the CKP data for watershed 417 will only be used for indicative purposes, to understand the proportionate change that may happen at Mabula Kapi site in terms mean annual runoff (volume), mean annual flow, flow duration and annual energy production.

(Source: *(World Bank, 2022)*

Figure 3-11: Watershed 417 – Climate Change Knowledge Portal for the World Bank

4 Chapter Four: Results

4.1 Rainfall-Runoff modelling

4.1.1 Purpose of modelling

The time series computed from the rating curve for Manangwa gauging station is not long enough for energy yield modelling. This observed data covers only two hydrological years, from October 2019 to September 2021. Typically, a minimum of 15 years of discharge time series is required for hydropower power plant energy modelling (Fitchner, 2015). A climate resilient guide published by the International Hydropower Association (IHA) recommends a time series of 30 years. It this study, the Author therefore opted to extend the observed time series to 30 years. The extension of the time series was achieved using the PITMAN model.

4.1.2 PITMAN model set up and input data

As previously stated, the Pitman Model was selected for hydrologic modelling on Mabula Kapi project. The model requires substantial manipulation of the input data, to arrange it in the format required in the model. The input data that was added to the model is listed the Table 4-1 below:

Table 4-1: Input data for PITMAN model

(Source: Author's compilation)

S/N	Input Data Type	Description
1	Catchment area	Delineated using GIS software – 511 km2
2	Rainfall	CHIRPS time series from October 1981 to September 2021
3	Pan evaporation	Monthly averages from 1930 to 1995 (JICA, 1995)
4	Observed discharge	Time series from October 2019 to September 2021

Ideally, the rainfall input time series used in hydrologic modelling of the catchment is based on the average depth of precipitation over the catchment. This average is

usually calculated using time series from rain gauges evenly distributed within the catchment. Due to the unavailability of rain gauges on Mabula Kapi catchment, the average depth of precipitation over the catchment could not be determined.

The relative location of rainfall stations reasonably near to Mabula Kapi catchment is shown on the isohyetal map shown in Figure 4.1. This map was published by the Water Resources Management Authority (WARMA) with the help of the Federal Institute of Geosciences and Natural Resources (BGR) of Germany. The isohyets on the map were constructed based on a 30 year (1983 -2012) temporary consistent rainfall data set for Africa (Version 2) known as Tropical Applications of Meteorology using satellite and ground-based observations (TAMSAT). The rainfall data was provided by the Maproom of the Zambia Meteorological Department.

A comparison of annual rainfall values from the isohyetal map in Figure 8 -1 and from CHIRPS data was done as compiled in the in Table 4-2 below.

Table 4-2: Comparison of average annual rainfall – CHIRPS vs BGR Isohyet map (1983 to 2012)

[*Source: Author's compilation*]

Site	Average annual rainfall (BGR Isohyet Map)	Average annual rainfall (CHIRPS data)
Mabula Kapi catchment area (polygon)	950mm – 1050mm	1078 mm
Serenje Met. Station	1000 mm to 1050mm	1023 mm (point)
Mpika Met. Station	950mm – 1000mm	953 mm (point)

Table 4-2 indicates that CHIRPS point data downloaded as average rainfall over the catchment seems to overestimate the rainfall over the catchment. Thus, caution was applied when using it in modelling of the catchment. A decision was made to carry out independent simulations using CHIRPS point rainfall (for Serenje and Mpika) and the average catchment rainfall point data over Mabula Kapi catchment. The data set

that would yield good calibration results in the model would be adopted for extension of time series at Manangwa gauging station.

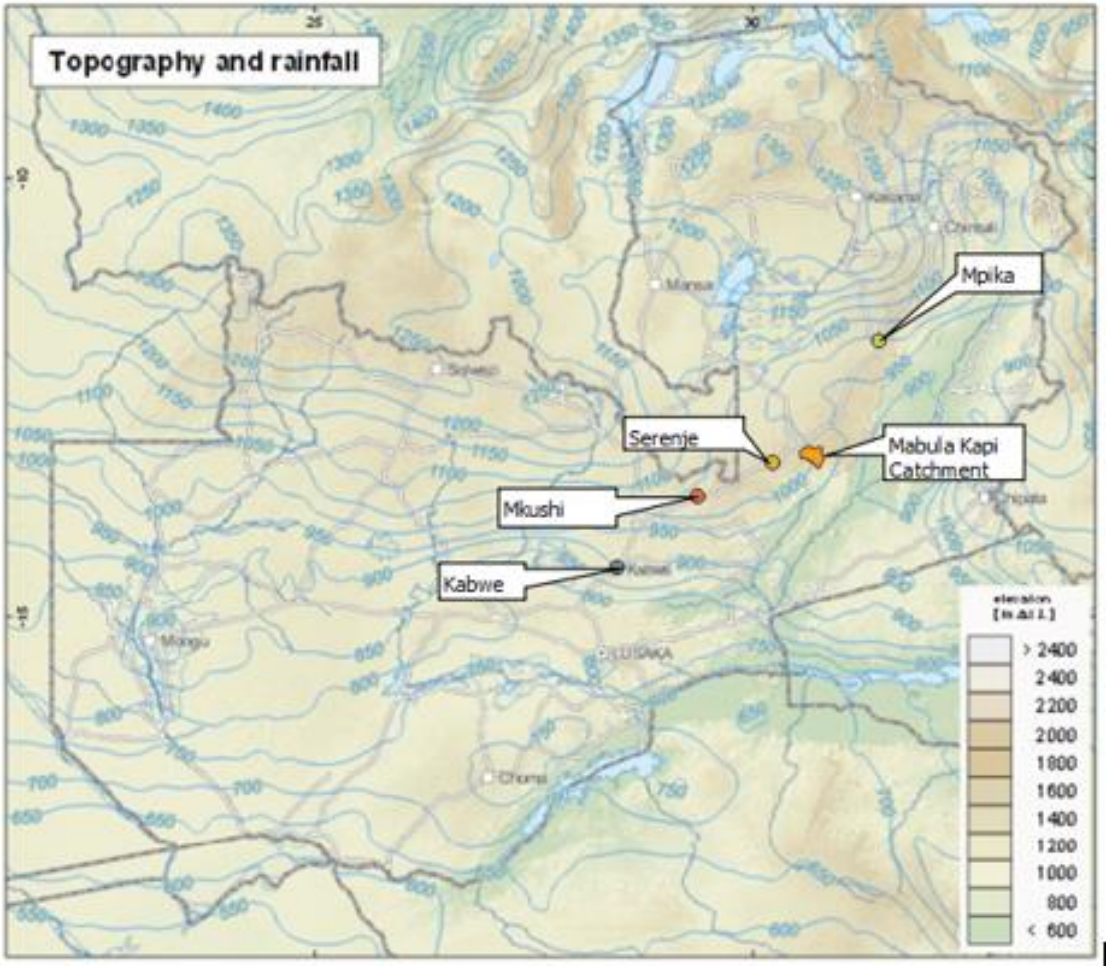

[Source: BGR]

Figure 4-1: Isohyetal Map of Zambia (1983 -2013)

A model network was created for Mabula Kapi with appropriate modules for the catchment. The schematic network diagram in Figure 4-2 below shows a simple representation of the model for Mabula Kapi catchment on Kaombe River. It shows the catchment area (runoff module), river reaches (route) and a stream flow gauge.

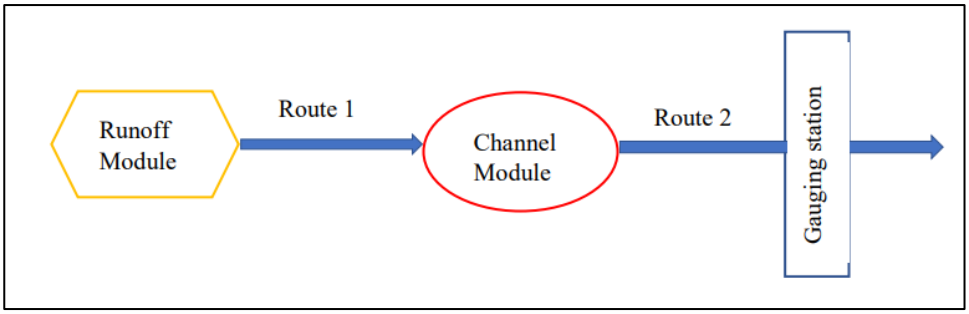

(Source: Author's created in MS word)

Figure 4-2: Network diagram for Mabula Kapi model

4.1.3 Model simulations

Upon completion of the model setup, a first simulation was initiated in the PIMAN model with the default parameters which govern the amount, rate and timing of the runoff generated. Thereafter, the default parameters were changed with good judgement, based on knowledge of catchment characteristics, to match or calibrate the simulated and observed flows as closely as possible.

Selecting the correct parameters when calibrating the model was an iterative process. Most of the parameters are not quantifiable, and the exact values are unknown to the user at the start of the calibration process. The calibration parameters are chosen based on the fit between observed and simulated flows, rather than a predetermined parameter value which determines the flows. Therefore, the (fit of) flows determine the parameters, and it is not a case of the 'known' parameters determining the flows. It is consequently not a case of choosing a 'correct' parameter for the catchment at the outset, generating the 'correct' simulated flows using the 'correct' calibration parameter. It is rather a case of iteratively changing the parameters which drive the flows to be as close as possible to the observed data. The simulated flows are a function of these parameters; therefore, the result of this process is the calibration parameters, as they are the factors which dictate the simulated flows (EDF-GIBB, 2019).

Each time a parameter was changed the model was re-run and the results re-valuated. The results were assessed by means of the numerical statistics and the graphical results generated. This process was carried out for the Mabula Kapi catchment and repeated after each parameter change, until the simulated flows were as similar as possible to

the observed flows for the gauging station. Simulations were done independently using CHIRPS rainfall time series point data for Serenje, Mpika and Mabula Kapi catchment average rainfall point data. The average catchment rainfall point data for Mabula Kapi catchment and the point data at Serenje station could not yield satisfactory calibration results, despite multiple simulation runs.

On the other hand, simulations using CHIRPS point data at Mpika station were satisfactory and yielded reasonable results. The final runoff module calibration parameters used to arrive at a reasonable fit are shown in figure 4-3 below.

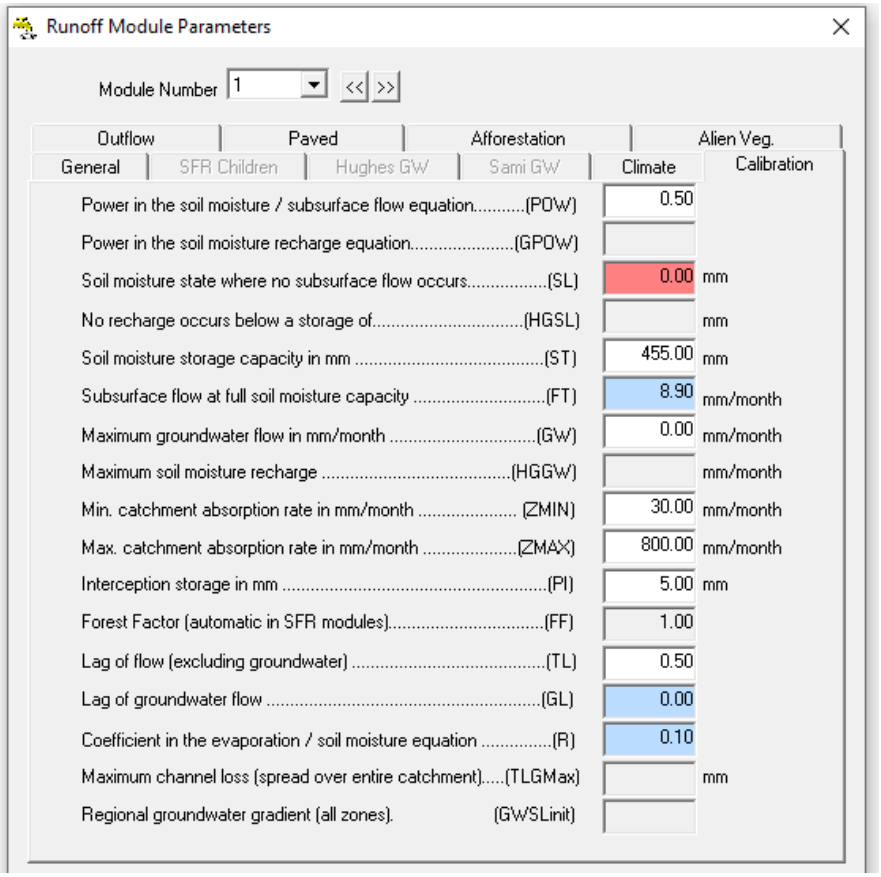

(Source: Author's simulation using PITMAN model)

Figure 4-3: Runoff Module Parameters used to achieve reasonable fit between observed and simulated flows

4.1.4 Calibration results

Once all the data has been entered into the various modules and routes, the graphs and statistics are used to check on the calibration between simulated and observed

(known) streamflow and storage. Streamflow can be checked at any route where there are observed stream flows. There are no firm criteria as to what constitutes a "good fit" but one can use the following guidelines (Pitman, et al., 2015):

- Error in MAR and mean (log): < 4%
- Error in std. dev (natural & log): < 6%
- Error in seasonal index:< 8%

The final calibration results statistics are for Mabula Kapi catchment indicating the closeness of fit between simulated flows and observed flows are presented in Table 4-3.

Table 4-3: Route 2 Statistics (Simulated vs Observed)

[Source: Author's compilation from PITMAN model]

S/N	Statistic	Observed	Simulated	Percentage difference	Remarks
1	Mean Annual Runoff (MAR)	70.63	71.02	0.55%	Good fit
2	Mean (Log)	1.83	1.83	0%	Good fit
3	Standard Deviation	30.90	31.05	0.48%	Good fit
4	Log Standard Deviation	0.20	0.20	0%	Good fit
5	Seasonal Index	40.11	39.46	1.62%	Good fit

The annual hydrograph for the final calibration is shown in Figure 4-4 below. The fit for observed versus simulated flows for Manangwa gauging station is considered reasonable. However, it is evident that for very high flows, the model is unable to accurately simulate these closely. However, the troughs are very well simulated, as are the mean monthly flows which indicate the distribution of rainfall over the year.

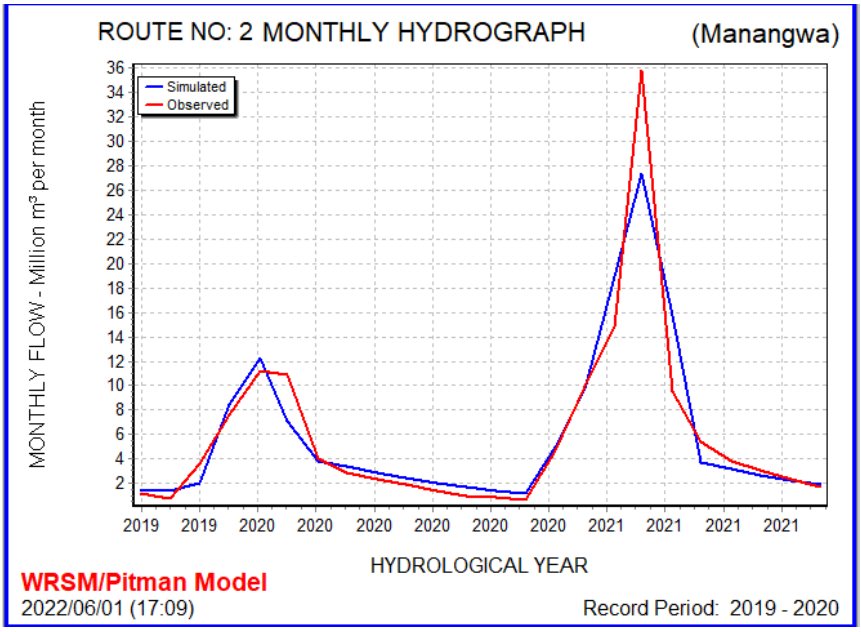

[Source: Author's simulation using PITMAN model]

Figure 4-4:Annual Hydrograph for Manangwa gauging station (Simulated vs Observed)

The coefficient of determination r^2, was calculated using Microsoft excel as 0.885 while the Nash-Sutcliffe coefficient of efficiency was computed as 0.882. This shows a good fit as both figures are close to 1. Figure 4-5 below shows the scatter plot between observed and simulated flows in MS excel.

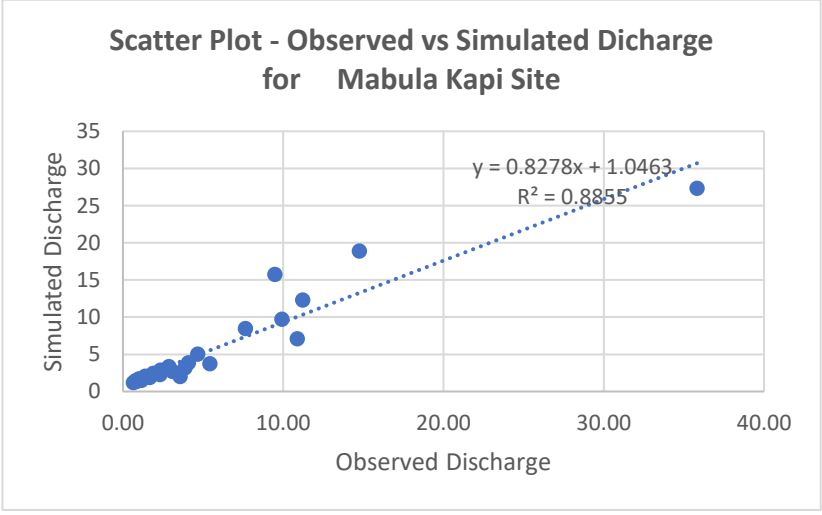

*(*Source: Author's computation using MS excel)

Figure 4-5: Scatter Plot - Observed vs Simulated flows

The PITMAN model has therefore been used to simulate runoff and to extend the discharge time series at Manangwa gaging station. A 30-year long discharge time series has accurately been obtained for Manangwa gauging station, running from October 1991 to September 2021. The time series are plotted on the annual hydrograph shown in Figure 4-6.

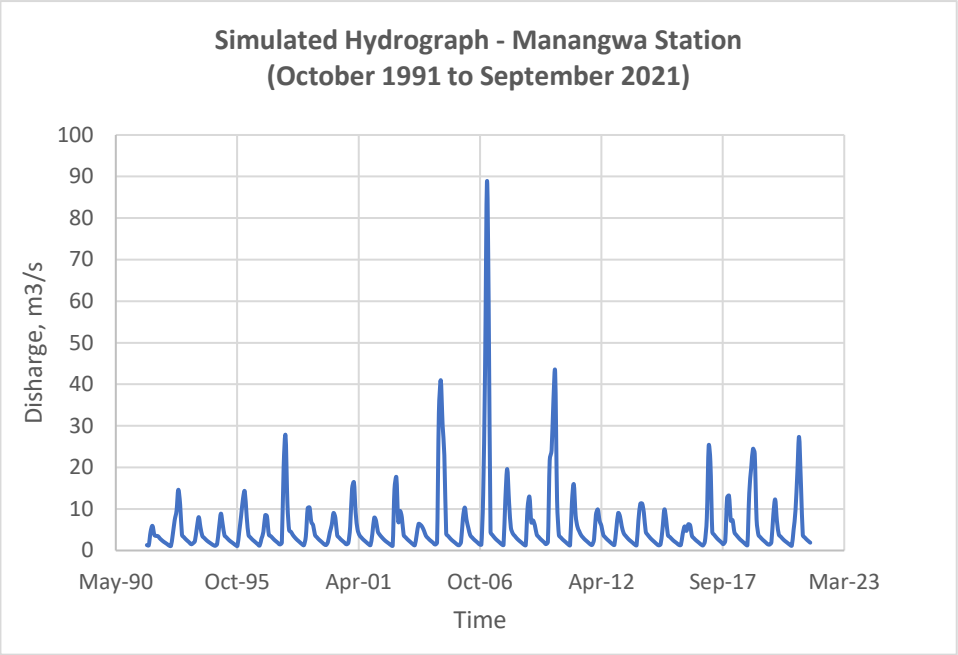

(Source: Author's computation using results from PITMAN model)

Figure 4-6: Simulated hydrograph – 30-year time series

4.2 Installed Capacity and Annual Energy

The simulated 30-year time series was analysed to determine the design discharge to be used in evaluating the power potential at Mabula Kapi site. Since Mabula Kapi site is envisaged to run as a run-of-river plant, a flow duration was used to evaluate the energy potential of the site. A flow duration curve (FDC) is important for selection of plant design discharge. The derived flow duration curve using the simulated 30-year data is shown in Figure 4-7 below.

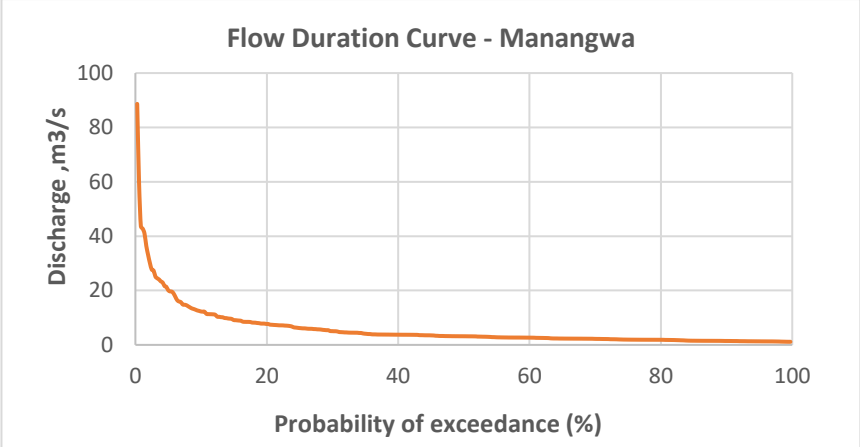

[Source: Author's creation using PITMAN model results]

Figure 4-7: Flow duration curve – Manangwa Gauging Station (1991 -2021)

In order to determine the design discharge and optimum installed capacity for Mabula Kapi site, an energy yield analysis has been carried out, taking into account the associated capital cost for each installed capacity. A basic costing model accounting for the cost of civil works, electro-mechanical works, hydro-mechanical works, and administration and engineering fees was applied in the RETScreen Energy Model. The major input parameters and assumptions added to the model are indicated in Table 4-4 below. Some parameters such as gross head are based on the findings of the prefeasibility study done in 2018 (ZESCO, 2018)

Table 4-4: Main parameters and assumptions used in RETScreen software

[Source : (ZESCO, 2018)]

S/N	Description	Value
1	Gross head	203.38m
2	Turbine type/Number of turbines	Pelton/3
3	Residual (e) flow – 10% mean flow	0.58 m^3/s
4	Firm flow	90% Probability exceedance
5	Maximum hydraulic losses	4%
6	Turbine efficiency	88%
7	Generator efficiency	97%
8	Plant availability	90%

The power and annual energy for Mabula Kapi HPP based on design discharge at different probability exceedance of flow are summarized in Table 4 -5 below.

Table 4-5: Comparison of Design Discharge against CAPEX and Annual Energy

(Source: Author's computation using results from PITMAN model)

Design Discharge (m^3/s)	Probability of exceedance (%)	Installed Capacity (MW)	Capacity Factor (%)	Annual Energy (GWh)	Estimated CAPEX (Millions USD)
12.29	10	20.49	30.60%	54.86	60.33
9.13	15	15.13	37.50%	49.65	48.38
7.69	20	12.70	41.70%	46.42	42.26
6.20	25	10.20	47.10%	42.11	35.77
5.02	30	8.20	52.70%	37.94	28.70
4.12	35	6.70	58.10%	34.23	24.86
3.73	40	6.07	61.00%	32.46	23.16
3.49	45	5.68	62.90%	31.28	22.11
3.18	50	5.16	65.60%	29.65	20.73
2.79	55	4.52	69.10%	27.32	18.97
2.66	60	4.30	70.20%	26.46	18.37
2.32	65	3.74	73.60%	24.12	16.80
2.20	70	3.54	74.80%	23.22	16.79
1.93	75	3.10	77.60%	21.07	14.95
1.86	80	2.99	78.30%	20.49	14.62
1.52	85	2.43	81.90%	17.45	12.95

Assuming a run of river scheme, installed capacities and annual energies for plant sizes using different design flows were computed. A basic costing model accounting for the cost of civil works, electro-mechanical works, hydro-mechanical works, and administration and engineering fees was applied in the RETScreen Energy Model. Indicative project cost estimates obtained were plotted against the average annual energy generation for each plant size as shown in Figure 4 - 8 below.

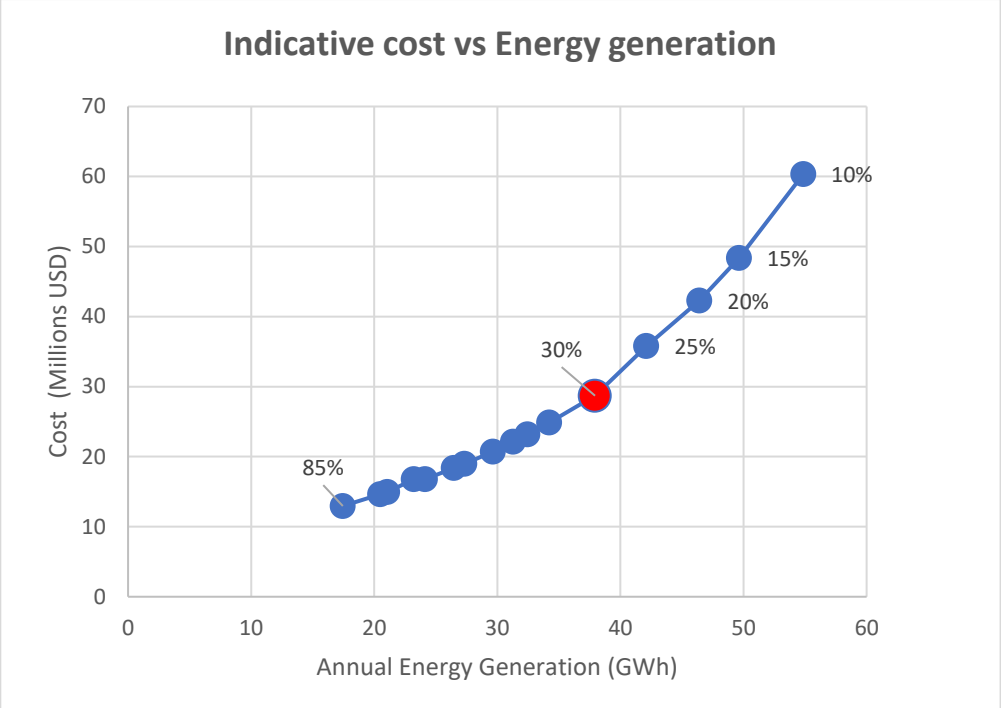

(Source: Author's plot using MS excel)

Figure 4-8: Indicative cost vs energy generation graph

It can be seen from the above graph that when the design discharge falls below the probability of exceedance of 30%, there is a sharp change in the slope of the graph. This implies that beyond 30%, additional energy generation is not justified by additional plant costs. The increase of design discharge is only reasonable to 30% probability of exceedance. Therefore, the optimum plant size for the proposed Mabula Kapi site HPP was be selected at the probability exceedance of 30% (P30).

In this case, Mabula Kapi site will have an installed capacity of 8.2MW and annual energy of 37.94 GWh. The Power duration curve computed using RETScreen software is shown on Figure 4 -9 below.

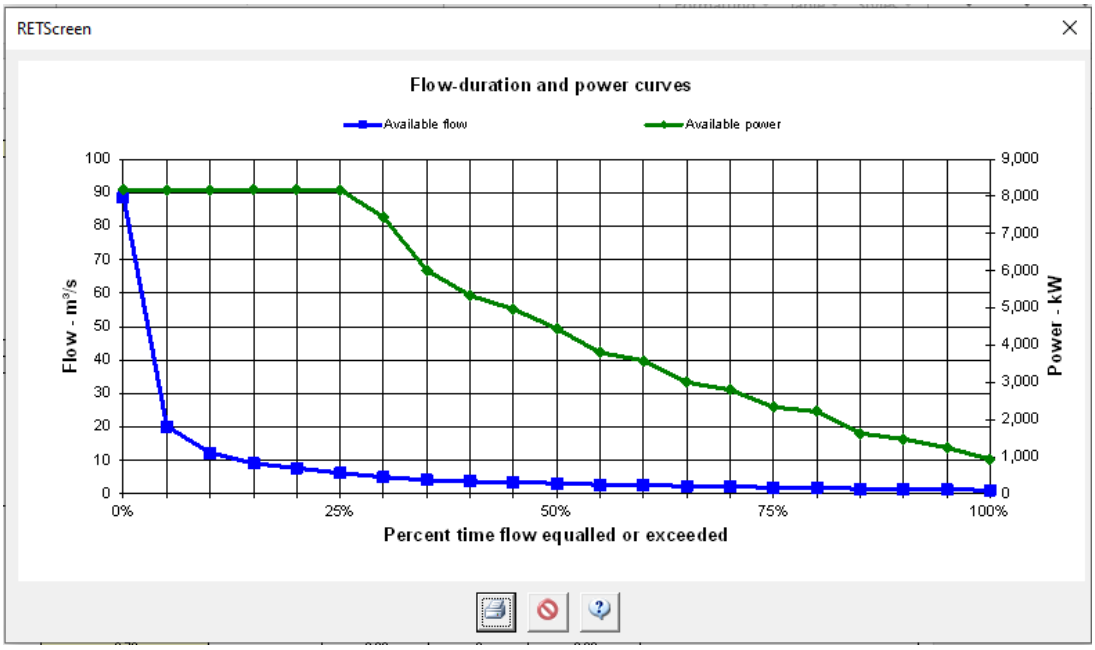

(Source: Author's computation using RETScreen)

Figure 4-9: Flow and Power Duration Curves

4.3 Design Flood Estimation

Estimation of design flood for Mabula Kapi site was done using statistical analysis or flood frequency probability analysis. This is because of the low risk of negative impacts that would arise downstream in case of failure of its hydraulic structures.

Mean daily data are traditionally used for flood frequency analysis instead of monthly data. The monthly time series simulated and used for estimating the installed capacity and energy could not be used for flood estimation purposes. Therefore, the PITMAN daily time step model was used to simulate daily flows. The flows were simulated as naturalised flows in the model. Naturalised flows are appropriate in flood estimation because such flows reflect a worst-case scenario where there are no artificial influences. (Government of Alberta, 2020)

The daily naturalised flows were simulated using parameters from the calibrated monthly model. Conversion factors suggested in the PITMAN model were applied accordingly. The calibration parameters used in the model and the simulated hydrograph are shown in Figures 4-10 and 4 -11 respectively.

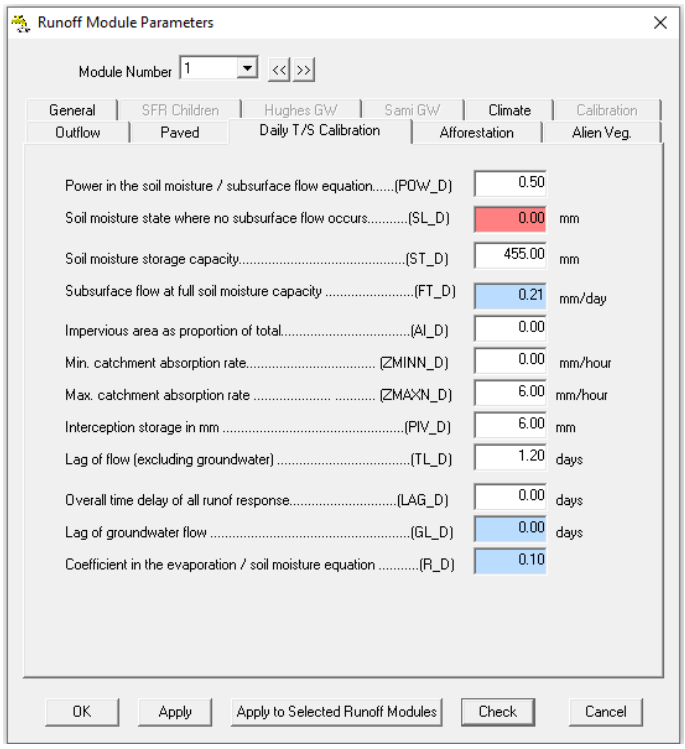

(Source: Author's simulation in PITMAN model)

Figure 4-10: Daily time step calibration parameters

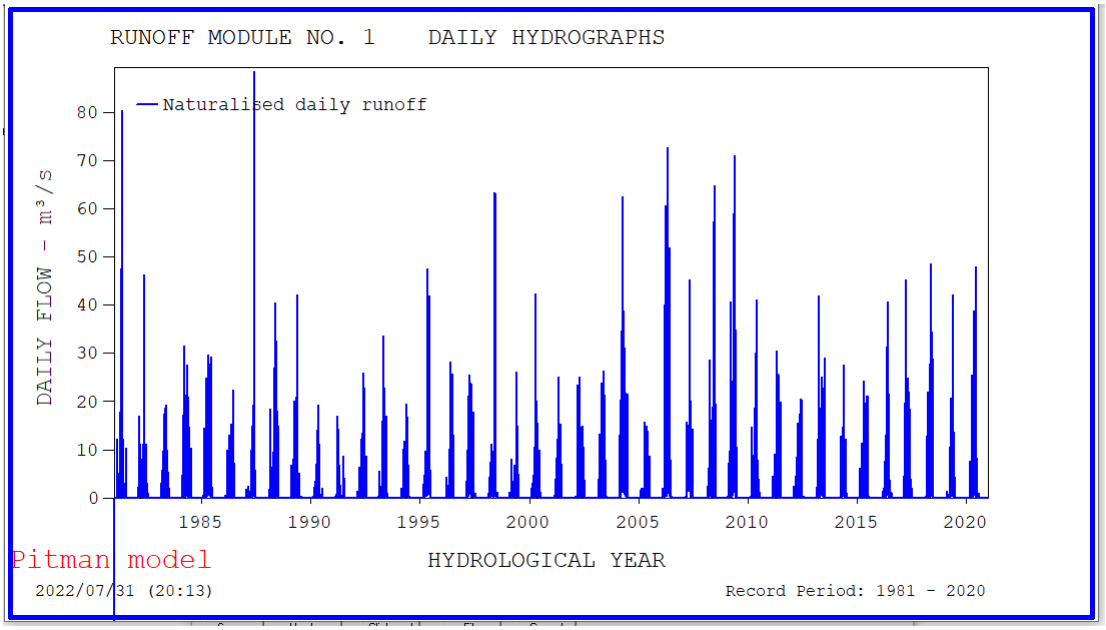

(Source: Author's simulation in PITMAN model)

Figure 4-11: Simulated Daily Naturalised Flows for Mabula Kapi Site

The simulated naturalised discharge time series were used to perform flood frequency analysis, with the purpose of estimating a design flood for sizing of the spillway on

the weir or dam. Annual maximum flows were selected for each year from the 40-year time series as shown in the Table 4-6.

The series of annual maxima was analysed using different frequency distributions as shown in Figure 4-12 and the log-normal distribution was found to give the nearest fit to the data.

Table 4-6: Annual maximum flows

(Source: Author's compilation in MS excel)

YEAR	Annual Max Flood
1982	90.77
1983	81.05
1984	73.77
1985	71.04
1986	65.97
1987	64.87
1988	63.89
1989	63.35
1990	55.77
1991	49.25
1992	49.25
1993	48.64
1994	47.56
1995	47.27
1996	46.02
1997	43.77
1998	43.58
1999	43.05
2000	42.91
2001	42.18
2002	41.60
2003	36.64
2004	32.34
2005	32.00
2006	31.47
2007	29.26
2008	28.95
2009	28.74

Table 4-6 Continued

YEAR	Annual Max Flood
2010	27.87
2011	27.17
2012	26.42
2013	25.90
2014	25.68
2015	25.59
2016	25.34
2017	24.36
2018	23.15
2019	20.46
2020	20.21
2021	12.00

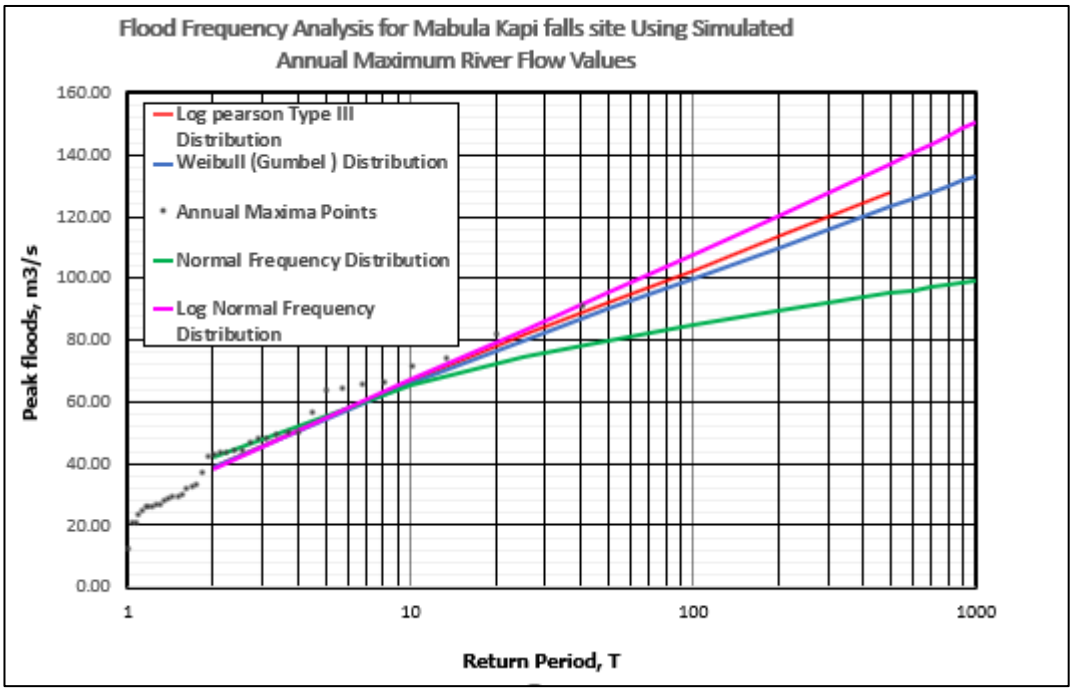

(Source: Author's computation and plot in excel)

Figure 4-12: Flood frequency analysis for Mabula Kapi HPP site

The fitted data and peak flow estimates are given in Table 4-7 below for return periods up to 1:1000 years. A return period of 200 years was selected for Mabula Kapi site for design flood estimation. This return period was selected because of the low risk of negative impacts that may otherwise arise at the site in case of failure of hydraulic structures. Mabula Kapi HPP is expected to have a weir as a diversion structure. A 1:200-year design flood corresponds to 120 m^3/s.

Table 4-7: Peak Flood Discharges – Lognormal Distribution

(Source: Author's computation using excel)

Return period, T years	K(T) Frequency Factor	Estimated Peak Flood (m3/s)
2	0.00	38.26
10	1.28	67.55
25	1.75	83.19
50	2.06	95.16
100	2.33	107.39
200	2.58	119.95
500	2.88	137.17
600	2.94	140.68
700	2.98	143.67
800	3.02	146.29
900	3.06	148.61
1000	3.09	150.69

4.4 Comparison of Results from Previous Studies

Table 4-8 below shows a comparison of the parameters and results between the previous prefeasibility study and the current study. The comparison indicates an improvement in the prediction of design flood, residual flow and the design discharge. The increase in the design discharge leads to a corresponding improvement in installed capacity and annual energy.

Table 4-8: Comparison of results between previous and current study

(Source: Author's computation)

S/N	Description	Previous study (Prefeasibility)	Current study	Remarks
1	Gross head	203.38m	203.38m	
2	Turbine type/Number of turbines	Pelton/3	Pelton/3	
3	Residual (e) flow	0.20 m^3/s (5% of mean flow)	0.58 m^3/s (10% of mean flow)	Improvement
4	Firm flow	90% Probability exceedance	90% Probability exceedance	
5	Maximum hydraulic losses	4%	4%	
6	Turbine efficiency	88%	88%	
7	Generator efficiency	97%	97%	
8	Plant availability	90%	90%	
9	Time series duration	9 years	30 years	
10	Design flood	59 m^3/s	120 m^3/s	Improvement
10	Design Discharge (30% Probability of exceedance)	4.5 m^3/s	5.0 m^3/s	Improvement
11	Capacity factor	52%	52.7%	
12	Installed capacity	7.4 MW	8.2 MW	Improvement
13	Annual Energy	34 GWh	38 GWh	Improvement

4.5 Climate risks assessment

4.5.1 Need for Mabula Kapi climate assessment

An assessment was done to determine if a climate risk assessment was required for Mabula Kapi site. Table 4-9 below shows the answers for the proposed power plant.

Table 4-9: Typical Questions for Climate Risk Assessment

(Source: Author's compilation)

Could a change of the hydrological regime significantly affect the hydropower project's economic viability?	Yes
Could a change in the hydrological regime affect service continuity/access to electricity in the region it serves?	Yes
Could any of the performance metrics for the project be unachievable by potential climate change effects?	Yes
Would a breach of the project's main dam or other associated infrastructure have significant adverse consequences on downstream populations, strategic infrastructure or protected ecosystems?	No

It can be seen from above that the answer to at least one question is yes. Therefore, a climate risk assessment is imperative for Mabula Kapi site.

4.5.2 Future climate scenarios and climate test for Mabula Kapi catchment

The climate indicators were downloaded from the CKP of the World Bank and used in climate assessment of Mabula Kapi site are precipitation/rainfall and temperature.

4.5.3 Rainfall future scenarios

Figures 4-13 and 4-14 show the projected climatology for rainfall for a SSP 2.6 and SSP 8.5 respectively. They also include historical reference data from 1914 to 1995.

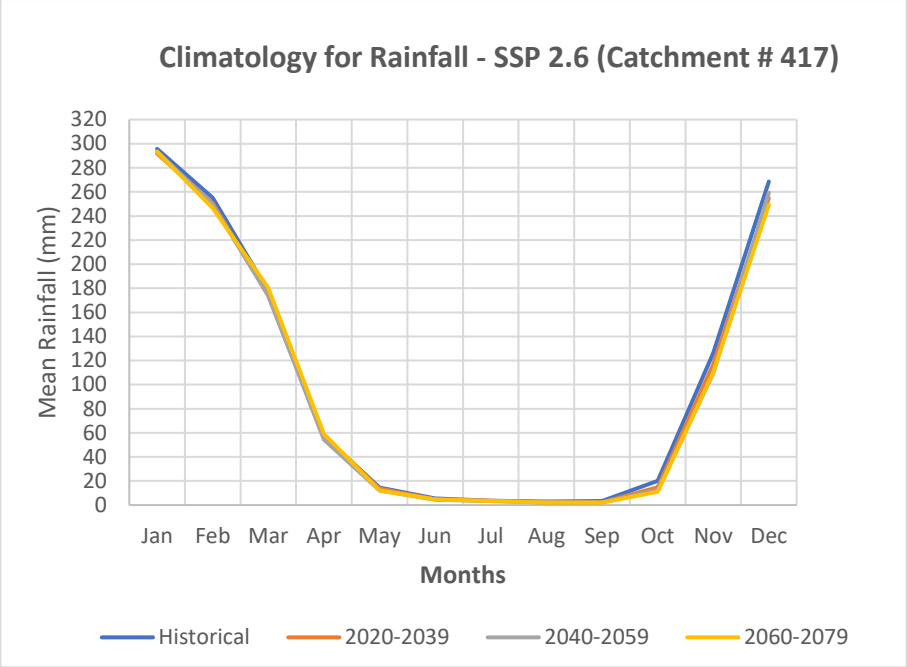

[Source: *(World Bank, 2022)*]

Figure 4-13: Changes in Rainfall – SSP 2.6 (CKP data)

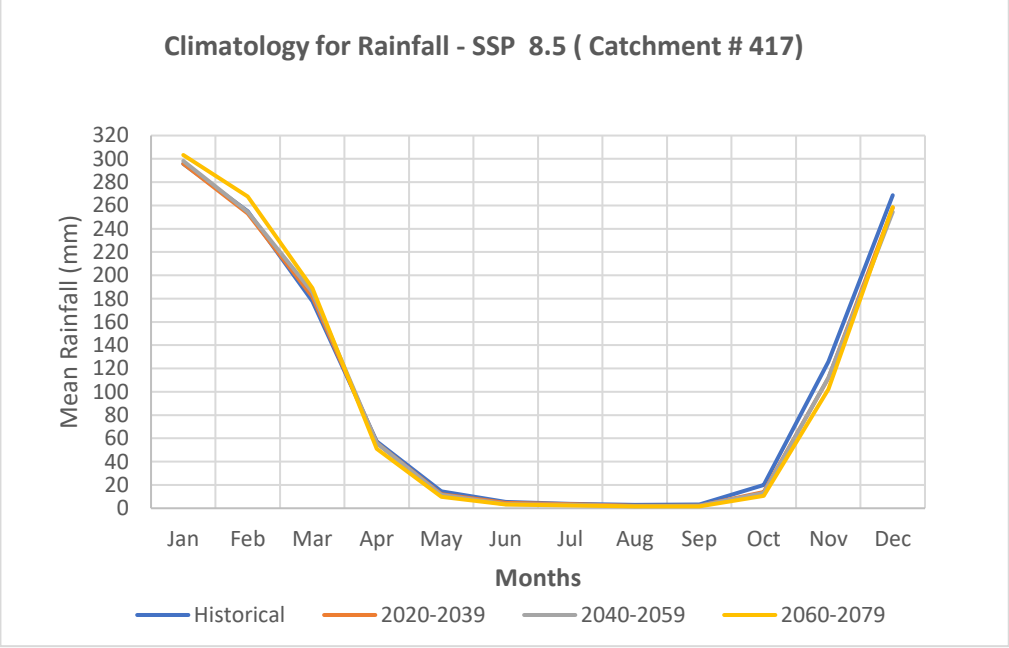

[Source: *(World Bank, 2022)*]

Figure 4-14: Changes in Rainfall – SSP 8.5 (CKP data

The changes in rainfall can also be illustrated in terms of anomalies for the SSP 2.6 and SSP scenarios as shown from Figure 4-15 to 4-20 below.

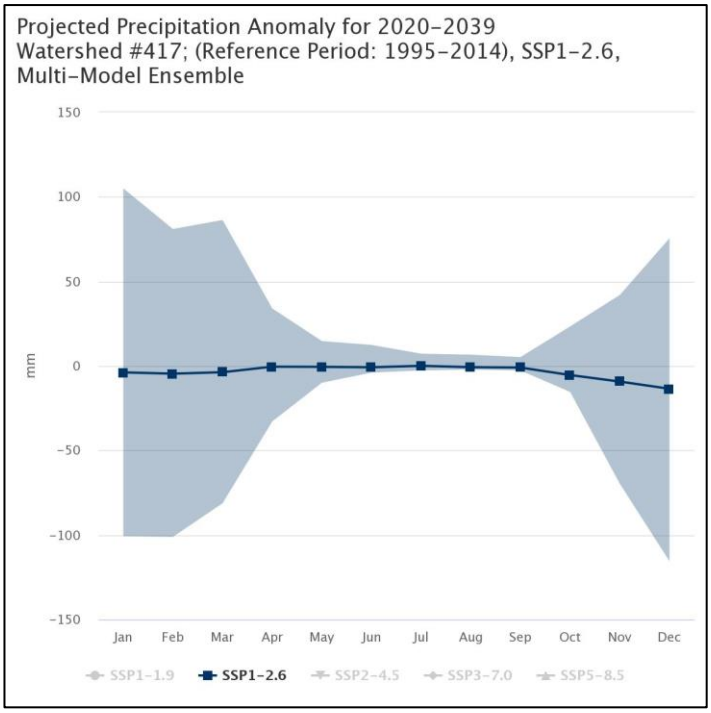

[Source: *(World Bank, 2022)*]

Figure 4-15: Projected precipitation Anomaly for 2020-2039 (SSP 2.6)

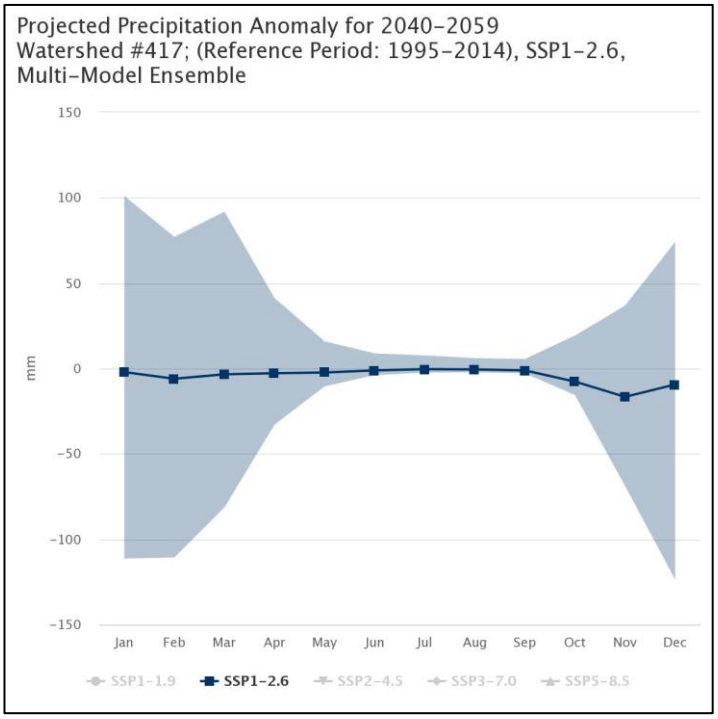

[Source: *(World Bank, 2022)*]

Figure 4-16: Projected precipitation Anomaly for 2040-2059 (SSP 2.6)

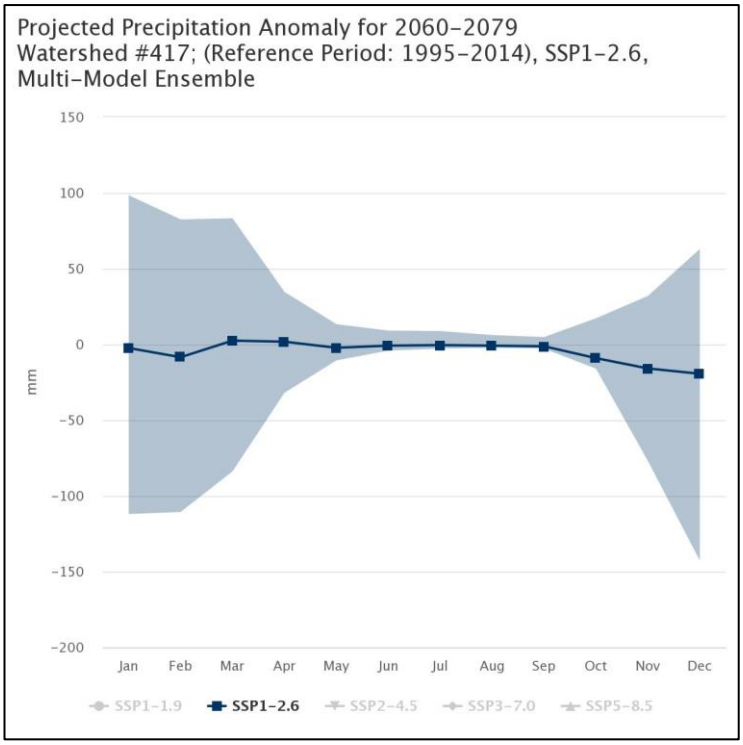

[Source: *(World Bank, 2022)*]

Figure 4-17: Projected precipitation Anomaly for 2060 -2079 (SSP 2.6)

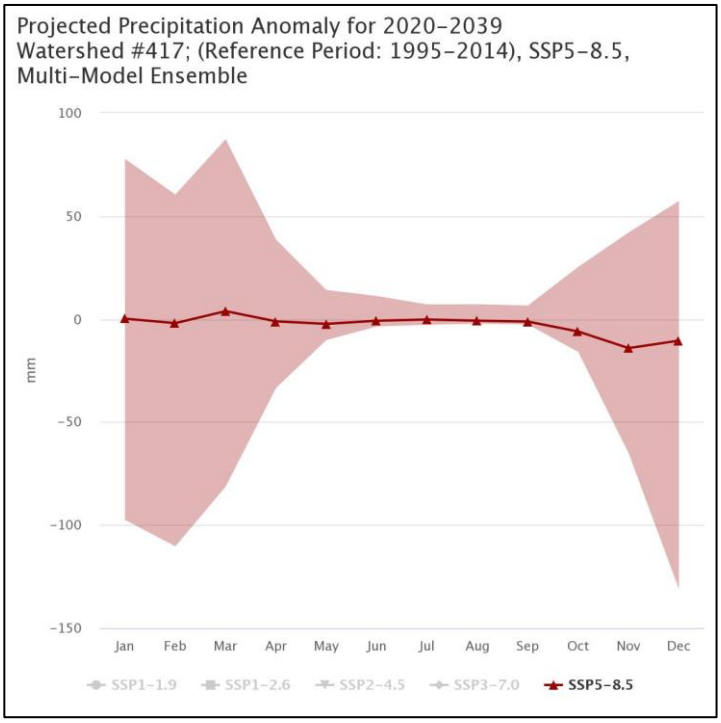

[Source: *(World Bank, 2022)*]

Figure 4-18: Projected precipitation Anomaly for 2020 -2039 (SSP 8.5)

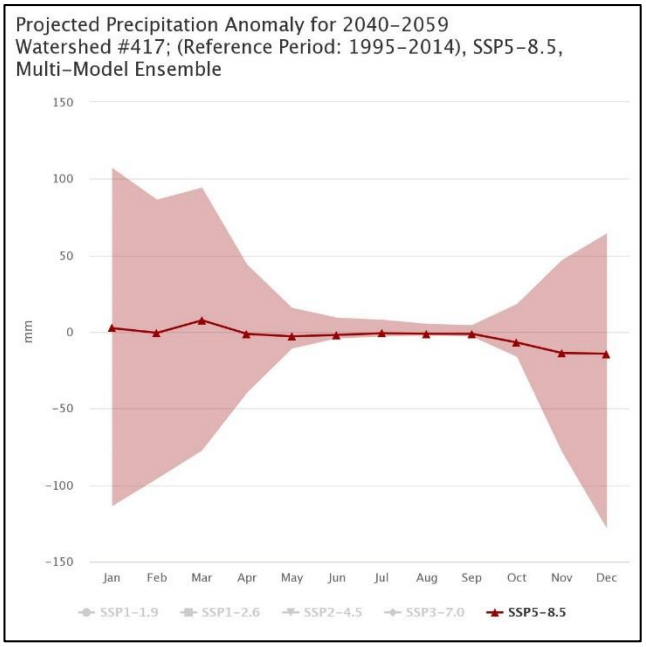

[Source: *(World Bank, 2022)*]

Figure 4-19: Projected precipitation Anomaly for 2040 -2059 (SSP 8.5)

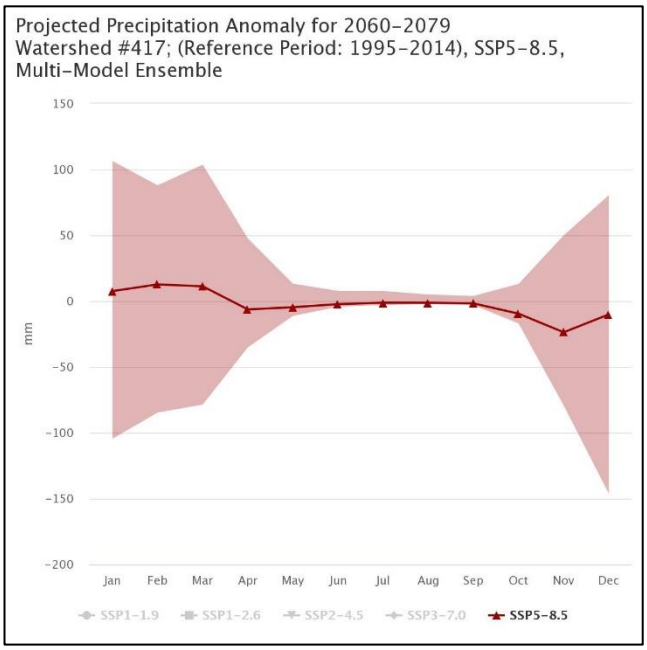

[Source: *(World Bank, 2022)*]

Figure 4-20: Projected precipitation Anomaly for 2060 -2079 (SSP 8.5)

From the graphs above, climatic projections up to the year 2079 indicate that in the optimistic emission scenario RCP 2.6, the annual rainfall is on average expected to

reduce moderately in the wet months and reduce significantly in the dry months of the year. On the other hand, for the pessimistic scenario RCP 8.5, the annual rainfall is on average expected to significantly increase over the wet months and significantly reduce over the dry months of the year.

4.5.4 Temperature future scenarios

Figure 4-21 and 4-22 show the projected climatology for mean temperature for SSP 2.6 and SSP 8.5 respectively. They also include historical reference data from 1914 to 1995.

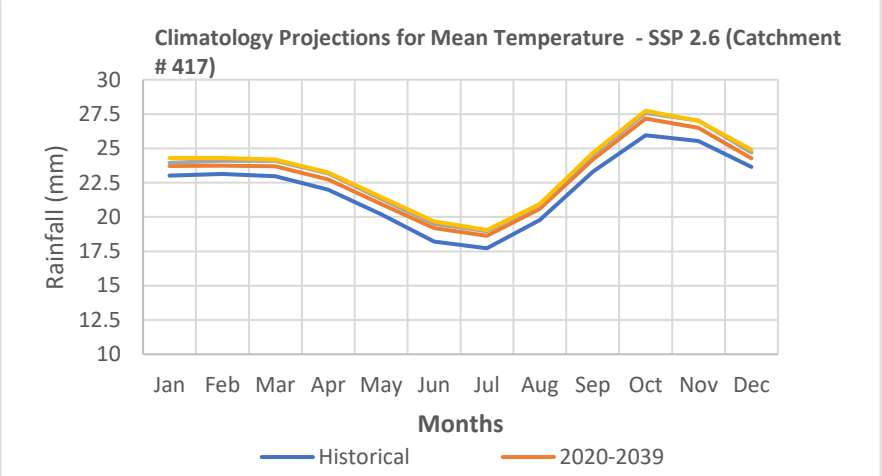

[Source: *(World Bank, 2022)*]

Figure 4-21: Climatology projections – Mean Temperature (SSP 2.6)

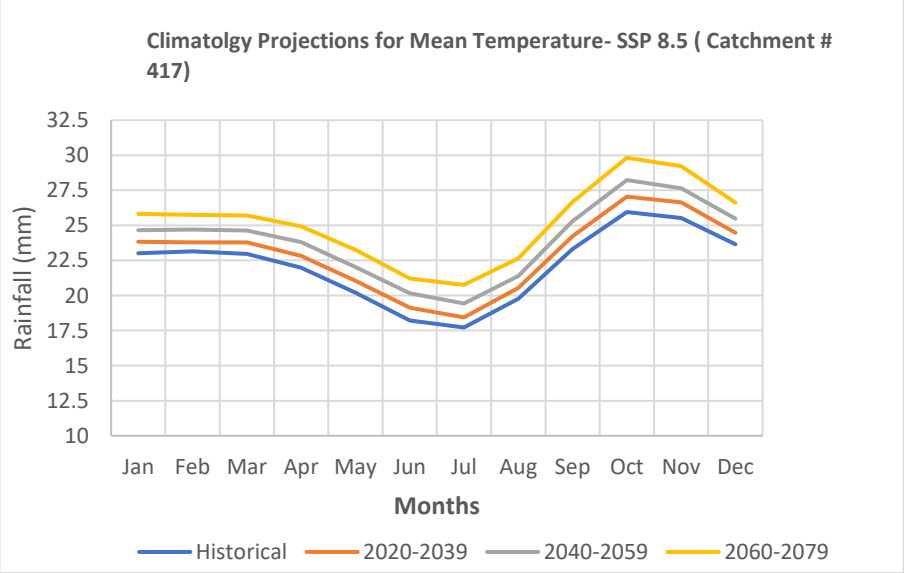

[Source: *(World Bank, 2022)*]

Figure 4-22: Climatology projections – Mean Temperature (SSP 8.5)

The changes in mean temperature can also be illustrated in terms of anomalies for the SSP 2.6 and SSP scenarios as shown from figure 4-23 to 4-28 below.

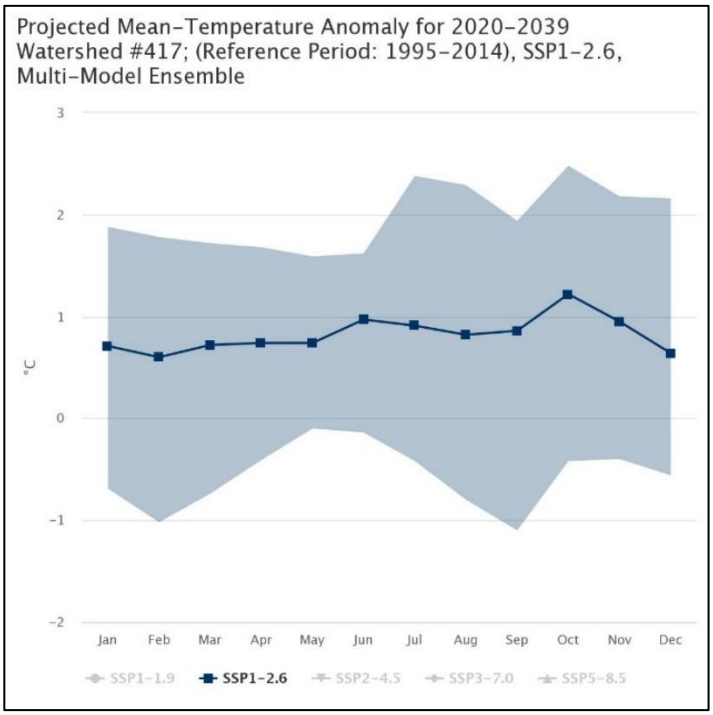

[Source: *(World Bank, 2022)*]

Figure 4-23: Projected Mean Temperature Anomaly for 2020 -2039 (SSP 2.6)

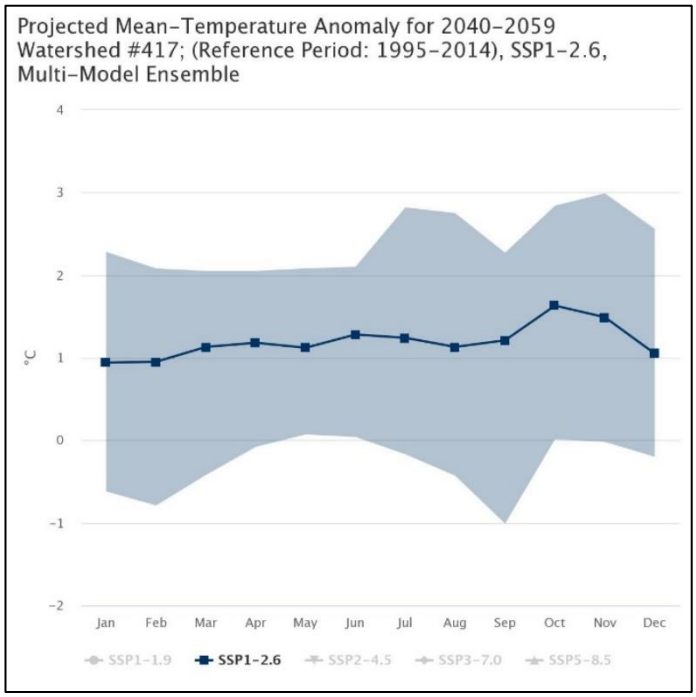

[Source: *(World Bank, 2022)*]

Figure 4-24: Projected Mean Temperature Anomaly for 2040 -2059 (SSP 2.6)

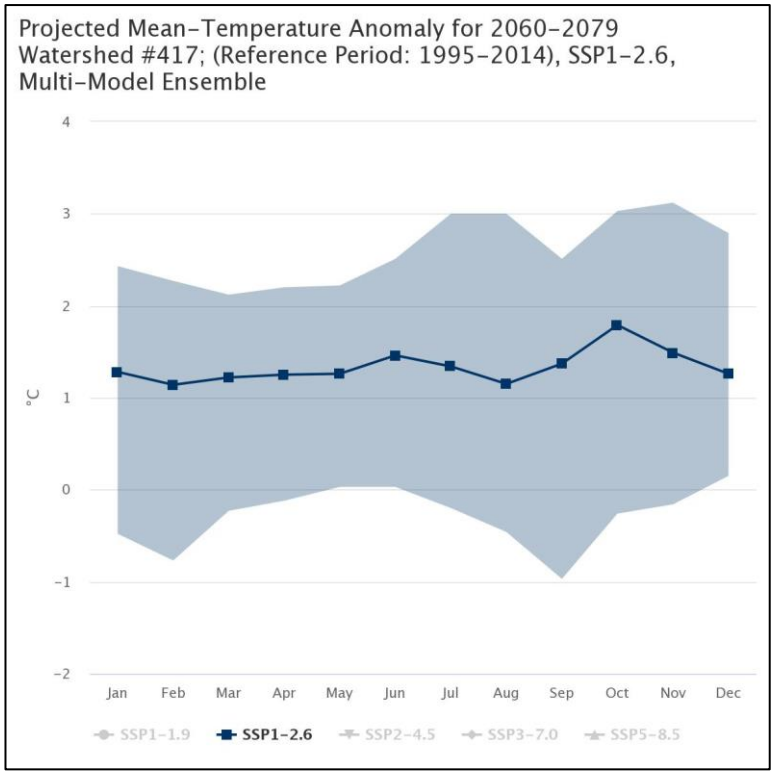

[Source: *(World Bank, 2022)*]

Figure 4-25: Projected Mean Temperature Anomaly for 2060 -2079 (SSP 2.6)

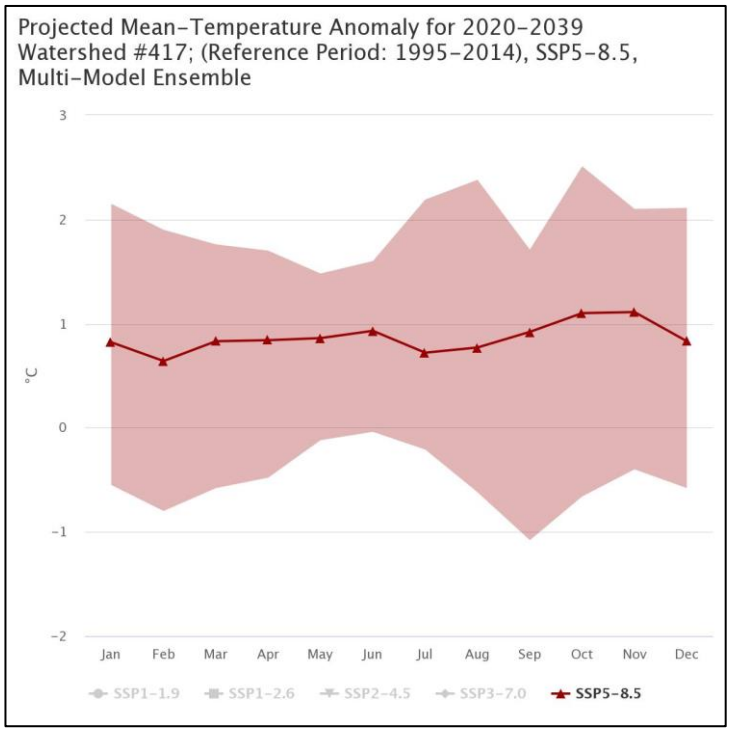

[Source: *(World Bank, 2022)*]

Figure 4-26: Projected Mean Temperature Anomaly for 2020 -2039 (SSP 8.5)

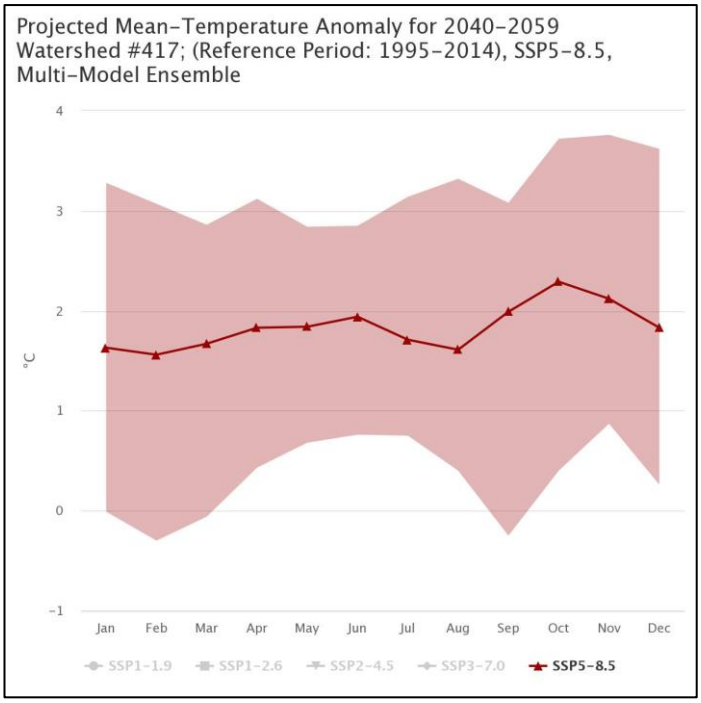

[Source: *(World Bank, 2022)*]

Figure 4-27: Projected Mean Temperature Anomaly for 2040 -2059 (SSP 8.5)

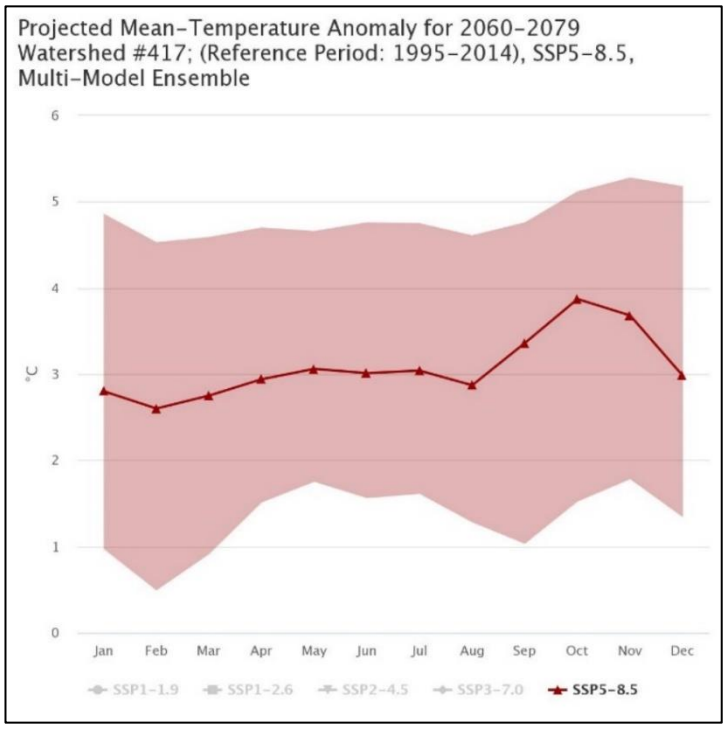

[Source: *(World Bank, 2022)*]

Figure 4-28: Projected Mean Temperature Anomaly for 2060 -2079 (SSP 8.5)

From the mean temperature climatology graphs above, projections to the year 2079 indicate that in the optimistic emission scenario SSP 2.6, mean annual temperatures are expected to rise significantly. In the pessimistic scenario SSP 8.5, the mean annual temperatures are expected to have a significantly higher increase compared to the SSP 2.6 scenario.

4.5.5 Climate test for proposed Mabula Kapi HPP

The calibrated Mabula Kapi PITMAN rainfall-runoff model was used to simulate runoff and understand how the runoff would be affected by the anticipated future climatic changes up to the year 2079. Since the model uses pan evaporation data as an input, temperature input data downloaded from the CKP was used in CROPWAT software to estimate reference crop evapotranspiration which was then converted to pan evaporation for use in the PITMAN model. Due to lack of sufficient data on pan evaporation factors, a Kpan factor of 0.7 was adopted in converting the estimated reference crop evapotranspiration to pan evaporation. The data sets used in rainfall-runoff modelling of future climatic conditions are listed below in Table 4-10:

Table 4-10: Input data – Future Climatology

(Source: Author's compilation)

S/N	Input Data Type	Description
1	Catchment area	Delineated using GIS software – 511 km2
2	Rainfall	• Historical reference precipitation for **1995 - 2014** period downloaded from the CKP of the world bank • Mean monthly precipitation for **2020-2039** period downloaded from the CKP of the World Bank • Mean monthly precipitation for **2040 - 2059** period downloaded from the CKP of the World Bank • Mean monthly precipitation for **2060 - 2079** period downloaded from the CKP of the World Bank

Table 4-10 Continued

S/N	Input Data Type	Description
3	Pan evaporation	• Pan evaporation estimated using reference crop evapotranspiration ○ Reference crop evapotranspiration calculated in CROPWAT software using minimum and maximum temperature projections for 2020 – 2039, 2040-2059 and 2060-2079 downloaded from the CKP of the world bank ○ Relative humidity, wind speed and sunshine hours used to calculate reference crop evapotranspiration are for Serenje meteorological station

The results for the Mabula Kapi Catchment hydrologic modelling are presented in Table 4-11 below. It should be noted that these are merely indicative results to be used to understand the proportionate impact of climate change on Mabula Kapi site.

It can be seen from the Table below that rainfall-runoff modelling was done comparing the performance of historical data and future climatic data in the model. Future climatic conditions were simulated for both the optimistic scenario SSP 2.6 and the pessimistic SSP 8.5.

Table 4-11: Results for future catchment hydrologic modelling of Mabula Kapi Catchment

(Source: Author's computation)

		Mean annual Runoff ($Mm^3/yr.$)	Mean Annual Flow (m^3/s)	30% PoE flow on FDC (m^3/s)
Historical (1995 -2014)		70.03	5.82	7.64
SSP 2.6	**2020 -2039**	64.58	5.37	7.64
	2040-2059	62.21	5.17	6.47
	2060-2079	60.84	5.05	5.81
SSP 8.5	**2020 -2039**	67.78	5.63	6.7
	2040-2059	63.91	5.3	6.18
	2060-2079	67.03	5.56	6.34

The results of the simulation can further be analysed by considering the percentage change expected with reference to the historical scenario. Tables 4-12 to 4-14 shows the expected percentage reductions in mean annual runoff, mean annual flow and the flow with 30% probability of exceedance.

Table 4-12: Percentage reduction of mean annual runoff

(Source: Author's computation)

		Mean annual Runoff ($Mm^3/yr.$)	% Reduction from historical mean annual runoff
Historical (1995 -2014)		70.03	
SSP 2.6	**2020 -2039**	64.58	7.75
	2040-2059	62.21	11.50
	2060-2079	60.84	13.10
SSP 8.5	**2020 -2039**	67.78	3.20
	2040-2059	63.91	8.70
	2060-2079	67.03	4.30

Table 4-13: Percentage reduction of mean annual flow

(Source: Author's computation)

		Mean Annual Flow (m^3/s)	% Reduction from historical mean annual flow
Historical (1995 -2014)		5.82	
SSP 2.6	**2020 -2039**	5.37	11.10
	2040-2059	5.17	11.16
	2060-2079	5.05	13.23
SSP 8.5	**2020 -2039**	5.63	3.26
	2040-2059	5.3	8.93
	2060-2079	5.56	4.46

Table 4-14: Percentage reduction of mean annual flow

(Source: Author's computation)

		30% PoE flow on FDC (m^3/s)	% Reduction from historical 30% PoE flow
Historical (1995 -2014)		7.64	
SSP 2.6	**2020 -2039**	7.64	0
	2040-2059	6.47	15.31
	2060-2079	5.81	23.95
SSP 8.5	**2020 -2039**	6.7	12.30
	2040-2059	6.18	19.10
	2060-2079	6.34	17.01

It can be seen from the above that power production at Mabula Kapi is likely to be impacted by the effects of climate change over its operation life. The operational period for Mabula Kapi is assumed to be 30 years. The mean annual runoff (volume) and the mean annual flow may reduce up to 11% in the SSP 2.6 scenario. However, being a run-of-river power plant, the main concern will be how climate change affects the flow duration. The simulation results indicate that the reduction in the discharge with 30% probability of exceedance is likely to be about 12% from 2020 to 2039 and 19 % from 2040 to 2059 in the pessimistic SSP 8.5 scenario, with reference to the historical time series. This translates to average annual energy reductions of 11 % during the life of the project as computed using RETscreen energy software. This reduction should be taken into account in the economic and financial analysis for the project.

5 Chapter 5: Conclusions and Recommendations

5.1 Conclusions

An accurate design discharge time series for Mabula Kapi catchment site has been predicted by using the rainfall-runoff modelling method, selected from a review of several statistical and empirical discharge prediction methods. The Author selected a computer-based rainfall-runoff model known as the PITMAN model to perform modelling and prediction of discharge for the Mabula Kapi catchment. The PITMAN model can create a conceptual representation of relevant processes and storages in a hydrologic catchment such as interception, soil moisture capacity, groundwater flow, wetlands, lakes, and attenuation in channel systems.

Data collected from a newly installed gauging station known as Manangwa gauging station made possible the calibration of the Mabula Kapi PITMAN model. Water levels and their corresponding discharges measured at Manangwa were used to derive a rating curve from which time series of observed discharge were computed from October 2019 to September 2021. Since this short-range time series would not be adequate for hydropower energy modelling, which typically requires a minimum period of 15 years, the PITMAN model was used to simulate longer time series. This was done by calibrating the model through the matching of the observed discharge with the simulated discharge time series. The simulated time series which ran from September 1981 to October 2021 were derived using satellite-based CHIRPS rainfall data. This is because CHIRPS data was found to have a good correlation with ground measured data from meteorological stations located in the vicinity of Mabula Kapi catchment.

Based on the simulated longer discharge time series from the model, the design discharge and the design flood for the proposed Mabula Kapi HPP were estimated as 5 m^3/s and 108 m^3/s respectively. Using the design discharge, the Installed Capacity was computed in RETscreen software to be 8.2 MW and the average annual energy output was found to be 38 GWh. These results are an improvement from the prefeasibility study done in 2018 where the installed capacity was estimated to be 7.4 MW and the annual energy as 34 GWh.

Climate risk assessments and tests were conducted on Mabula Kapi catchment and it was found that the catchment is likely to be affected by the impacts of climate change. The assessments were based on climate projections obtained from the Climate Knowledge Portal (CKP) of the World Bank. The CKP data sets are provided based on different greenhouse emission scenarios known as Shared Social Pathways (SSPs) or Representative Concentration Pathways (RCPs). The Author downloaded climate data projections for the optimistic SSP 2.6 and the pessimistic SSP 8.5 scenarios for assessment of Mabula Kapi site. Since the resolution of the CKP climate data sets is not as accurate as the CHIRPS data, the CKP data was only used for indicative purposes, to understand the proportionate change that may happen at Mabula Kapi site over the life of the project in terms mean annual runoff, (volume), mean annual flow, flow duration and annual energy production. The operational life of the small hydropower plant was assumed to be 30 years, which may run up to the year 2059.

Hydrologic modelling was done using the PITMAN model to simulate future runoff. Rainfall data from CKP was directly used as an input to the model. However, since the PITMAN model uses average pan evaporation values instead of evapotranspiration values, minimum and maximum temperature data downloaded from the CKP was first imputed in CROPWAT software for calculation of reference crop evapotranspiration. The reference crop evapotranspiration was then converted into pan evaporation and used in the PITMAN model for simulation of average future runoff conditions for 2020 -2039, 2040 -2059 and 2060 -2079.

Mabula Kapi is likely to be impacted by the effects of climate change over its operation life. The mean annual runoff (volume) and the mean annual flow may reduce up to 11% in the SSP 2.6 scenario. However, being a run-of-river power plant, the main concern will be how climate change affects the flow duration. The simulation results indicate that the reduction in the discharge with 30% probability of exceedance is likely to be about 12% from 2020 to 2039 and 19 % from 2040 to 2059 in the pessimistic SSP 8.5 scenario, with reference to the historical time series. This translates to average annual energy reductions of 11 % during the life of the project as computed using RETscreen energy software.

5.2 Recommendations

Section 3.2 of this report discussed the derivation of the discharge rating curve. The rating curve was derived using eight (8) measured corresponding values of discharge and stage. It was observed that most measurements were taken in the lower ranges of stage. More discharge measurements are required to fully cover the upper ranges of stage at Manangwa gauging station. It is therefore recommended that KGRTC conduct additional streamflow measurements in the flood season to improve the accuracy of the rating curve.

Section 4.5 of this report discussed climate risk assessment for the proposed Mabula Kapi HPP. It is understood that the proposed Mabula Kapi HPP is likely to be impacted by the effects of climate change over its operation life. The mean annual energy may reduce by 11% over the life of the project. It is therefore recommended that the economic and financial analysis take into account the anticipated energy reduction.

In this study, a hydrologic model has been established and calibrated using the PITMAN model. However, validation of the model was not done due to limited observed discharge time series. It is therefore recommended that validation be conducted in future as more and more observed discharge data becomes available.

6 References

Alam, J. & Mohammad, M., 2018. *A Spreadsheet Approach for Prediction of Rating Curve Parameters,* Uttar Pradesh: Springer Nature.

Bedient, Huber & Baxter, 2013. *Hydrology and Floodplan Analysis.* 5th ed. Reading: PEARSON.

Boiten, W., 2003. *Hydrometry.* Paperpack ed. Delft: A. A. Balkema.

Davie, T., 2008. *Fundamentals of Hydrology.* 2nd ed. London: Routledge.

DeCoursey, W., 2013. *Statistics and Probability for Engineering Applications.* 1st ed. Newyork: Newness.

Desert Research Institute, 2021. *Climate engine.* [Online]
Available at: https://app.climateengine.com/climateEngine
[Accessed 9 October 2021].

Devore, J., 2012. *Probability and Statistics for Engineering and Sciences.* 8th ed. Boston: CENGAGE Learning.

EDF-GIBB, 2019. *Prefeasibility Study Report for Luapula River Hydropower Development* , Johanesburg: EDF-GIBB.

Eijkelkamp, 2009. *Evaporation Pan,* Giesbeek: Eijkelkamp.

Eldho, T., 2015. *Hydrologic Modelling.* Mumbai: Indian Institute of Technonolgy Bombay.

ESHA, 2004. *Guide on How to Develop a Small Hydropower Plant,* Brussels: s.n.

FICHTNER, 2015. *Hydroelectric Power - A Guide for Developers and Investors,* Germany: International Finance Corporation.

Food and Agriculture Organization of the United Nations, 2021. *FAO.* [Online]
Available at: https://www.fao.org/3/x0490e/x0490e08.htm#pan%20evaporation%20method
[Accessed 1 November November 2021].

Government of Alberta, 2020. *Peace River Flood Study,* Alberta: Government of Alberta.

Hamududu, S., 2021. *Assessing impacts of Climate change on Hydropower Batoka GHES Case: Zambezi River*. Trondheim, International Centre for Hydropower.

Helsel & Hirsch, 2002. *Statistical Methods in Water Resources.* 1st ed. Newyork: US Geological Survey.

Hughes, D., Andersson , J. & Wilk, J., 2006. *Regional Calibration of the Okavango River,* Johannesburg: J. Hydro.

IHA, 2019. *Hydropower Climate Resilience Guide,* London: IHA.

IIT, 2008. *Water Resources Engineering,* Kharagpur: Indian Institute of Technology.

INSHP, 2019. *Technical Guidelines for the Development of Hydropower Plants (Part 2) - Hydrology*. Hangzhou: UNIDO.

Irish Aid, 2018. *Zambia Climate Risk Screening Report,* Belfast: Resilience and Economic Inclusion Team, Policy Unit.

Jha, R. & Smakhtin, V., 2008. *A Review of Methods of Hydrological Estimation at Ungauged Sites in India,* Delhi: IWMI.

JICA, 1995. *National Water Resources Master Plan for Zambia,* Tokyo: Ministry of Energy and Water Resources Development .

Johnson, L., 2009. *Geogpahic Information Systems in Water Resources Engineering.* 1st ed. London: CRC Press.

KGRTC, 2021. *Mission Report: 3rd Flow Measurement - Mabula Kapi Small Hydropower Project Site,* Lusaka: Kafue Gorge Regional Training Center.

Mwelwa, E., 2004. *The Application of the monthly time step Pitman Rainfall-Runoff,* Grahamstown: Rhodes University.

NASA, 2021. *Alaska Satelite Facility.* [Online]
Available at: https://asf.alaska.edu/data-sets/derived-data-sets/alos-palsar-rtc/alos-palsar-radiometric-terrain-correction/
[Accessed 10th November 2021].

New Zealand Government, 2018. *Climate Change Projections for New Zealand,* Manatu Mo Te Taiao: Ministry for the Environment.

Novak, P., Moffat, A., Naluri, C. & Narayanan, R., 2007. *Hydraulic Structures.* 4th ed. London: Taylor & Francis.

Nruthya, K. & Srinivas, V., 2015. *Evaluating Methods to Predict Streamflow at Ungauged Sites using Regional Flow Duration Curves: A Case Study.* Bangalore, ELSEVIER.

Pitman , B. & Bailey, A., 2012. *Water Resources of South Africa 2012 Study,* Johannesburg: RoyalHaskoningDHV.

Pitman & Bailey, 2021. *Can CHIRPS fill the gap left by the decline in the availability of.* Johannesburg, Bailey and Pitman Water Resources (PTY) Ltd.

Pitman, B., Bailey, K. & Kakebeeke, J., 2015. *Users Manual - WRSM/PITMAN Water Resources Simulation Model for Windows,* Johannesburg: Royal HaskoningDHV.

Rainville, F. et al., 2016. *Hydrometric Manual – Data Computations,* Toronto: Water Survey of Canada.

Raphael , M., Tshimanga & Hughes , D., 2014. *Basin-scale performance of a semidistributed rainfall-runoff model for hydrological predictions and water resources assesement of large rivers: The Congo River,* Johannesburg: Advancing Earth and Space Science.

Republic of Zambia, 2015. *2015 Living Conditions Monitoring Survey Report* , Lusaka: Central Statistical Office.

Republic of Zambia, 2016. *Report of the Committee on Lands, Environment and Tourism on the National Assembly Approval to Ratify the Paris Agreement on Climate Change,* Lusaka: National Assembly of Zambia.

RETScreen International , 2004. *RETSceen Software Online User Manual,* Ottawa: Minister of Natural Resources Canada.

RMetS, 2018. Validation of the CHIRPS satellite rainfall estimates over eastern Africa. *Quaterly Journal of the Royal Meteorological Society,* 1(10.1002/qj.3244), pp. 1-21.

Singh, V. P., 1995. *Computer Models for Watershed Hydrology,* Colorado: Water Resouces Publications.

Sitterson, J. et al., 2017. *An Overview of Rainfall-Runoff Model Types,* Athens: United States Environmental Protection Agency.

Stretta, E., 1983. *Problems of Water Resources in Zambia ,* Lusaka: UNESCO.

Subramanya, K., 2008. *Engineering Hydrology.* 3rd ed. New Delhi: The McGrawHill Companies.

Tilrem, O., 1997. *Manual on Procedures in Operational Hydrology,* Oslo: Norwegian Water Resources and Energy Administration - NVE.

Tokyo Electric Power Company, 2008. *Rural Electrification Master Plan for Zambia 2008 - 2030,* Tokyo: JICA.

Wilson D, L. D. H. L. E., 2011. *A Review of NEV's Flood Frequency Estimation Procedures,* Oslo: Norwegian Water Resources and Energy Directorate.

World Bank, 2022. *Climate Change Knowledge Portal.* [Online]
Available at: https://climateknowledgeportal.worldbank.org
[Accessed 10 July 2022].

World Meteorological Organization , 2010. *Manual On Stream Gauging,* Geneva: WMO.

Yilmaz, M. & Onoz, B., 2020. *A Comparative Study of Statistical Methods for Daily Streamflow Estimation at Ungauged Basins in Turkey.* Istanbul, MDPI.

ZESCO, 2018. *Prefeasibility Study for Kaombe Hydropower Potential Site,* Lusaka: ZESCO.

7 Appendices

7.1 Appendix 1: Ethical Approval Letter

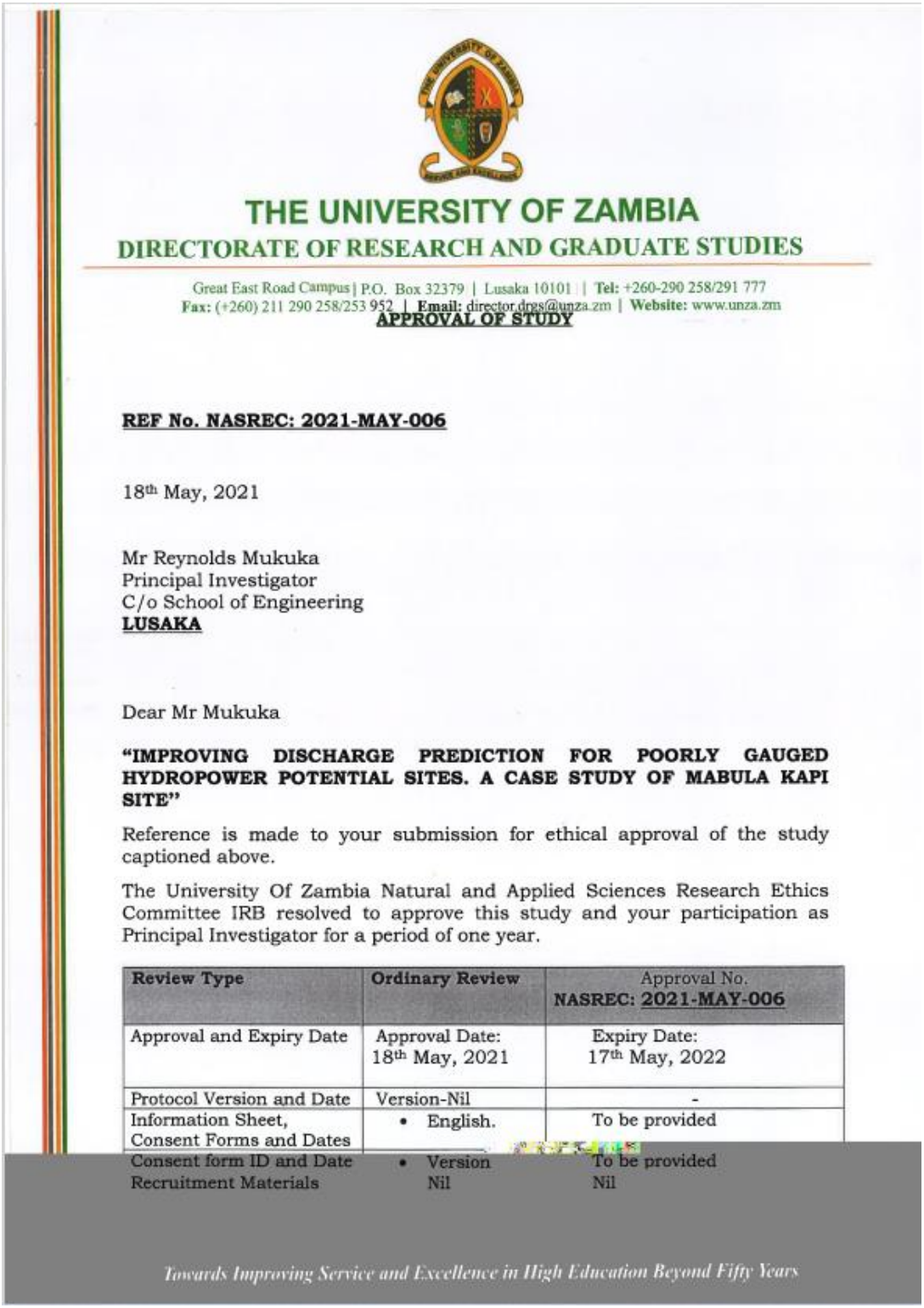

THE UNIVERSITY OF ZAMBIA

DIRECTORATE OF RESEARCH AND GRADUATE STUDIES

Great East Road Campus | P.O. Box 32379 | Lusaka 10101 | **Tel:** +260-290 258/291 777
Fax: (+260) 211 290 258/253 952 | **Email:** director.drgs@unza.zm | **Website:** www.unza.zm

APPROVAL OF STUDY

REF No. NASREC: 2021-MAY-006

18th May, 2021

Mr Reynolds Mukuka
Principal Investigator
C/o School of Engineering
LUSAKA

Dear Mr Mukuka

"IMPROVING DISCHARGE PREDICTION FOR POORLY GAUGED HYDROPOWER POTENTIAL SITES. A CASE STUDY OF MABULA KAPI SITE"

Reference is made to your submission for ethical approval of the study captioned above.

The University Of Zambia Natural and Applied Sciences Research Ethics Committee IRB resolved to approve this study and your participation as Principal Investigator for a period of one year.

Review Type	**Ordinary Review**	Approval No. **NASREC: 2021-MAY-006**
Approval and Expiry Date	Approval Date: 18th May, 2021	Expiry Date: 17th May, 2022
Protocol Version and Date	Version-Nil	-
Information Sheet, Consent Forms and Dates	• English.	To be provided
Consent form ID and Date	• Version Nil	To be provided Nil
Recruitment Materials		

Towards Improving Service and Excellence in High Education Beyond Fifty Years

Specific conditions will apply to this approval. As Principal Investigator it is your responsibility to ensure that the contents of this letter are adhered to. If these are not adhered to, the approval may be suspended. Should the study be suspended, study sponsors and other regulatory authorities will be informed.

Conditions of Approval

- No participant may be involved in any study procedure prior to the study approval or after the expiration date.
- All unanticipated or Serious Adverse Events (SAEs) must be reported to NASREC within 5 days.
- All protocol modifications must be approved by NASREC prior to implementation unless they are intended to reduce risk (but must still be reported for approval). Modifications will include any change of investigator/s or site address.
- All protocol deviations must be reported to NASREC within 5 working days.
- All recruitment materials must be approved by NASREC prior to being used.
- Principal investigators are responsible for initiating Continuing Review proceedings. HSSRECwill only approve a study for a period of 12 months.
- It is the responsibility of the PI to renew his/her ethics approval through a renewal application to NASREC.
- Where the PI desires to extend the study after expiry of the study period, documents for study extension must be received by NASREC at least 30 days before the expiry date. This is for the purpose of facilitating the review process. Documents received within 30 days after expiry will be labelled "late submissions" and will incur a penaltyfee of K500.00. No study shall be renewed whose documents are submitted for renewal 30 days after expiry of the certificate.
- Every 6 (six) months a progress report form supplied by The University of Zambia Humanities and Social Sciences Research Ethics Committee as an IRB must be filled in and submitted to us. There is a penalty of K500.00 for failure to submit the report.
- When closing a project, the PI is responsible for notifying, in writing or using the Research Ethics and Management Online (REMO),both NASREC and the National Health Research Authority (NHRA) when ethics certification is no longer required for a project.
- In order to close an approved study, a Closing Report must be submitted in writing or through the REMO system. A Closing Report should be filed when data collection has ended and the study team will no longer be using human participants or animals or secondary data or have any direct or indirect contact with the research participants or animals for the study.

- Filing a closing report (rather than just letting your approval lapse) is important as it assists NASREC in efficiently tracking and reporting on projects. Note that some funding agencies and sponsors require a notice of closure from the IRB which had approved the study and can only be generated after the Closing Report has been filed.
- A reprint of this letter shall be done at a fee.
- All protocol modifications must be approved by NASREC by way of an application for an amendment prior to implementation unless they are intended to reduce risk (but must still be reported for approval). Modifications will include any change of investigator/s or site address or methodology and methods. Many modifications entail minimal risk adjustments to a protocol and/or consent form and can be made on an Expedited basis (via the IRB Chair). Some examples are: format changes, correcting spelling errors, adding key personnel, minor changes to questionnaires, recruiting and changes, and so forth. Other, more substantive changes, especially those that may alter the risk-benefit ratio, may require Full Board review. In all cases, except where noted above regarding subject safety, any changes to any protocol document or procedure must first be approved by NASREC before they can be implemented.

Should you have any questions regarding anything indicated in this letter, please do not hesitate to get in touch with us at the above indicated address.

On behalf of NASREC, we would like to wish you all the success as you carry out your study.

Yours faithfully,

Dr. E. Mwanaumo

CHAIRPERSON
THE UNIVERSITY OF ZAMBIA NATURAL AND APPLIED SCIENCES
RESEARCH ETHICS COMMITTEE IRB

cc Director, Directorate of Research and Graduate Studies
Assistant Registrar (Research), Directorate of Research and Graduate Studies
Acting Senior Administration (R), Directorate of Research and Graduate Studies

7.2 Appendix 2: Article Publication Acceptance Letter

Gmail

Reynolds Mukuka <rmukuka22@gmail.com>

Paper Acceptance Notification for Paper ID "IJISRT23FEB1183"

1 message

Ijisrt digital library <editor@ijisrt.com> Mon, Feb 27, 2023 at 1:52 PM
Reply-To: "ijisrt@gmail.com" <ijisrt@gmail.com>
To: rmukuka22@gmail.com
Cc: ijisrt@gmail.com

Hello Author ,

Greetings of the day .....

Paper ID: *"IJISRT23FEB1183"*

Paper Title: *"IMPROVING DISCHARGE PREDICTION FOR POORLY GAUGED HYDROPOWER POTENTIAL SITES – A CASE STUDY OF MABULA KAPI SITE"*

Congratulations.....

We are happy to inform you that your research paper has been "Accepted" for publishing in "International Journal of Innovative Science and Research Technology". After completion of the registration processes, your research paper will be available on IJISRT official website in Volume 8 - 2023 - Issue 2 - February.

Registration Amount :- 50 $

Submit Publication Fee :-

You can Pay by Debit Card / Credit Card / Net Banking . For Submit Registration Fee click at given Link.

https://ijisrt.com/ijisrt-foreign-gateway

OR

If you are not able to submit your registration fee via given link then you may use below payment link.

https://pages.razorpay.com/ijisrt

OR

Bank Details

A/C Number :- 430305500051

A/C Holder Name :- IJISRT PUBLICATION

Swift Code :- ICICINBBNRI

IFSC Code :- ICIC0004303

Bank :- ICICI

A/C type :- Current

Country :- India

City :- Jaipur

Street :- Patrakar Colony

Purpose Code :- P1017

(Important) In order to the complete registration you must finish following steps.

1. Download and complete the Copyright Form enclosed in this mail. In the Attachment , you will get Pdf/.Doc both Format. You can download as per suitable format.

2. Login and submit Copyrightform, Payment Slip and Paper (.doc, .docx) till the last date.

Important Dates:-

Last Date For Submission of Registration Fee ,Copyright Form and Paper :- 07/03/2023(DD/MM/YYYY)

For any query please login to account and use Help & Support.

Click here for Login.

Thanks.

Yours sincerely,
Editor-in-Chief International Journal of Innovative Science and Research Technology(IJISRT)
www.ijisrt.com
ISSN No :- 2456-2165
Impact Factor :- 6.253

2 attachments

1624772649.pdf
40K

1624772649.docx
117K

7.3 Appendix 3: Author Certificate by IJISRT

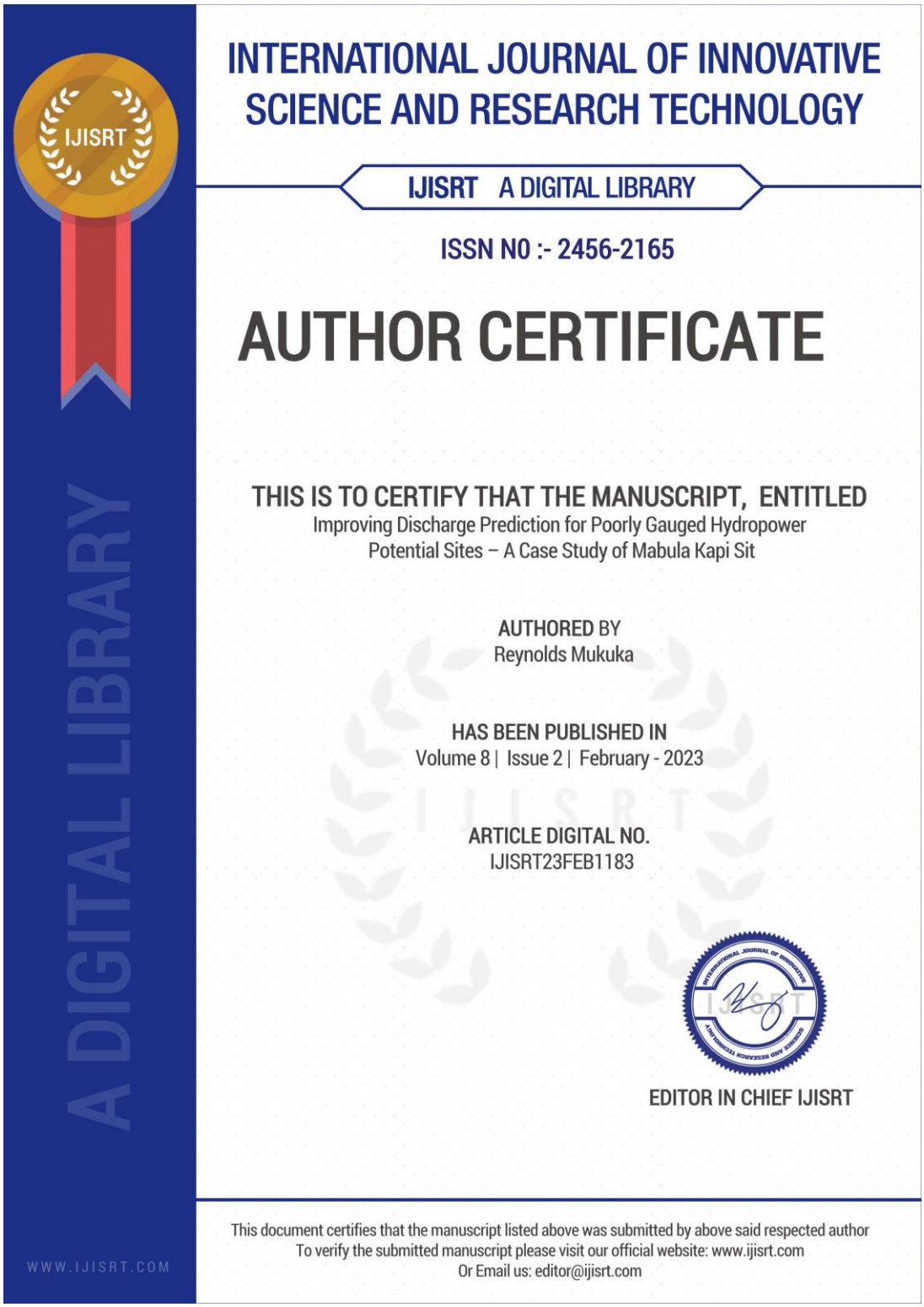

INTERNATIONAL JOURNAL OF INNOVATIVE SCIENCE AND RESEARCH TECHNOLOGY

IJISRT A DIGITAL LIBRARY

ISSN NO :- 2456-2165

AUTHOR CERTIFICATE

THIS IS TO CERTIFY THAT THE MANUSCRIPT, ENTITLED

Improving Discharge Prediction for Poorly Gauged Hydropower Potential Sites – A Case Study of Mabula Kapi Sit

AUTHORED BY

Reynolds Mukuka

HAS BEEN PUBLISHED IN

Volume 8 | Issue 2 | February - 2023

ARTICLE DIGITAL NO.

IJISRT23FEB1183

EDITOR IN CHIEF IJISRT

This document certifies that the manuscript listed above was submitted by above said respected author
To verify the submitted manuscript please visit our official website: www.ijisrt.com
Or Email us: editor@ijisrt.com

A DIGITAL LIBRARY

WWW.IJISRT.COM

7.4 Appendix 4: RETScreen Hydro Turbine Analysis Results

RETScreen Energy Model - Power project ☐ Show alternative units

Proposed case power system

Technology		Hydro turbine
Analysis type		○ Method 1 ⊙ Method 2
Resource assessment		
Proposed project		Run-of-river
Hydrology method		User-defined
Gross head	m	203.0
Maximum tailwater effect	m	0.00
Residual flow	m³/s	0.580
Percent time firm flow available	%	90.0%
Firm flow	m³/s	0.85
Hydro turbine		
Design flow	m³/s	5.000
Type		Pelton
Turbine efficiency		Standard
Number of jets for impulse turbine	jet	2
Number of turbines		3
Manufacturer		
Model		
Efficiency adjustment	%	0.0%
Turbine peak efficiency	%	89.7%
Flow at peak efficiency	m³/s	3.3
Turbine efficiency at design flow	%	88.1%

See product database

Show figure

%	Flow m³/s	Turbine efficiency	Number of turbines	Combined efficiency
0%	88.67	0.00	0	0.00
5%	20.14	0.16	1	0.66
10%	12.29	0.47	1	0.87
15%	9.13	0.66	1	0.90
20%	7.69	0.77	1	0.90
25%	6.20	0.84	1	0.90
30%	5.02	0.87	1	0.90
35%	4.12	0.89	2	0.90
40%	3.73	0.89	2	0.90
45%	3.49	0.90	2	0.90
50%	3.18	0.90	2	0.90
55%	2.79	0.90	2	0.90
60%	2.66	0.90	2	0.90
65%	2.32	0.90	2	0.89
70%	2.20	0.90	3	0.90
75%	1.93	0.90	3	0.90
80%	1.86	0.90	3	0.90
85%	1.52	0.90	3	0.90
90%	1.43	0.90	3	0.90
95%	1.30	0.89	3	0.89
100%	1.13	0.88	3	0.88

Show figure

Maximum hydraulic losses	%	4.0%	
Miscellaneous losses	%	0.0%	
Generator efficiency	%	97.0%	
Availability	%	90.0%	
Summary			Firm
Power capacity	kW	8,173	1,470
Available flow adjustment factor		1.00	
Capacity factor	%	52.8%	
Electricity exported to grid	MWh	37,786	
Electricity export rate	$/MWh		

7.5 Appendix 5 : Simulated Times Series for Mabula Kapi Catchment

Table 7-1: Simulated Time Series for Mabula Kapi Catchment

(Source: Author's computation)

	Oct	Nov	Dec	Jan	Feb	Mar	Apr	May	Jun	Jul	Aug	Sep
1991	1.31	1.26	4.49	5.93	3.73	3.51	3.45	2.92	2.50	2.14	1.83	1.52
1992	1.19	1.13	3.88	7.30	9.64	14.60	11.04	3.79	3.22	2.73	2.31	1.91
1993	1.50	1.78	2.32	5.47	8.04	5.64	3.53	3.05	2.59	2.20	1.88	1.56
1994	1.28	1.14	1.59	5.39	8.87	6.46	3.68	3.20	2.70	2.30	1.96	1.62
1995	1.29	1.14	4.58	8.43	12.50	14.20	8.15	3.74	3.15	2.67	2.27	1.88
1996	1.49	1.22	2.86	4.48	8.48	8.23	3.80	3.48	3.01	2.55	2.17	1.79
1997	1.44	1.93	20.14	27.69	11.29	4.92	4.50	3.75	3.18	2.70	2.29	1.89
1998	1.50	1.31	3.34	10.15	10.35	6.92	6.08	3.77	3.19	2.70	2.29	1.89
1999	1.49	1.33	2.09	4.37	6.14	9.01	7.83	3.69	3.12	2.64	2.25	1.86
2000	1.48	1.88	5.72	14.85	16.42	9.13	5.10	3.74	3.17	2.68	2.28	1.88
2001	1.51	1.32	3.98	7.84	7.07	4.59	3.80	3.27	2.77	2.35	2.00	1.66
2002	1.32	1.16	14.77	17.62	7.01	9.53	7.99	3.76	3.18	2.70	2.29	1.89
2003	1.50	1.30	3.72	6.37	6.20	5.70	4.72	3.56	3.03	2.57	2.19	1.81
2004	1.42	1.94	33.07	41.00	30.04	22.94	4.06	3.52	2.98	2.53	2.15	1.78
2005	1.40	1.28	2.08	7.68	10.34	7.45	5.40	3.71	3.15	2.67	2.27	1.88
2006	1.48	1.44	13.42	43.68	88.67	60.07	4.47	3.75	3.18	2.69	2.29	1.89
2007	1.50	1.34	12.22	19.61	11.42	5.53	4.12	3.57	3.01	2.56	2.17	1.80
2008	1.42	1.29	10.19	12.95	6.76	7.25	6.00	3.85	3.28	2.78	2.36	1.95
2009	1.53	2.08	21.67	24.06	36.38	42.77	12.21	3.73	3.15	2.67	2.27	1.87
2010	1.48	1.27	11.32	15.96	8.46	5.82	4.65	3.72	3.15	2.67	2.27	1.87
2011	1.49	1.37	2.68	8.54	9.89	7.19	5.92	3.78	3.20	2.72	2.31	1.90
2012	1.53	1.36	5.06	8.94	8.18	5.90	4.22	3.59	3.05	2.59	2.20	1.82
2013	1.44	1.28	7.19	11.22	11.29	9.08	4.52	3.81	3.24	2.75	2.33	1.92
2014	1.52	1.24	1.50	5.01	9.84	7.69	3.70	3.28	2.81	2.38	2.03	1.68
2015	1.33	1.36	3.99	5.80	4.72	6.29	6.07	3.53	2.98	2.53	2.15	1.78
2016	1.41	1.25	2.22	7.81	25.16	21.34	4.46	3.81	3.23	2.74	2.33	1.92
2017	1.54	2.36	12.67	13.21	7.17	7.34	4.38	3.73	3.19	2.70	2.30	1.90
2018	1.49	1.29	13.80	19.68	24.50	23.35	7.40	3.79	3.21	2.72	2.31	1.91
2019	1.51	1.43	2.00	8.46	12.29	7.10	3.86	3.36	2.85	2.42	2.06	1.71
2020	1.37	1.19	5.02	9.70	18.90	27.34	15.73	3.74	3.16	2.68	2.27	1.88

7.6 Appendix 6: Rainfall time series for local stations

Table 7-2: Serenje rainfall time series

(Source: ZMD)

Year	Jan	Feb	Mar	Apr	May	Jun	Jul	Aug	Sep	Oct	Nov	Dec
1981	124.6	179.5	190.1	26.4	0	0	0	0	0	0.5	86.4	102.3
1982	367.7	287.2	24.2	42.6	22.6	0	0	0	0	12.4	162	168.2
1983	295	248.5	14.2	21.8	1.2	0	2.7	0	0	0	55.8	242.6
1984	304.8	174.9	166.3	6.6	0	0	0	0	0	1.3	124.1	387.5
1985	231.4	299.2	146.1	68.2	2	299.1	0	0	0	13.7	143.4	221.4
1986	326	302.6	152.8	125.5	0	0.3	0	0	0	34.8	68.2	243.6
1987	436.6	142.4	132.3	28.4	0	0	0	0	0	0	102.9	197.2
1988	278.3	335.2	253.4	49.3	0.2	0	0	0	0	20.8	29	164.5
1989	394.3	201.7	187.1	27.7	0	0	0	0	0	4.5	60.8	317.2
1990	339.5	158.7	90.1	72.1	17.7	9	0	0.4	0	0	33.2	180.5
1991	313.2	193.7	45.3	47.1	9.8	0	0	0	0	48.6	74.9	236.9
1992	127.4	118.9	156.5	0.7	4.8	0	0	0	0	0	170.1	291.9
1993	389.7	261.1	185.9	57.3	0	0	0	0	0	0	156.1	99.7
1994	215.4	271.3	3.5	12.8	0	0	0	0	0	111.4	62.3	157.2
1995	185.9	152	68.5	7.7	0	0	0	0	0	3.6	28.6	179.1
1996	206.9	182.6	99.6	10.1	31	0	0	0	1.7	0	74.8	262.1
1997	257.7	266.3	55.9	111.2	0	0	2.3	0	21	5.9	145	383.2
1998	232	91	142.1	0.5	0	0	0	0	0	3	98.7	131.7
1999	238.1	270.5	333.8	4.8	0	0	0	0	0	0	67.8	170.9
2000	237.3	257.6	206.3	6.5	2.3	0	0	0	0	0.9	183	305.1
2001	363	221.1	178.4	47.1	0	0	0	0	0	0	0	229.2
2002	239.9	170.7	199.2	37.6	0	0	0	0	1.4	5.7	47.7	297.8
2003	112.8	259.6	187.1	72.6	0	0	1.9	0	0	29.3	24.6	139.6
2004	300.6	239.6	186.2	84.3	0	0	0	0	0	0	84.1	310.8
2005	346	106	83	0	0	0	5	0	3.3	0	15.6	513.6
2006	318.7	189.9	268.1	2.7	0	0	0	0	0	34.9	86	334.2
2007	361.8	246.4	107.1	15.3	0	0	0	0	2.7	11.7	-	-
2008	185.4	223	72.2	0	0	0	0	0	-	0.5	121.4	201.9
2009	291.5	400.7	254.4	31.6	0	0	0	0	0	0.5	189.3	170.3
2010	182.4	274.5	250.2	9.1	0	0	0	0.5	0	0	187.7	296.1
2011	235	132	266.2	25.1	0	-	-	0	0	-	74.1	128.5
2012	345.5	284.9	291.3	38.7	0	0	0	-	-	-	-	-
2013	-	-	-	-	-	-	-	-	-	-	-	-
2014	-	-	-	-	-	-	-	-	-	-	-	-
2015	-	-	-	-	-	-	-	-	-	-	-	-
2016	171.1	205	283.8	6.3	-	0	0	0	0	0	56.1	124.2
2017	-	-	-	-	-	-	0	0	0	9.2	247.3	195.3

Table 7-3: Kabwe station rainfall time series

(Source: ZMD)

Year	Jan	Feb	Mar	Apr	May	Jun	Jul	Aug	Sep	Oct	Nov	Dec
1981	274.9	281.5	165	85.1	0	0	0	0	0	0	90.4	35.2
1982	271.6	237.2	16.6	22.5	17.4	0	0	0	0	29.1	130.2	96.7
1983	318.9	183	174.2	64.2	1.1	0	0	0	0	18	105.2	199.4
1984	87.6	176.8	136.4	7.5	0	0	0	0	0	0	104.5	442.5
1985	247.8	181.6	191.1	10	3.9	0	0	0	0	29.2	53.5	316.7
1986	356	126.5	114.4	116.9	0	0	0	0	0	25.3	52.6	153
1987	286.7	34.9	50.3	0	0	0	0	0	0	1.3	20.4	264.8
1988	179.2	134.3	70.2	0	0	0	0	0	0	53.2	55.2	167.4
1989	245.7	262.5	94.6	0	0	0	0	0	0	0	48	141.7
1990	368.7	215.9	65.1	23.3	13.4	0	0	0	0	0	64.2	183.6
1991	326.1	180.7	42.3	0	0	0	0	0	0	31.9	45.7	81.3
1992	113.3	64.4	132.3	29.9	0	0	0	0	0	0.5	98	290
1993	225.8	188.6	136.5	34.5	0	0	0	0	2.6	98.3	-	91.9
1994	229.8	295.8	1.5	0.2	0	0	0	0	0	43.4	18.3	122.1
1995	170.3	148.8	10.7	0	0	0	0	0	0	-	-	-
1996	170.3	192.4	224.5	0.7	37.1	0	0	0	0	0	166	407.8
1997	290.1	178.8	151.1	133.7	0	0	0	0	5.7	0	167.9	407.8
1998	-	-	-	-	-	-	-	-	-	-	-	-
1999	-	-	-	-	-	-	-	-	-	0	-	-
2000	-	-	-	0	-	-	-	0	0	0	208	-
2001	-	-	-	-	-	-	-	-	-	-	-	-
2002	122.6	66.7	26.7	44.1	0	0	0	0	1.6	19.9	90.9	307
2003	-	328	202.2	3.1	0	0	0	0	0	20.8	87.7	221.8
2004	261.1	214.2	105.4	18.1	0	0	0	0	-	-	-	-
2005	-	-	-	-	-	-	-	-	-	-	-	-
2006	-	-	-	-	-	-	-	-	-	-	-	-
2007	-	-	-	-	-	-	-	-	-	-	-	-
2008	-	-	-	-	-	-	-	-	-	-	-	-
2009	-	-	-	0	70.4	0	0	0	0	3.1	171.4	103.6
2010	143.1	426.5	63.5	0	0	0	-	-	-	-	-	-
2011	299.4	47.4	-	-	-	-	-	-	-	-	-	-
2012	-	-	-	-	-	-	-	-	-	-	-	-
2013	-	-	-	-	-	-	-	-	-	-	-	-
2014	-	-	-	-	-	-	-	-	-	-	-	-
2015	-	-	-	-	-	-	0	0	0	0	31.3	-

Table 7-4: Mkushi station rainfall time series

(Source: ZMD)

Year	Jan	Feb	Mar	Apr	May	Jun	Jul	Aug	Sep	Oct	Nov	Dec
1993	282.5	304.3	336.9	63.1	0	0	0	0	0	18.3	59.5	193.8
1994	469.3	210.4	11.6	30.4	0	0	0	0	7.2	115.9	38.7	149.5
1995	177.7	277.1	90.5	15.2	0	0	0	0	0	37.2	87.8	302.2
1996	267	299.8	188.2	1.4	15.3	0	0	0	0	0.6	43	459.6
1997	425	251.1	56	102	3.7	0	0	0	95.7	-	-	321.8
1998	298.2	183.4	133.8	0	0	0	0	0	0	5.7	109.4	330.7
1999	322.1	267.2	501.7	2.8	6.1	0	0	0	0	29.8	120.7	141.1
2000	165.3	319.9	171.9	38	0	0	0	0	0	0	82.8	229.1
2001	222.7	51.2	239.1	53.5	0	0	0	0	0	20.1	124.2	165.2
2002	231.9	150.4	111.7	13.2	0	1.9	0	0	3.3	0	67.7	166
2003	279	202.2	212.5	31.6	0	0	0	0.7	0	43.1	33	135.1
2004	219.6	149.4	126.2	0	0	0	0	0	0	3.2	146.5	358.8
2005	380.4	82.1	81.2	5.3	0	0	0	0	0	0	177	169.7
2006	284	194.8	175.6	41.5	5.6	0	0	0	0	0	36.7	283.6
2007	535.6	260.9	127.4	30.9	1.7	0	0	0	0	5.9	21.4	283.9
2008	296.2	266.4	113.1	1.2	0	0	0	0	124.6	2.3	122.6	275.3
2009	163.2	217.8	206.5	37.2	2	0	0	0	0	1.6	200.5	238.3
2010	115.4	0	184.3	26	0	0	0	0	0	0	59.4	272.6
2011	165.4	203.2	181.7	27.1	0	0	0	0	0	14.2	100.1	129.1
2012	221.7	233.4	248.2	16.5	1.5	0	0	9.4	3	1.8	69.9	178
2013	341.8	202.3	56	1.1	-	-	-	-	-	-	33.1	197.5
2014	108.6	262.4	77.6	0	0	0	0	0	20.6	0	45.1	170
2015	503.4	109.6	70.4	109.4	0	0	-	-	-	-	-	-

Table 7-5: Mpika station rainfall time series

(Source: ZMD)

Year	Jan	Feb	Mar	Apr	May	Jun	Jul	Aug	Sep	Oct	Nov	Dec
1981	218.8	240.3	112.9	11.9	1.2	0	0	0	0	49.1	113.8	69.7
1982	328.4	286.9	125	26.2	12.2	0	0	0	0	9.4	176.3	154.7
1983	299.6	190.5	63.9	16.2	3.2	0	0.3	0	0	0.5	51.2	348.2
1984	212.8	298.3	49	18.7	0	0	0	0	0	0.1	207.8	393.4
1985	295.9	218.4	111.2	84.9	0	0	0	2	0	16.5	129	334.3
1986	367.7	172.6	222.5	26.4	0	0	0	0	0	46.7	90.3	252.6
1987	254.6	165	164.4	10.8	0	0	0	0	35.5	5.8	53.4	250.6
1988	253.7	305.7	357.6	17.5	11	1	0	0	0	12.7	179.4	184.1
1989	267.5	222.6	390	74.3	0	0	0	0	0	0	69.3	200.6
1990	195.7	308.4	32.5	13.9	0	0	0	0	2	0	37.4	145.4
1991	245.9	145.8	36.4	15.9	14.5	0	0	0	7.5	12.7	51.7	308.5
1992	149.2	67.1	154.1	19	6.2	0	0	0	0	0	104.2	219.7
1993	251.2	118.4	262.4	23.7	0	0	10	2.5	0.9	0	155.5	68.1
1994	277	210.7	62.2	4.8	0	0	0	0	0.3	48.9	19.8	107.2
1995	244.6	188.7	111.6	5.1	0	0	0	0	0	0	38	135.8
1996	135.6	259.4	218.9	26.2	0	0	0	0	0	6	1.2	280.9
1997	147.1	292.5	17.3	124.2	0	0	0.2	0	0	26.4	212.8	382.4
1998	343.4	257	106.3	21.4	0	0	0	0	0	0	56.4	112.8
1999	187.8	151.3	362.4	47.5	0	0	0	0	0	0	56.1	125.1
2000	230.7	178.6	411.3	3.7	0	0	0	0	0	9	95.9	359.2
2001	424.5	213.3	136.8	19.2	0	0	3.2	0	0	1.5	76.2	201.7
2002	231.9	150.4	111.7	13.2	0	1.9	0	0	3.3	0	67.7	166
2003	279	202.2	212.5	31.6	0	0	0	0.7	0	43.1	33	135.1
2004	219.6	149.4	126.2	0	0	0	0	0	0	3.2	146.5	358.8
2005	380.4	82.1	81.2	5.3	0	0	0	0	0	0	177	169.7
2006	284	194.8	175.6	41.5	5.6	0	0	0	0	0	36.7	283.6
2007	535.6	260.9	127.4	30.9	1.7	0	0	0	0	5.9	21.4	283.9
2008	296.2	266.4	113.1	1.2	0	0	0	0	124.6	2.3	122.6	275.3
2009	163.2	217.8	206.5	37.2	2	0	0	0	0	1.6	200.5	238.3
2010	115.4	0	184.3	26	0	0	0	0	0	0	59.4	272.6
2011	165.4	203.2	181.7	27.1	0	0	0	0	0	14.2	100.1	129.1
2012	221.7	233.4	248.2	16.5	1.5	0	0	9.4	3	1.8	69.9	178

7.7 Appendix 4: CHIRPS rainfall time series

Table 7-6: CHIRPS point data for Serenje station

(Source: DRI, 2021)

Year	Jan	Feb	Mar	Apr	May	Jun	Jul	Aug	Sep	Oct	Nov	Dec
1981	196.8	266.2	135.7	42.7	3.1	0.0	0.0	0.0	0.0	8.7	54.1	102.7
1982	340.7	267.1	49.4	47.1	6.2	0.0	0.0	0.0	0.6	15.9	149.0	181.7
1983	294.2	217.7	77.7	39.9	13.2	0.0	0.0	0.0	0.0	5.2	54.4	224.3
1984	183.3	212.1	115.3	14.3	0.0	0.0	0.0	0.0	0.0	0.0	105.1	307.3
1985	279.1	234.2	111.3	44.1	0.0	0.0	0.0	0.0	0.0	12.9	101.4	224.4
1986	336.2	207.0	124.3	117.3	0.0	0.0	0.0	0.0	0.0	32.2	83.2	205.3
1987	313.5	149.4	98.1	15.5	3.0	0.0	0.0	0.0	1.0	8.4	76.3	173.9
1988	298.1	310.8	162.8	36.2	0.0	0.0	0.0	0.0	0.0	11.8	34.6	163.1
1989	312.6	241.8	163.0	15.3	0.0	0.0	0.0	0.0	0.0	4.5	68.0	297.1
1990	291.8	219.3	102.4	33.8	11.2	0.0	0.0	0.0	0.0	0.0	50.5	169.2
1991	322.7	167.4	96.8	57.8	0.0	0.0	0.0	0.0	0.0	19.9	110.9	225.3
1992	147.1	84.7	136.6	27.6	0.0	0.0	0.0	0.0	0.0	0.0	69.0	277.4
1993	257.9	334.3	225.3	48.1	0.0	0.0	0.0	0.0	0.0	0.0	142.2	145.9
1994	284.3	221.5	32.9	17.3	0.0	0.0	0.0	0.0	1.2	36.4	27.2	164.7
1995	205.7	214.5	86.1	11.3	0.0	0.0	0.0	0.0	0.0	9.2	64.7	276.4
1996	250.8	216.2	114.0	15.5	5.0	0.0	0.0	0.0	0.0	0.0	67.3	281.7
1997	298.4	251.7	80.6	79.5	0.0	0.0	0.0	0.0	0.6	6.4	203.4	298.6
1998	287.0	175.2	108.1	11.4	0.0	0.0	0.0	0.0	0.0	0.0	96.9	225.6
1999	368.4	254.9	173.2	23.5	0.0	0.0	0.0	0.0	0.0	7.0	77.7	121.6
2000	301.5	271.5	227.4	17.3	0.0	0.0	0.0	0.0	0.0	7.1	136.1	208.9
2001	275.4	310.8	213.5	24.2	0.0	0.0	0.0	0.0	0.0	11.4	103.3	198.9
2002	213.8	141.4	59.2	31.3	0.0	0.0	0.0	0.0	0.9	10.8	77.9	326.0
2003	233.8	268.5	175.8	18.8	0.0	0.0	0.0	0.0	0.0	8.8	78.2	212.6
2004	259.4	203.2	163.7	51.5	0.0	0.0	0.0	0.0	0.0	5.8	115.7	361.9
2005	265.6	152.9	49.4	23.8	0.0	0.0	0.0	0.0	0.9	0.0	74.0	233.3
2006	301.4	287.0	199.4	22.2	3.6	0.0	0.0	0.0	0.0	4.1	112.9	241.0
2007	419.6	366.4	94.2	15.4	0.0	0.0	0.0	0.0	0.0	6.1	101.8	349.6
2008	358.4	179.9	103.8	21.7	0.0	0.0	0.0	0.0	0.0	0.0	118.6	342.7
2009	275.5	165.9	175.8	19.6	7.3	0.0	0.0	0.0	0.0	1.8	143.1	314.6
2010	189.4	431.4	191.6	53.3	0.0	0.0	0.0	0.0	0.0	0.0	73.6	340.7
2011	308.6	115.4	133.4	39.4	0.0	0.0	0.0	0.0	0.0	7.3	109.6	202.7
2012	340.0	286.7	217.1	36.5	0.0	0.0	0.0	0.0	0.0	0.0	50.8	221.2
2013	253.2	229.1	76.3	28.3	0.0	0.0	0.0	0.0	0.0	6.6	72.1	200.8
2014	225.7	242.3	112.1	37.4	0.0	0.0	0.0	0.0	0.0	3.0	20.3	171.6
2015	268.1	232.4	76.8	117.5	0.0	0.0	0.0	0.0	0.0	7.1	83.7	163.6
2016	213.7	133.2	233.3	20.6	0.0	0.0	0.0	0.0	0.0	0.0	121.1	203.3
2017	419.4	328.0	121.1	101.2	5.1	0.0	0.0	0.0	0.0	17.0	214.3	242.4
2018	107.2	306.8	188.2	54.1	0.0	0.0	0.0	0.0	0.0	6.2	53.9	207.2
2019	263.6	214.5	101.9	69.8	5.1	0.0	0.0	0.0	0.0	2.9	117.5	136.4
2020	240.8	220.4	70.1	26.7	11.3	0.3	0.0	0.0	0.1	5.6	49.7	312.5
2021	389.5	302.4	356.7	14.7	5.2	0.0	0.0	0.0	0.0	0.0	0.0	0.0

Table 7-7: CHIRPS point data for Kabwe station

(Source: DRI, 2021)

Year	Jan	Feb	Mar	Apr	May	Jun	Jul	Aug	Sep	Oct	Nov	Dec
1981	212.7	255.6	125.8	57.1	0.0	0.0	0.0	0.0	0.0	9.3	61.8	62.0
1982	269.9	264.4	44.2	37.4	0.0	0.0	0.0	0.0	0.0	35.9	167.7	154.7
1983	234.1	160.7	86.5	38.1	6.0	0.0	0.0	0.0	0.0	16.8	92.1	215.5
1984	129.8	194.7	107.2	10.4	0.0	0.0	0.0	0.0	0.0	7.5	132.8	357.7
1985	247.9	178.0	158.8	23.0	0.0	0.0	0.0	0.0	0.0	21.0	57.5	271.4
1986	324.9	143.2	108.8	96.3	0.0	0.0	0.0	0.0	1.7	40.5	54.1	193.7
1987	248.5	105.8	68.4	6.5	0.0	0.0	0.0	0.0	1.3	7.0	49.0	228.9
1988	183.2	195.6	128.5	5.4	0.0	0.0	0.0	0.0	0.0	22.6	41.8	170.4
1989	256.3	285.4	140.2	9.8	0.0	0.0	0.0	0.0	0.0	5.7	68.6	171.7
1990	330.4	177.3	93.2	22.3	0.0	0.0	0.0	0.0	0.0	17.2	77.1	161.2
1991	303.9	162.5	93.0	14.3	0.0	0.0	0.0	0.0	0.9	27.2	57.4	140.1
1992	104.7	82.9	177.5	31.9	0.0	0.0	0.0	0.0	0.0	7.5	65.1	284.2
1993	184.4	182.7	207.7	26.7	0.0	0.0	0.0	0.0	0.0	7.9	102.6	123.1
1994	232.4	159.2	16.3	8.6	0.0	0.0	0.0	0.0	0.0	38.3	29.0	153.6
1995	159.8	198.5	47.1	5.7	0.0	0.0	0.0	0.0	0.0	30.7	119.3	142.2
1996	206.5	199.0	127.8	0.0	4.2	0.0	0.0	0.0	0.0	5.7	119.0	278.9
1997	302.7	212.3	78.0	94.5	0.0	0.0	0.0	0.0	0.0	5.5	146.9	235.5
1998	291.0	71.1	89.6	8.2	0.0	0.0	0.0	0.0	0.0	5.7	66.3	296.4
1999	303.5	214.4	104.1	0.0	0.0	0.0	0.0	0.0	0.0	14.1	52.2	135.6
2000	255.9	222.6	207.9	5.5	0.0	0.0	0.0	0.0	0.0	10.3	151.0	223.3
2001	237.9	329.9	233.1	6.3	0.0	0.0	0.0	0.0	0.0	10.4	114.9	205.1
2002	130.2	76.0	55.0	46.5	0.0	0.0	0.0	0.0	0.0	18.4	89.3	263.3
2003	168.0	256.9	220.0	13.4	0.0	0.0	0.0	0.0	0.0	15.1	91.2	188.5
2004	241.5	225.7	137.3	22.4	0.0	0.0	0.0	0.0	0.0	18.2	89.6	320.7
2005	194.6	62.2	64.9	10.8	0.0	0.0	0.0	0.0	0.0	0.0	109.4	301.2
2006	226.4	196.5	183.7	9.0	0.0	0.0	0.0	0.0	0.0	6.2	101.5	183.8
2007	284.1	277.5	62.0	16.3	0.0	0.0	0.0	0.0	0.0	7.9	139.2	339.3
2008	293.6	92.3	114.5	0.0	0.0	0.0	0.0	0.0	0.0	7.2	156.4	261.0
2009	283.6	109.5	200.4	5.7	14.3	0.0	0.0	0.0	0.0	5.2	201.1	177.7
2010	154.3	330.6	202.7	45.7	0.0	0.0	0.0	0.0	0.0	0.0	123.6	267.5
2011	252.6	76.3	140.3	20.7	0.0	0.0	0.0	0.0	0.0	10.9	130.9	150.6
2012	262.4	186.1	170.5	20.6	0.0	0.0	0.0	0.0	0.0	6.4	83.4	246.3
2013	284.1	205.3	55.3	27.4	0.0	0.0	0.0	0.0	0.0	23.9	55.1	223.8
2014	213.5	178.2	103.5	40.5	0.0	0.0	0.0	0.0	0.0	8.4	48.1	211.9
2015	227.0	197.5	82.6	105.4	0.0	0.0	0.0	0.0	0.0	9.5	58.9	160.8
2016	247.1	100.0	233.5	25.8	0.0	0.0	0.0	0.0	0.0	8.2	190.1	197.1
2017	328.4	314.6	124.7	62.7	0.0	0.0	0.0	0.0	0.0	25.2	149.2	220.5
2018	79.5	323.2	191.3	17.7	15.2	0.0	0.0	0.0	0.0	6.9	42.3	143.1
2019	184.8	152.2	53.8	55.0	0.0	0.0	0.0	0.0	0.0	7.4	85.2	65.6
2020	257.3	243.0	65.8	6.8	0.1	0.1	0.0	0.0	0.3	11.4	82.9	354.3
2021	324.3	293.8	164.1	0.0	0.0	0.0	0.0	0.0	0.0	0.0	0.0	0.0

Table 7-8: CHIRPS point data for Mkushi station

(Source: DRI, 2021)

Year	Jan	Feb	Mar	Apr	May	Jun	Jul	Aug	Sep	Oct	Nov	Dec
1981	179.3	294.9	117.9	25.9	0.0	0.0	0.0	0.0	0.0	7.9	59.6	85.3
1982	297.2	314.5	24.1	20.7	6.1	0.0	0.1	0.0	0.0	13.2	99.1	171.9
1983	260.9	220.9	58.4	19.6	6.2	0.0	0.0	0.0	0.1	11.2	59.5	234.3
1984	179.7	259.8	94.9	7.9	0.0	0.0	0.0	0.0	0.0	7.9	84.3	290.0
1985	236.8	234.8	129.4	20.9	7.7	0.0	0.0	0.0	0.0	12.0	81.6	231.3
1986	335.6	210.9	75.8	34.1	4.4	0.0	0.0	0.0	0.0	31.3	54.2	187.8
1987	290.0	119.4	95.8	5.9	2.8	0.0	0.1	0.0	1.4	9.7	72.3	201.7
1988	254.6	367.2	105.5	10.5	0.0	0.0	0.0	0.0	0.0	15.5	41.5	152.6
1989	278.2	276.5	114.1	11.5	0.0	0.0	0.0	0.0	0.0	4.4	67.0	226.7
1990	291.6	249.4	127.7	17.7	0.0	0.0	0.0	0.0	0.0	0.0	54.1	176.4
1991	290.3	219.4	70.1	20.0	0.0	0.0	0.0	0.0	0.0	23.7	72.5	189.6
1992	167.7	95.3	100.1	12.4	0.0	0.0	0.0	0.0	0.0	5.5	62.1	313.2
1993	222.7	315.6	141.2	17.6	0.0	0.0	0.0	0.0	0.0	5.4	123.1	142.3
1994	307.0	271.5	20.8	8.9	0.0	0.0	0.0	0.0	1.2	23.0	39.4	132.8
1995	180.2	210.9	60.0	0.0	0.0	0.0	0.0	0.0	0.0	11.6	111.2	245.1
1996	225.1	263.7	102.7	6.2	6.8	0.0	0.0	0.0	0.0	0.0	63.3	360.3
1997	288.1	209.8	80.4	57.8	0.0	0.0	0.0	0.0	0.7	5.2	139.8	314.5
1998	247.3	158.7	99.9	0.0	0.0	0.0	0.0	0.0	0.0	0.0	70.2	312.7
1999	321.4	301.2	107.2	6.0	0.0	0.0	0.0	0.0	0.0	8.8	56.5	135.6
2000	240.8	296.8	220.9	5.5	0.0	0.0	0.0	0.0	0.0	10.7	112.1	248.2
2001	266.1	385.7	228.2	7.0	0.0	0.0	0.0	0.0	0.0	11.1	108.4	189.1
2002	177.2	145.0	43.3	29.9	0.0	0.0	0.0	0.0	0.0	10.3	98.1	302.2
2003	179.7	310.0	214.8	9.8	0.0	0.0	0.0	0.0	0.0	12.2	73.7	227.2
2004	256.4	285.3	123.8	21.9	0.0	0.0	0.0	0.6	0.0	12.2	88.9	336.1
2005	209.2	131.8	34.4	9.4	0.0	0.0	0.0	0.0	0.0	0.0	75.5	285.6
2006	230.1	304.3	163.9	7.6	0.0	0.0	0.0	0.0	0.0	2.2	80.0	211.6
2007	304.6	286.8	63.0	8.6	0.0	0.0	0.0	0.0	0.7	6.0	80.0	341.3
2008	295.4	134.0	93.9	5.9	0.0	0.0	0.0	0.0	0.0	6.3	123.6	284.3
2009	307.0	118.3	150.2	0.0	14.4	0.0	0.0	0.0	0.0	5.1	135.4	239.2
2010	171.2	372.8	132.9	29.1	0.0	0.0	0.0	0.0	0.0	0.0	67.8	286.2
2011	243.2	130.3	125.1	16.5	0.0	0.0	0.0	0.0	0.0	7.2	96.1	167.6
2012	279.2	232.5	150.5	12.0	0.0	0.0	0.0	0.0	0.0	5.7	50.0	250.6
2013	287.7	249.2	59.1	9.4	0.0	0.0	0.0	0.0	0.0	9.9	53.6	217.6
2014	225.9	246.8	92.4	11.7	0.0	0.0	0.0	0.0	0.0	0.0	31.4	196.2
2015	275.1	234.8	64.9	54.9	0.0	0.0	0.0	0.0	0.0	5.9	72.1	177.1
2016	250.6	113.4	176.9	6.9	0.0	0.0	0.0	0.0	0.7	0.0	129.8	208.3
2017	363.4	369.9	112.7	31.8	8.3	0.0	0.0	0.0	0.0	16.8	148.7	251.7
2018	106.6	355.5	145.2	9.5	5.2	0.0	0.0	0.6	0.0	5.7	41.3	211.5
2019	182.5	262.7	52.4	32.1	7.3	0.5	0.0	0.0	0.0	4.4	87.9	97.6
2020	245.3	251.4	52.0	6.3	2.3	0.8	0.0	0.0	0.3	6.4	48.0	312.4
2021	313.2	362.6	265.0	0.0	6.1	0.0	0.0	0.0	0.0	0.0	0.0	0.0

Table 7-9: CHIRPS point data for Mpika station

(Source: DRI, 2021)

Year	Jan	Feb	Mar	Apr	May	Jun	Jul	Aug	Sep	Oct	Nov	Dec
1981	203.9	248.5	100.1	13.5	0.0	0.0	0.0	0.0	0.0	14.6	64.1	78.0
1982	267.9	312.8	80.8	37.8	0.0	0.0	0.0	0.0	0.0	14.8	167.1	249.1
1983	190.2	172.9	86.7	26.1	0.0	0.0	0.0	0.0	0.3	4.2	44.4	227.4
1984	163.5	244.0	79.4	16.9	0.0	0.0	0.0	0.0	0.0	0.0	134.9	391.5
1985	228.5	159.8	159.6	37.3	0.0	0.0	0.0	0.0	0.0	17.0	179.3	353.8
1986	255.5	198.1	117.9	31.0	0.0	0.0	0.0	0.0	0.0	30.9	84.2	258.2
1987	198.9	150.1	129.6	14.0	1.9	0.0	0.0	0.0	0.0	19.7	67.5	137.6
1988	220.8	273.6	239.8	12.9	0.0	0.0	0.0	0.0	0.0	8.8	103.4	210.9
1989	214.7	285.0	193.8	34.2	0.0	0.0	0.0	0.0	0.0	5.0	101.1	275.8
1990	190.0	232.6	62.3	11.6	6.1	0.0	0.0	0.0	0.0	0.0	39.8	167.3
1991	271.7	168.2	76.8	23.8	0.0	0.0	0.0	0.0	0.0	14.5	77.2	226.6
1992	156.7	65.6	129.0	17.2	6.3	0.0	0.0	0.0	0.0	0.0	78.1	215.0
1993	221.5	244.6	217.0	24.6	0.0	0.0	0.0	0.0	0.0	0.0	137.4	104.2
1994	229.4	209.0	48.1	9.8	0.0	0.0	0.0	0.0	1.5	23.4	30.2	126.2
1995	233.4	227.6	92.8	9.3	0.0	0.0	0.0	0.0	0.0	6.8	50.4	231.8
1996	229.4	278.2	176.0	10.6	0.0	0.0	0.0	0.0	0.0	6.9	24.6	191.4
1997	168.7	257.6	79.8	83.9	0.0	0.0	0.0	0.0	0.0	17.7	148.0	369.6
1998	286.7	131.4	132.7	20.1	0.0	0.0	0.0	0.0	0.0	5.4	61.5	200.4
1999	275.6	176.0	208.6	15.8	0.0	0.0	0.0	0.0	0.0	0.0	74.5	145.8
2000	198.5	194.7	247.0	14.6	0.0	0.0	0.0	0.0	0.0	9.4	144.6	235.6
2001	303.8	210.1	152.7	14.2	0.0	0.0	0.0	0.0	0.0	14.5	49.7	217.3
2002	231.3	163.6	107.3	10.0	0.0	0.0	0.0	0.0	0.0	5.1	54.3	340.1
2003	202.0	198.9	204.1	16.9	0.0	0.0	0.0	0.0	0.0	8.3	50.4	211.5
2004	204.2	181.7	169.6	31.4	0.0	0.0	0.0	0.0	0.0	0.0	152.4	441.5
2005	290.5	204.5	77.4	14.0	0.0	0.0	0.0	0.0	1.2	0.0	79.2	145.6
2006	262.0	215.0	189.8	19.0	2.2	0.0	0.0	0.0	0.0	3.5	98.5	327.5
2007	435.4	361.4	128.1	16.0	0.0	0.0	0.0	0.0	0.0	7.4	70.7	319.3
2008	280.1	186.9	91.2	11.0	0.0	0.0	0.0	0.0	0.0	5.9	70.6	301.8
2009	202.4	191.8	204.2	25.5	3.6	0.0	0.0	0.0	0.0	0.0	156.1	378.2
2010	206.6	324.0	178.2	8.9	0.0	0.0	0.0	0.0	0.0	3.3	54.2	312.6
2011	242.0	184.3	151.9	21.9	0.0	0.0	0.0	0.0	0.0	9.5	77.3	174.5
2012	264.9	193.1	204.3	23.0	0.0	0.0	0.0	0.0	0.0	15.5	58.9	237.6
2013	231.2	201.3	127.0	32.3	0.0	0.0	0.0	0.0	0.0	5.5	63.4	269.7
2014	232.3	258.6	132.2	33.2	0.0	0.0	0.0	0.0	0.0	4.5	25.2	113.4
2015	229.1	249.9	84.2	37.5	0.0	0.0	0.0	0.0	0.0	6.2	101.3	212.0
2016	178.7	142.0	215.5	11.7	0.0	0.0	0.0	0.0	0.0	4.2	63.5	159.1
2017	261.1	366.7	121.9	28.7	0.0	0.0	0.0	0.0	1.3	15.3	167.8	312.6
2018	142.9	231.4	127.0	35.6	2.0	0.0	0.0	0.0	0.0	0.0	60.5	332.3
2019	260.5	280.7	159.4	26.8	0.0	0.0	0.0	0.0	1.2	3.3	92.0	173.7
2020	274.3	235.5	82.7	15.5	0.8	0.2	0.0	0.0	0.5	9.0	44.9	239.7
2021	244.2	322.2	193.0	10.3	0.0	0.0	0.0	0.0	0.0	0.0	0.0	0.0

Table 7-10: CHIRPS gridded data over Mabula Kapi catchment

(Source: DRI, 2021)

Year	Jan	Feb	Mar	Apr	May	Jun	Jul	Aug	Sep	Oct	Nov	Dec
1981	217.9	276.1	170.8	25.6	2.0	0.0	0.0	0.0	0.0	13.2	56.4	95.2
1982	328.0	249.0	76.1	40.0	11.1	0.0	0.1	0.0	0.3	18.2	156.6	202.7
1983	276.0	225.8	117.9	25.4	9.0	0.0	0.0	0.0	0.0	6.7	52.2	213.0
1984	142.7	244.7	124.8	17.6	2.4	0.0	0.0	0.0	0.0	6.6	99.7	283.9
1985	311.7	244.7	229.8	49.8	4.4	0.0	0.0	0.0	0.0	17.9	104.7	249.4
1986	369.8	277.0	166.7	73.7	2.0	0.0	0.0	0.0	0.0	29.6	78.7	247.9
1987	299.6	139.4	139.1	15.1	4.9	0.0	0.4	0.0	2.0	14.4	85.1	156.7
1988	257.8	320.3	253.9	17.1	5.3	0.0	0.0	0.0	0.0	19.6	57.8	159.0
1989	316.6	276.0	196.2	34.4	2.6	0.0	0.0	0.0	0.0	7.2	70.2	307.8
1990	300.5	243.4	87.5	29.6	13.2	0.0	0.0	0.2	0.0	4.3	56.8	153.6
1991	278.3	204.3	91.3	44.2	8.6	0.0	0.0	0.0	0.0	23.1	92.4	256.0
1992	164.2	81.5	199.6	19.6	8.8	0.0	0.0	0.0	0.2	6.1	71.2	265.6
1993	226.1	346.3	240.5	37.9	2.3	0.0	0.0	0.0	0.0	6.3	126.5	132.9
1994	324.1	243.1	37.5	13.6	2.7	0.0	0.0	0.0	2.0	40.2	32.1	150.3
1995	205.9	228.2	92.9	10.3	2.6	0.0	0.0	0.0	0.0	8.9	47.7	318.7
1996	278.7	221.0	134.0	12.3	7.9	0.0	0.0	0.0	0.0	6.1	51.1	271.9
1997	336.1	280.2	78.3	78.1	3.3	0.0	0.0	0.2	0.3	12.4	180.2	266.2
1998	304.5	175.2	165.0	15.1	2.7	0.0	0.0	0.0	0.0	8.5	94.2	200.5
1999	350.1	291.5	243.0	19.6	3.9	0.0	0.0	0.0	0.0	6.6	89.8	122.0
2000	293.1	273.2	259.7	16.6	3.0	0.0	0.0	0.0	0.0	6.5	126.2	195.2
2001	309.7	305.3	241.2	24.3	2.5	0.0	0.0	0.0	0.0	12.9	91.1	215.6
2002	248.1	188.7	71.6	29.6	1.8	0.4	0.1	0.1	0.0	9.2	72.8	345.5
2003	225.6	249.4	240.5	20.5	2.0	0.0	0.0	0.0	0.0	11.4	61.0	208.4
2004	274.9	224.4	209.0	44.5	1.7	0.0	0.0	0.2	0.0	7.6	108.1	386.4
2005	280.9	188.5	53.9	16.5	2.0	0.0	0.0	0.0	1.3	6.2	77.2	190.7
2006	357.2	258.8	249.6	20.1	1.7	0.0	0.0	0.0	0.2	8.8	112.4	285.0
2007	534.3	377.5	130.8	19.3	1.6	0.0	0.0	0.0	0.0	9.0	87.2	369.8
2008	412.2	206.8	91.9	16.1	1.6	0.0	0.0	0.0	0.0	7.2	76.8	338.0
2009	260.7	177.2	216.2	23.7	12.6	0.0	0.1	0.0	0.0	6.0	157.9	325.5
2010	199.7	499.4	227.1	37.4	2.6	0.0	0.0	0.0	0.0	5.5	61.3	321.7
2011	329.7	134.2	154.8	38.5	3.2	0.0	0.0	0.0	0.0	9.4	100.1	212.9
2012	354.2	297.4	254.5	50.8	1.7	0.0	0.0	0.0	0.0	7.9	55.8	215.5
2013	242.3	247.5	92.9	35.2	5.1	0.0	0.0	0.0	0.0	10.1	66.1	218.9
2014	213.9	239.4	121.3	27.9	1.8	0.0	0.0	0.0	0.0	5.7	18.7	164.2
2015	277.0	252.1	87.2	95.0	1.9	0.0	0.0	0.0	0.0	11.0	72.1	174.9
2016	196.5	166.0	293.9	18.3	1.9	0.0	0.0	0.2	0.0	8.0	100.6	179.4
2017	401.5	315.5	132.7	70.3	8.0	0.0	0.0	0.2	0.0	18.6	203.7	262.7
2018	105.3	297.0	223.9	44.9	5.5	0.0	0.0	0.5	0.1	9.7	58.0	240.0
2019	295.4	260.2	138.1	47.7	5.9	0.7	0.0	0.0	0.0	8.5	90.4	136.7
2020	247.1	251.8	71.4	19.9	5.7	1.3	0.3	0.0	0.5	11.6	38.2	311.2
2021	381.4	318.0	438.0	11.2	8.0	0.0	0.0	0.0	0.0	0.0	0.0	0.0

7.8 Appendix 5: Location map

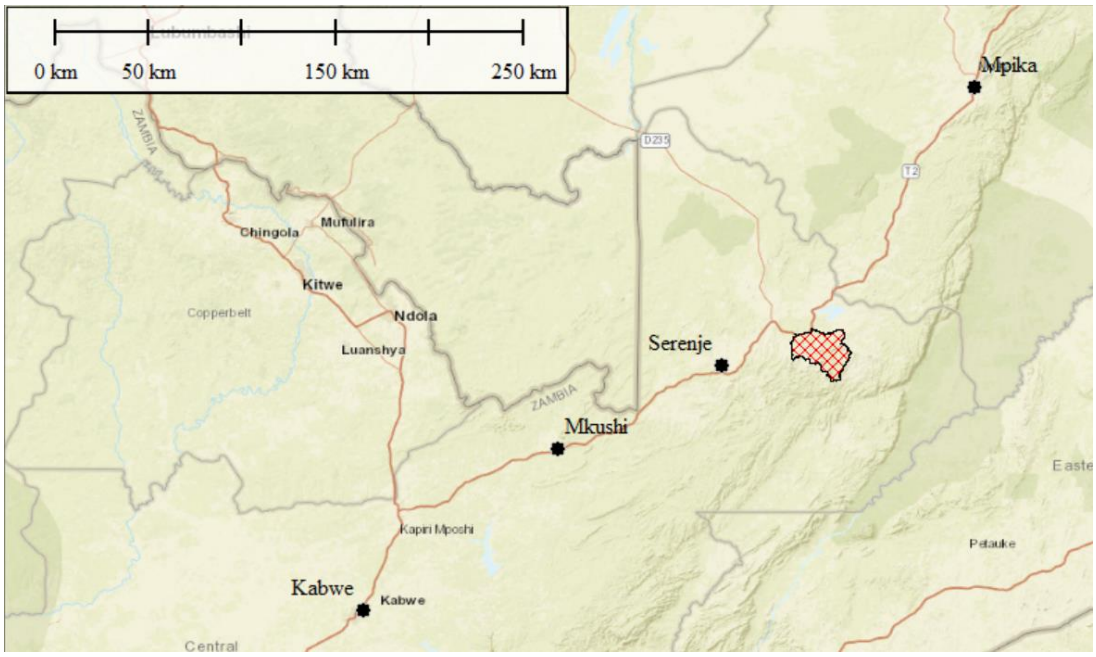

Figure 7-1: Location map - Mabula Kapi catchment and local meteorological stations

7.9 Appendix 6 : Training in rainfall-runoff modelling

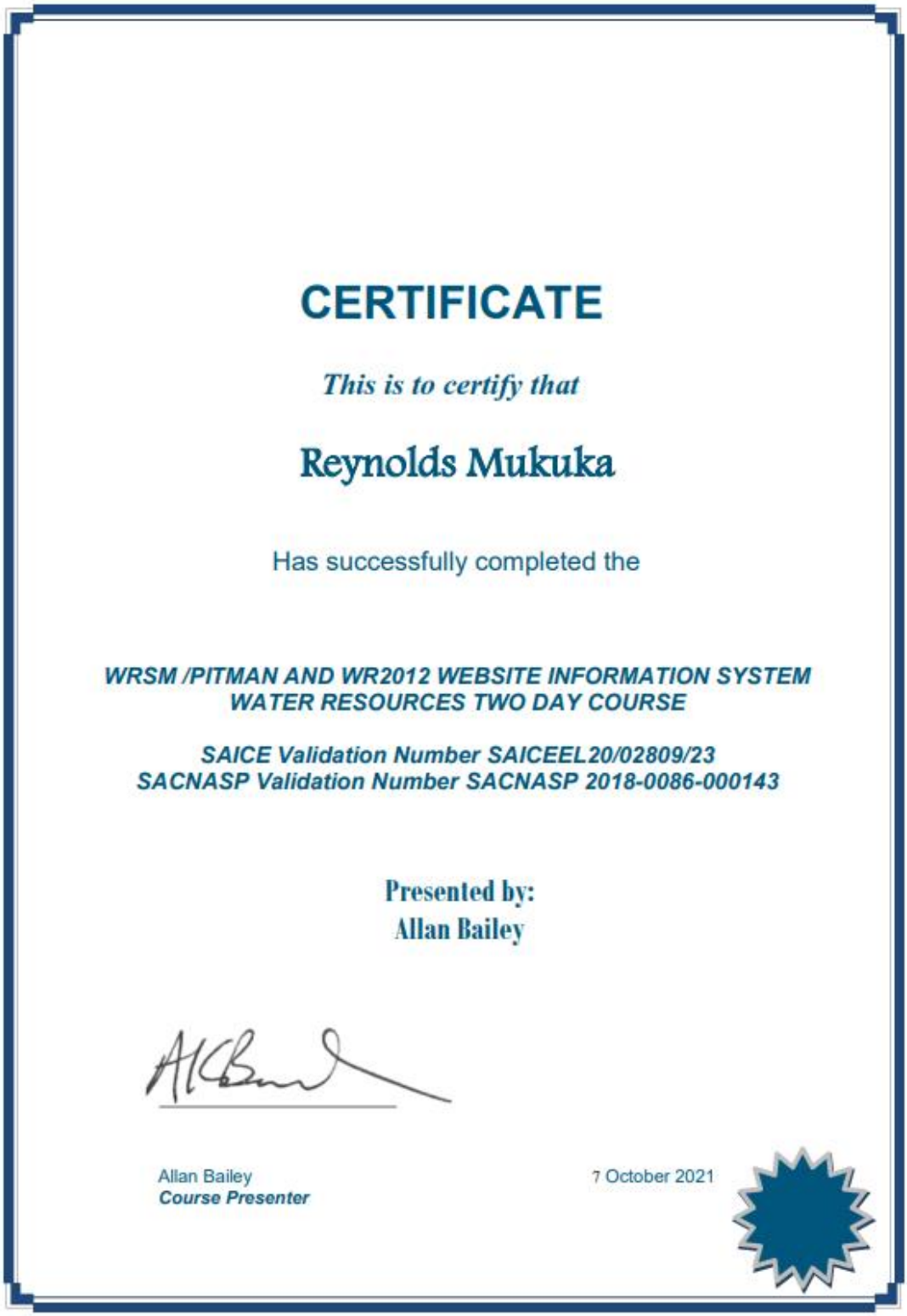

CERTIFICATE

This is to certify that

Reynolds Mukuka

Has successfully completed the

WRSM /PITMAN AND WR2012 WEBSITE INFORMATION SYSTEM
WATER RESOURCES TWO DAY COURSE

SAICE Validation Number SAICEEL20/02809/23
SACNASP Validation Number SACNASP 2018-0086-000143

Presented by:
Allan Bailey

Allan Bailey
Course Presenter

7 October 2021

Figure 7-2: Certificates of training for PITMAN rainfall-runoff model

7.10 Appendix 7: Photo gallery – Site visit at Manangwa station